5-2013

PIM KINASE INHIBITION: SINGLE AGENT AND COMBINATION APPROACHES IN B-CELL LYMPHOMA

Qingshan Yang

PIM KINASE INHIBITION: SINGLE AGENT AND COMBINATION

APPROACHES IN B-CELL LYMPHOMA

by

Qingshan Yang, B.A.

Approved:

_____
Varsha Gandhi, Ph.D.
Advisor

_____
Hesham Amin, M.D.

_____
Jan Burger, M.D.

_____
Joya Chandra, Ph.D.

_____
Peng Huang, M.D., Ph.D.

Approved:

_____
Dean, The University of Texas
Graduate School of Biomedical Sciences at Houston

PIM KINASE INHIBITION: SINGLE AGENT AND COMBINATION

APPROACHES IN B-CELL LYMPHOMA

A

DISSERTATION

Presented to the Faculty of

The University of Texas

Health Science Center at Houston

and

The University of Texas

MD Anderson Cancer Center

Graduate School of Biomedical Sciences at Houston

in Partial Fulfillment

of the Requirements

for the Degree of

DOCTOR OF PHILOSOPHY

by

Qingshan Yang, B.A.

Houston, Texas

May, 2013

Copyright

Dedication

To my loving and supportive parents, grandparents, and uncle David.

Your passion in science has inspired me and guided me to where I am today.

Acknowledgement

I would like to extend my deepest gratitude towards my Ph.D. advisor, Dr. Varsha Gandhi. Your support teaching and mentorship on my academia career development endeavors has been the most invaluable experience of my graduate training; your dedication to science and education has made you my role model and life-time mentor. Without your generous support, I could not have reached the finish line in such efficiency!

I would also like to express my biggest thank you to my Ph.D. mentor and good friend, Dr. Lisa Chen. You have taught me much more than laboratory techniques and scientific writing. Also thank you for holding my hand through each milestone during my training, I could not have done it without you!

Special thank you to all of my committee members, Drs. Hesham Amin, Jan Burger, Joya Chandra and Peng Huang! Thank you for providing helpful advises on my thesis projects through the past 3 years, and helping me to become a better scientist.

Additional thank you to Bill, for your support and help along the way, and thank you for all the helpful suggestions from lab meetings on my projects, and the very supportive recommendation letters as well as the thoughtful notes you passed to me on various occasions.

Many thanks to…

My current lab mates, Shadia Zaman and Viral Patel, Fabiola Gomez, Yingjun Jiang and Prexy Shah, for providing good company and very helpful tips and suggestions during my thesis writing, and throughout my Ph.D. training.

Every member of the Cellular and Molecular Pharmacology group! Thank you for providing valuable assistance throughout my Ph.D. training here, for all the protocols, reagents, trouble-shootings and also for all the moral supports! I am so fortunate to be in this group!

PIM KINASE INHIBITION: SINGLE AGENT AND COMBINATION
APPROACHES IN B-CELL LYMPHOMA

Publication no._____

Qingshan Yang, B.A.

Advisor: Varsha Gandhi, Ph.D.

Proviral integration site for Moloney murine leukemia virus (Pim) kinases are Ser/Thr/Tyr kinases. They modulate B-cell development but become oncoproteins and promote cancer development once overexpressed. Containing three isoforms, Pim-1, -2 and -3 are known to phosphorylate various substrates that regulate transcription, translation, cell cycle, and survival pathways in both hematological and solid tumors.

Mantle cell lymphoma (MCL) is an aggressive B-cell lymphoma. Elevated Pim kinase levels are common in MCL, and it negatively correlates with patient outcome. SGI-1776 is a small molecule inhibitor selective for Pim-1/-3. We hypothesize that SGI-1776 treatment in MCL will inhibit Pim kinase function, and inhibition of downstream substrates phosphorylation will disrupt transcriptional, translational, and cell cycle processes while promoting apoptosis.

SGI-1776 treatment induced moderate to high levels of apoptosis in four MCL cell lines (JeKo-1, Mino, SP-53 and Granta-519) and peripheral blood mononuclear cells (PBMCs) from MCL patients. Phosphorylation of transcription and translation regulators, c-Myc and 4E-BP1 declined in both model systems. Additionally, levels of short-lived Mcl-1 mRNA and protein also decreased and correlated with decline of global RNA synthesis. Collectively, our investigations highlight Pim kinases as viable drug targets in MCL and emphasize their roles in transcriptional and translational regulation.

We further investigated a combination strategy using SGI-1776 with bendamustine, an FDA-approved DNA-damaging alkylating agent for treating non-Hodgkin's lymphoma. We hypothesized this combination will enhance SGI-1776-induced transcription and translation inhibition, while promoting bendamustine-triggered DNA damage and inducing additive to synergistic cytotoxicity in B-cell lymphoma.

Bendamustine alone resulted in moderate levels of apoptosis induction in MCL cell lines (JeKo-1 and Mino), and in MCL and splenic marginal zone lymphoma (a type of B-cell lymphoma) primary cells. An additive effect in cell killing was observed when combined with SGI-1776. Expectedly, SGI-1776 effectively decreased global RNA and protein synthesis levels, while bendamustine significantly inhibited DNA synthesis and generated DNA damage response. In combination, intensified inhibitory effects in DNA, RNA and protein syntheses were observed. Together, these data suggested feasibility of using Pim kinase inhibitor in combination with chemotherapeutic agents such as bendamustine in B-cell lymphoma, and provided foundation of their mechanism of actions in lymphoma cells.

Table of Contents

CHAPTER 1. Introduction

CHAPTER 2. Materials and Methods

CHAPTER 3. SGI-1776 single agent treatment in MCL

Aim 1. Analyze the biological consequences of SGI-1776 in MCL cells.

Aim 2. Identify the biological function of Pim kinases in their signaling pathways and biomarkers impacted by SGI-1776 in MCL cells.

CHAPTER 4. Combination of bendamustine and SGI-1776 in B-cell lymphoma

Aim 3. Explore the combination strategy of bendamustine and SGI-1776 to identify primary mechanism of actions of cytotoxicity induction in B-cell lymphoma.

CHAPTER 5. Discussion and Conclusion

List of Figures

List of Tables

List of Abbreviations

4E-BP1	eukaryotic translation initiation factor 4E-binding protein 1
ABCB1	multidrug resistant protein 1
ABCG2	breast cancer resistance protein
AIF	apoptosis-inducing factor
Akt	protein kinase B
AML	acute myeloid leukemia
ATM	ataxia telangiectasia mutated
ATP	adenosine 5'-triphosphate
Bad	Bcl-2–associeated death promoter
BAFF	B-cell activating factor
Bcl-2	B-cell lymphoma 2
Bcl-X_L	B-cell lymphoma-extra large
BCR	B-cell receptor
BLyS	B lymphocyte stimulator
BSA	bovine serum albumin
CD	cluster of differentiation
CDC25A/C	cell division cycle 25A/C
CDK	cyclin-dependent kinase
CDKN1B (p27)	cyclin-dependent kinase inhibitor 1B
CHOP/R-CHOP	cyclophosphamide, doxorubicin, vincristine, prednisone ± rituximab
CLL	chronic lymphocytic leukemia
c-Myc	myelocytomatosis viral oncogen homolog
DHAP	dexamethasone, cytarabine and cisplatin
DLBCL	diffused large B-cell lymphoma

DMSO	dimethyl sulfoxide
DPM	disintegration per minute
4E-BP1	eukaryotic translation initiation factor 4E-binding protein 1
eIF4	eukaryotic initiation factor 4
FBS	fetal bovine serum
FL	follicular lymphoma
Flt3	Fms-like tyrosine kinase 3
GC	germinal center
H2AX	Histone 2A variant X
HSP	heat shock protein
IC50	half-maximal inhibitory concentration
Ig	immunoglobulin
JAK	Janus kinase
LDH	lactic acid dehydrogenase
MCL	mantle cell lymphoma
Mcl-1	induced myeloid leukemia cell differentiation protein
MDM2	mouse double minute 2 homolog
MM	multiple myeloma
mRNA	messenger ribonucleic acid
mTOR	mammalian target of rapamycin
NF-κB	nuclear factor kappa-light-chain-enhancer of activated B cells
NHL	non-Hodgkin's lymphoma
NOXA	Phorbol-12-myristate-13-acetate-induced protein 1
PARP	poly (ADP-ribose) polymerase
PBMC	peripheral blood mononuclear cells
PBS	phosphate-buffered saline

PI3K	phosphatidylinositide 3-kinases
RB1	retinoblastoma protein
RCC	renal cell carcinoma
RICE	ifosfamide, carboplatin and etoposide with rituximab
RPPA	reverse-phase protein microarray
RUNX	runt-related transcription factors
p21	cyclin-dependent kinase inhibitor 1
p27	cyclin-dependent kinase inhibitor 1B
Pim	proviral integration site for Moloney murine leukemia virus
rpm	rotations per minute
RT-PCR	reverse transcription polymerase chain reaction
SEM	standard error of the mean
SHM	somatic hypermutation
siRNA	small interfering ribonucleic acid
SMZL	small marginal zone lymphoma
SOCS	signaling transducer and suppressor of cytokine signaling
SOX11	sry-related high-mobility-group box 11
STAT	signal transducer and activator of transcription
TrkA	transforming tyrosine kinase protein

CHAPTER 1. Introduction

I.   Pim kinases and their role in physiology and tumorigenesis

<u>Pim kinase oncogenes</u>

Proviral integration site for Moloney murine leukemia virus (Pim) kinases are Ser/Thr/Tyr kinases (Selten 1986; Telerman 1988; Hoover 1991) and Pim-1 (the founding member of the Pim kinase family) was first discovered in 1980s (Selten 1986; Telerman 1988). Oncogenic feature of *PIM1* gene was revealed as it contains a small region of murine chromosome, to which murine leukemia virus (MuLV) frequently integrate itself. This integration site is associated with transcription activation that leads to activation of *PIM1* gene, which ultimately induced development of T-cell lymphoma with high incidence in the MuLV-infected murine models (Cuypers 1984).

To date, there are three identified isoforms, Pim-1, -2 and -3, located at different chromosomes in the mouse and human genomes and they share structural and functional similarities (Figure 1). Amino acid sequence of *PIM2* and *PIM3* share 61% and 71% similarity of *PIM1* sequence, respectively (Mikkers 2004). Pim kinases, especially Pim-1 and Pim-2, are expressed in hematological systems, whereas Pim-1 and Pim-3 are expressed in other organs such as testis, kidney and brain (Konietzko 1999; Mikkers 2004). Pim-1 was first reported as a cytoplasmic kinase, however, recent studies has shown that once truncated at C-terminus, Pim-1 can become nuclear and play a role in chemoresistance induction (Telerman 1988; Walpen 2012). Pim-2 is known to be both nuclear and cytoplasmic (Gomez-Abad 2011; Levy 2012), and it works in cytoplasm to enhance functions of other transcription factors such as NF-κB (Hammerman 2004; Chen 2005). In colon cancer cells, it appears that Pim-3 expression is sub-nuclear or cytoplasmic (Popivanova 2007). These Pim kinases functionally compensate one another as confirmed by Pim-1/-2 double knockout or Pim-1/-2/-3 triple knockout studies in mice (Mikkers 2004; An 2013).

Figure 1.
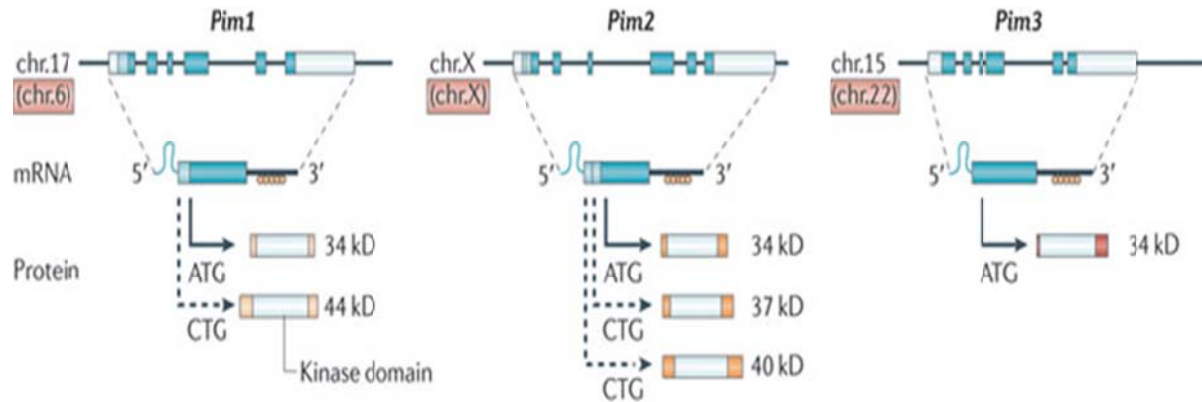
Figure 1. Pim kinase genes, transcripts and proteins.

Pim kinase genes are in both mouse and human genomes. Plain black letters indicate the Pim kinase genes' loci in mouse genome and the letters in orange boxes indicate their loci in human. Each Pim kinase gene is composed of six exons and large untranslated regions at the 5' and 3' ends, indicated by dark blue boxes and light blue boxes. In the Pim kinase mRNAs, G/C rich regions are indicated by light blue lariats, and at the 3' end, there are five copies of AUUUA destabilization motifs indicated by light orange circles. Pim-1, and Pim-2 proteins are synthesized into different isoforms by alternative starting sites (ATG, CTG), indicated by different molecular weights with different initiation codons for each.

The transcripts of all three Pim kinases are encoded by six exons, along with large untranslated regions (UTRs) at 5' and 3' ends as depicted in the figure. At the 5' end of these transcripts, there are G/C-rich regions (blue lariats) and 5 copies of AUUUA destabilizing motifs (orange circles) making them labile and short-lived mRNAs (Mikkers 2004). Translation of Pim-1 and Pim-2 proteins are initiated at alternative sites (light blue boxes and solid or dashed arrows), generating protein isoforms of different molecular weights. However, the kinase domains are highly -conserved among all three Pim kinases (white boxes) and their functional activity are retained (Mikkers 2004). Pim kinases are constitutively active as they do not require post-translational modification to activate the proteins (Qian 2005). However, there are reported phosphorylation sites mediated by tyrosine kinase ETK at Y218 or autophosphorylation at S8, and the former is known to enhance Pim kinase activity (Kim 2004; Bullock 2005). Pim kinase stability is regulated by ubiquitylation and proteasome degradation processes, as well as microRNAs (Thomas 2012) (Linn 2012).

Pim and Myc cooperation

It was reported that activation of c-Myc proto-oncogene was observed when MuLV-proviral DNA insertion leads to B-cell lymphoma development, which suggested a potential collaboration of Pim kinase and c-Myc in the process tumorigenesis (Selten 1986). This phenomenon was later confirmed by transgenic mice study of co-expressing the two proto-oncogenes (*Eμ-Pim1;Eμ-Myc*), which lead to prenatal development of lymphomas (Verbeek 1991). Interestingly, *Eμ-Myc* transgenic mice deficient for Pim-1showed delayed development of lymphoma, indicating the dependency of Myc-driven tumorigenesis on Pim kinase expression levels (Verbeek 1991). It was later confirmed that such synergism in tumorigenesis was also observed between Pim-2 and c-Myc, further suggesting Pim-2 as proto-oncogene and indicating its role in lymphomagenesis (Allen 1997). In addition, Pim-3 can substitute for Pim-1/-2 condition as it becomes activated by proviral insertion in

Pim-1/-2-deficient state, which also indicates the importance of Pim/Myc axis in lymphomagenesis (Mikkers 2004).

Pim kinase and early response genes

Pim kinases genes are early response genes (Polotskaya 1993). The 5' UTR site of Pim kinase transcripts contain a long G/C rich region, render them unstable transcripts and hence require cap-dependent translation (Domen 1987; Hoover 1997). There has been evidence that Pim-1 protein expression is dramatically increased after 5'UTR is depleted or translation initiation factor E4 (eIF4E) is overexpressed (Hoover 1997). This event triggers the assembly process of eIF4E complex and recruitment of 40S ribosomal subunit to bind to the "capped" 5'-m^{7}G translation initiation site of *PIM1* mRNA (Hoover 1997; Richter 2005). In addition, the *PIM1* 3' UTR also binds to eIF4E specifically, and induces nuclear export of the *PIM1* transcript which enhances translation activity (Culjkovic 2006). Notably, in absence of eIF4E, this process did not occur, further suggesting that Pim kinase translation is cap-dependent (Hoover 1997).

Pim kinase in B-cell development and hematological malignancies

Pim kinases are known to be involved in production, proliferation, and survival of normal blood cells. For instance, in hematological system, Pim-1 and Pim-2 proteins expression can be induced by multiple cytokines, mitogens and growth factors, suggesting their role in mediating signal transduction pathways (Dautry 1988; Mikkers 2004). During fetal hematopoiesis, Pim-1 is expressed at high levels in liver and spleen, whereas in adults, it is only detected in circulating granulocytes (Amson 1989).

However, Pim kinases are dispensable in nature, as Pim-1/-2/-3 triple knockout mouse remain viable and fertile (Mikkers 2004). However, these animals were smaller in size at birth and throughout their life span (Mikkers 2004). Meanwhile, they show deficiency in hematological system such as anemia, erythrocyte microcytosis, reduced peripheral T- and B-cell numbers, and

4

impaired responses of hematopoietic cell population to a distinct range of growth factors such as IL-2, IL-3 and IL-7 (Mikkers 2004; An 2013), which are all evidence for the importance of Pim kinases' physiological function during normal hematological development.

In contrast to normal hematopoiesis, Pim kinases are overexpressed in hematological malignancies and become oncogenic in nature as demonstrated by several reports. First, Pim kinases gene expression is regulated by signal transduction pathways initiated by growth factors and cytokines as mentioned above, most of which transduce their primary signal through Janus kinase/ signal transducer and activator of transcription (JAK/STAT) pathway, which are also oncogenic in nature (Mikkers 2004). Pim kinase is regulated by this pathway and also feeds back into it, and promotes G1-to-S cell cycle transition and prevent cell death (Shirogane 1999; Peltola 2004). Second, Pim kinases synergize with c-Myc, an important oncogenic transcription regulator that is also overexpressed in hematological malignancies and together they enhance transcription processes (Zippo 2007). Third, Pim kinases directly phosphorylate translation regulator eukaryotic translation initiation factor 4E-binding protein 1 (4E-BP1) that enhances translation (Fox 2003; Chen 2005; Tamburini 2009). Fourth, Pim kinases, especially Pim-1 and Pim-2, are known to regulate a variety of phosphorylation targets in cell death, cell cycle, and inflammation pathways, along with other transcription and translation regulators in both hematological and solid tumors (Brault L. 2010; Chen 2010). All of the above evidence suggests that Pim kinases have multitude of functions in tumor development and progression.

II.   B-cell lymphoma disease characteristics

<u>B-cell lymphoma overview</u>

Hematological malignancies are composed of lymphoma, leukemia, myeloma and myelodysplastic syndromes (MDS). Lymphoma, categorized into Hodgkin's and non-Hodgkin's subtypes, is the most common form of these hematological malignancies in the Western world

(National Cancer Institute, http://www.cancer.gov/researchandfunding/snapshots/lymphoma).
Incidence and mortality rate of non-Hodgkin's lymphoma (NHL) are much higher than that of
Hodgkin's lymphoma, while those of B-cell origin take up the vast majority (95%) of NHL cases
whereas the rest are of T-cell origin (Leukemia and Lymphoma Society, Facts and Statistics
http://www.lls.org/content/nationalcontent/resourcecenter/freeeducationmaterials/lymphoma/pdf/nhl.
pdf). There are 15 subtypes of B-cell lymphoma under the current lymphoma classification, and
about 60% of them are aggressive NHL while others are indolent (Leukemia and Lymphoma
Society).

B-cell lymphoma is classified based on the point during which their B-cell differentiation
process is disrupted (Kuppers 1999; Kuppers 2005). In classic NHL, such process is marked by the
specific structure of B-cell receptor (BCR), the key component that determines the faith of B-cells.
Properly developed BCR will guide cells towards normal differentiation or apoptosis that yields
healthy B-cells, whereas abnormally developed BCR leads to uncontrolled proliferation due to
termination of differentiation which causes B-cell lymphoma development (Greaves 1986; Kuppers
2005). BCR is composed of two identical copies of heavy and light-chain immunoglobulin (Ig). Only
B-cell precursors that successfully rearrange Ig heavy- and light-chain to make functional BCR will
differentiate into mature naïve B-cells, followed by antigen activation during immune responses
(Kuppers 1999). These antigen-activated B-cells undergo "clonal expansion" in the germinal center
(GC) of lymph nodes, where they proliferate, differentiate and mutate B-cell antibodies by further
modifying their Ig gens by somatic hypermutation or class switch –both are complicated processes to
introduce numerous mutations in Ig genes (Kuppers 2005).

Evidently, most types of B-cell lymphoma derive from GC or post-GC B-cells (Stevenson
2001). The BCR-guided lymphomagenesis is concluded by a hallmark feature known as "reciprocal
chromosomal translocation" between one of the Ig loci and a proto-oncogene, placing the proto-
oncogene in control of an active Ig locus promoter region, which leads to deregulated and

constitutive expression of this proto-oncogene and turn it into an oncogene (Kuppers 2001). *BCL2-IgH* translocation associated with follicular lymphoma and *CCDN1-IgVH* translocation featured in mantle cell lymphoma (MCL) are classic examples of this phenomenon.

Mantle cell lymphoma and its molecular pathogenesis

MCL is a form of aggressive B-cell lymphoma that it is very difficult to treat. It constitutes about 6% of all NHL cases with highest incidence in elderly Caucasian males. Patients typically present disseminated disease upon diagnosis, with leukemic phase in 20-30% of the cases (Perez-Galan 2011). Although standard frontline chemotherapies are not curative for MCL, they do contribute to high remission rates in previously untreated patients. Unfortunately, relapse is common within a few years; median survival is 5-7 years (Herrmann 2009). Tumor proliferation is a stronge indicator of survival in the clinic (Rosenwald 2003).

MCL has a genetic hallmark of translocation between 11q13 and 14q23, or t(11;14) (q13;q23), a molecular mechanism under overexpression of cyclin D1 in MCL cells. In cases where cyclin D1 is not overexpressed, cyclin D2 or D3 instead is detected at high levels (Rosenwald 2003). Notably, merely t(11;14) and cyclin D1 overexpression may not be sufficient for full transformation of the tumor cells and their aggressive phenotypes (Hinds 1994). A transgenic mice studies where *CCDN1* gene was linked to an immunoglobulin enhancer suggested that cyclin D1 overexpression alone did not lead to lymphomagenesis, but rather, spontaneous development of lymphoma required corporation with other oncogenes like *MYC* (Bodrug 1994; Lovec 1994).

As with other hematological malignancies, MCL also express a distinct set of CD surface markers, CD20+ (high levels), CD5+, CD23+/– (mostly negative, but up to 25% of cases are positive) and CD11c– (Klapper 2011). Newly identified transcription factor Sry-related high-mobility-group box 11 (SOX11) has been described as a diagnostic marker which is equally expressed in both cyclin D1-positive and -negative MCL cases (Ek 2008; Mozos 2009).

The labile and oncogenic cyclin D1 protein forms a complex with other cyclin-dependent kinases (CDK) 4 or 6 to enhance cell cycle entry. Consistently, both CDK4 and 6 are commonly expressed at high levels in MCL. Aside from cyclin D and CDK family proteins, multiple genetic lesions are also detected in MCL, such as Myc, MDM2 oncogene overexpression, and loss of tumor suppressor genes retinoblastoma protein (RB1), p53 and ataxia telangiectasia mutated (ATM) (Perez-Galan 2011). Important cancer-promoting signaling pathways, such as phosphatidylinositide 3-kinases (PI3K)/ protein kinase B (Akt), nuclear factor kappa-light-chain-enhancer of activated B cells (NF-κB) and JAK/STAT pathways are all upregulated, leading towards accumulation of genetic instability, increased transcription, translation and proliferation with less differentiation, all build on the augmentation of oncogenicity in MCL (Perez-Galan 2011).

<u>Pim kinases overexpression and lymphomagenesis in B-cell lymphoma</u>

PIM1 and *PIM2* mRNA are overexpressed at various incidences in B-cell hematological malignancies such as CLL, MCL, diffused large B-cell lymphoma (DLBCL), and follicular lymphoma (FL) (Gomez-Abad 2011). Such dysregulated *PIM* gene expression is not known to be caused by gene rearrangement or amplification (Sivertsen 2006), but rather through transcriptional regulation, such as JAK/STAT (Shirogane 1999) and NF-κB (Hammerman 2004), as well as aberrant somatic hypermutation (SHM) observed in NHL such as DLBCL and FL (Pasqualucci 2001; Halldorsdottir 2008). In addition, NHL-specific SHM in *PIM1* is often accompanies by SHM of other oncogenes such as *MYC*, which further promotes the *PIM*'s transformation power (Rossi 2006).

Notably, Pim kinases are constitutively active due to lack of regulatory domains (Fox 2003; Qian 2005). Post-translational regulations are mediated by heat shock proteins (HSP) 70/90, and also ubiquitylation processes, which dictates the degradation of these proteins (Shay K.P. 2005). In hematological malignancies, Pim kinases exert their lymphomagenesis capacity through

phosphorylating downstream targets in transcription and translation regulation, anti-apoptosis enhancement as well as cell cycle control processes (Figure 2) (Chen 2010).

III. Pim kinases substrates and functions

Pim kinases and transcription regulation

Myc heterodimerizes with Myc-associated factor X (Max) at E-box sequences, which forms a transcription activator complex that is speculated to regulate around 11% of human genes (Fernandez 2003). Under growth factor stimulation, Pim kinases bind with Myc/Max dimer complex as part of the transcription machinery (Zhang 2008). Pim-1 is also known to phosphorylate c-Myc (Ser62), whereas Pim-2 phosphorylates c-Myc (Ser329), both of which contribute to the Pim/Myc synergy to stabilize c-Myc protein and to enhance its transcriptional activity. Consistently, knocking down of either Pim-1 or Pim-2 dramatically decrease the endogenous level of c-Myc and also its oncogenecity (Zhang 2008). It was also demonstrated in human endothelial/epithelial cells that Myc helps to recruit Pim-1 to E-box and allows it to phosphorylate Histone H3 (Ser10) to enhance c-Myc oncogenecity through upregulated transcription (Zippo 2007).

In addition, Pim kinases are also known to phosphorylate and activate other transcription factors such as Myb, runt-related transcription factors 1 and 3 (RUNX1/3) and signaling transducer and suppressor of cytokine signaling 1 and 3 (SOCS1/3), etc. (Chen X.P. 2002; Winn 2003; Wang 2012).

Pim kinases and translation regulation

In translation regulation, Pim-1 and Pim-2 are known to phosphorylate 4E-BP1 (Thr37/46), the priming site of this translation inhibitor (Fox 2003). Once 4E-BP1 is primed, it triggers a hierarchical hyper-phosphorylation of this protein, causing it to dissociate with translation initiator

9

Figure 2. Pim kinase downstream phosphorylation substrates and Pim kinase-regulating pathways.

Pim kinases regulate multiple substrates four of the major pathways including transcription, translation, cell survival and cell cycle regulation.

This figure is adapted and altered from Chen L.S. *et al, Biochem Pharmacol.* 2010; 80,1936-45, after permission granted by *Biochemical Pharmacology* journal to use in dissertation.

Figure 2.
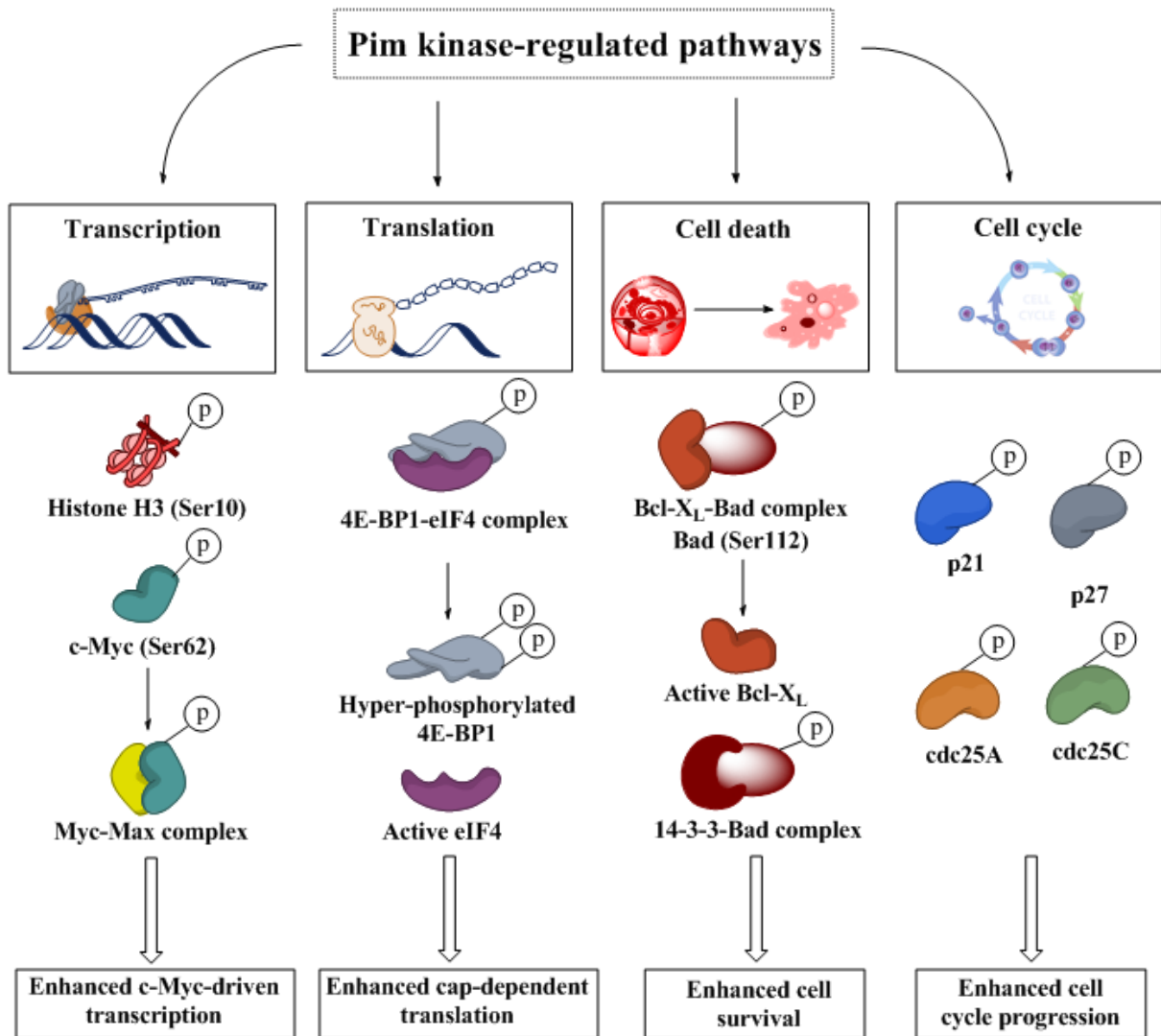
Adapted from Chen L.S. *et al, Biochem Pharmacol.* 2010; 80, 1936-45, with permission

eIF4E to activate cap-dependent translation process, which generates many early-response oncogenes including Pim kinases themselves (Gingras 2001; Trivigno 2013).

In addition, Pim-2 is known to phosphorylate 4E-BP1 (Ser65) through an unknown mechanism (Tamburini 2009). Pim-2 affects cap-dependent translation independently and in parallel of the PI3K/Akt/mTOR pathway (Fox 2003; Amaravadi R. 2005; Hammerman 2005). Interestingly, *PIM2* expression was associated with elevated eIF4E expression (both phospho- and total protein levels) compared to cells with constitutively active Akt (Hammerman 2005).

Pim kinases and cell survival regulation

In cell survival, Pim-1 and Pim-2 phosphorylate proapoptotic Bcl-2–associeated death promoter (Bad) at Ser112, 136 and 155, where Ser112 is the dominate site (Macdonald 2006). Inversely, Pim-3 mostly phosphorylates Ser136 and 155 sites instead of Ser112 (Macdonald 2006). These phosphorylation events lead to disruption of Bad binding with antiapoptotic Bcl-X_L, an anti-apoptotic member of the Bcl-2 family. This event sequesters proapoptotic function of Bad as the phosphorylated protein is now bound with scaffold protein 14-3-3, and also tips the balance in favor of cell survival by adding more players to the anti-apoptotic reservoir (Yan 2003; Macdonald 2006). Notably, phosphatase 2 (PP2A) is known to dephosphorylate Bad at Ser112 to reverse the above phenomenon (Chiang 2003). Pim-1 is also known to bind PP2A, which leads to destruction of Pim-1 through ubiquitylation degradation (Losman 2003).

In addition, Pim kinase may also contribute to cell survival through intervening with cellular metabolism machinery such as enhancing glycolysis by phosphorylating Bad at Ser155 (Danial 2003). Additionally, *PIM2* gene expression in growth factor-regulated cell line was able to increase glycolytic rate and induce cell survival associated with Bad phosphorylation (Fox 2003).

Pim kinases and cell cycle regulation

12

In addition, Pim kinases play an important role in upregulating cell cycle process. Cell cycle proteins cyclin-dependent kinase inhibitor 1 (p21), cyclin-dependent kinase inhibitor 1B (p27), as well as cdc25A/C are all known Pim kinase targets (Mochizuki 1999; Wang 2002; Morishita 2008).

Pim-1 phosphorylates cdc25A to enhances its effect in G1/S cell cycle entry; meanwhile, Pim-1 inactivates p21 through phosphorylation which also contribute to G1/S progression (Swords 2011). Pim kinases directly phosphorylate p27 to repress its activity as a tumor suppressor and G1/S modulator (Morishita 2008). In addition, Pim-1 phosphorylates G2/M cell cycle regulator cdc25C and pushes cells to enter mitosis (Bachmann 2006). Interestingly, it was also reported that Pim-2 induces proteasome-mediated degradation of cdc25A which leads to phosphorylation of CDK2 to trigger G1 cell cycle arrest (Levy 2012). Therefore, Pim kinases regulate cell cycle processes through promoting cell cycling, hereby enhancing tumor proliferation (Merkel 2012).

IV. Pim kinase inhibitor

It has been confirmed that Pim kinases gene and proteins are overexpressed in hematological malignancies and solid tumors, and their increased expression levels are indicative of poor prognosis in the clinic (Gomez-Abad 2011; Nawijn 2011). Their multitude of substrates and functions render them important oncogenes in these B-cell malignancies, and important drivers of lymphomagenesis (Chen 2010; Nawijn 2011). Importantly, Pim kinases are dispensable, confirmed by viable and fertile Pim triple knockout mice, making them druggable targets (Mikkers 2004).

Pim kinase small molecular inhibitor–SGI-1776

Pim kinase x-ray crystallography studies discovered a unique "fold-hinge-fold" structure of Pim kinases that provided the foundation of highly specific Pim kinase inhibitor development. In this region, a proline residue was found at position 123, followed by an additional amino acid, creating an unusual hydrophobic pocket for ATP binding –a site for highly selective structure-based drug design (Cheney 2007; Swords 2011). Large databases of virtual compounds were used for the high-

throughput screening, as well as predictive pharmaceutical properties calculations were performed to find "hits" as potential Pim kinase inhibitors (Chen 2009). Additional criteria such as solubility, permeability, molecular weight, drug-like properties etc. were used to narrow down the long list of potential hits, and imidazo[1,2-*b*]pyridazines structure was a final candidate, which was then used as the basics for developing SGI-1776 compound (Figure 3) (SuperGen,, now Astex Pharmaceuticals).

SGI-1776 was screened against a wide range of kinases using radiolabeled biochemical assays, and it showed high specificity towards Pim-1, and Pim-3, as well as Fms-like tyrosine kinase 3 (FLT-3) and transforming tyrosine kinase protein (TrkA), both are cell membrane-bound kinase receptors (Chen 2009). The half-maximal inhibitory concentration (IC50) of SGI-1776 is 7 nM, 363 nM, and 69 nM for Pim-1, -2 and -3, respectively, indicating the compound is less specific for Pim-2 compared to the other Pim kinases (Chen 2009).

Other Pim kinase inhibitors

Currently, several groups from both academia and industry are developing Pim kinase inhibitors, such as pan Pim kinase inhibitors SMI-4a (University of South Carolina) and AZD-1208 (AstraZeneca plc), and GNE-652(Genentech, Inc.) and more (Beharry 2011; Keeton 2011; Munugalavadla 2011; Blanco-Aparicio 2012; Keeton 2012). These inhibitors are either in pre-clinical trial (GNE-652) or clinical trial (AZD-1208), among them, AZD-1208 has shown favorable safety and patient tolerability in refractory AML patients.

V. Bendamustine

Bendamustine is an FDA-approved second-line chemotherapeutic agent for treating B-cell lymphoma and CLL (National Cancer Institute). Bendamustine hydrochloride (TRENDA®, Cephalon, Inc.) is the intravenously-administered drug that is used to treat indolent B-cell lymphoma that has progressed during the six months of rituximab or rituximab-containing regimens (National Cancer Institute).

Figure 3.
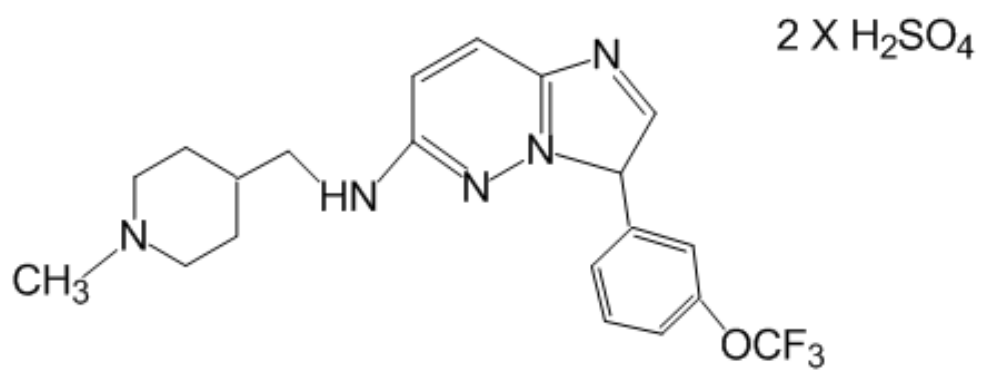
Figure 3. Chemical structure of Pim kinase inhibitor, SGI-1776.

Bendamustine is not a novel anticancer drug per se, as it was first synthesized in the 1960s and was quite extensively in Europe during the following decades, but in the US, it was not wildly used as much and was not approved by the FDA until 2008 (Gandhi 2009).

Bendamustine is an alkylating agent with the active component of nitrogen mustard (Figure 4) (Leoni 2008). Bendamustine is known to induce intra- and inter-strand DNA crosslinks, leading to initiation to DNA repair response, which is a slower process compared to other alkylating agents (Gandhi 2009; Leoni 2011). These types of DNA damage causes impaired DNA replication, and also disrupts transcription process in both replicating and quiescent cells, making it a drug-of-choice for indolent diseases (Leoni 2008; Gandhi 2009). Bendamustine presents a unique mechanism of action in cell killing, as it activate p53-dependent DNA damage stress response, producing higher levels of p21 and Phorbol-12-myristate-13-acetate-induced protein 1 (NOXA) compare to other alkylating agents (Leoni 2011).

In addition, release of apoptosis-inducing factor (AIF) from mitochondria following bendamustine treatment was also observed, and that oxidative stress is an important mediator of caspase-independent cell killing in CLL and MCL (Roue 2008). Importantly, bendamustine does not show cross-resistance with other alkylating agents, and shows synergism with nucleoside analogs (Roue 2008; Gandhi 2009).

Figure 4.
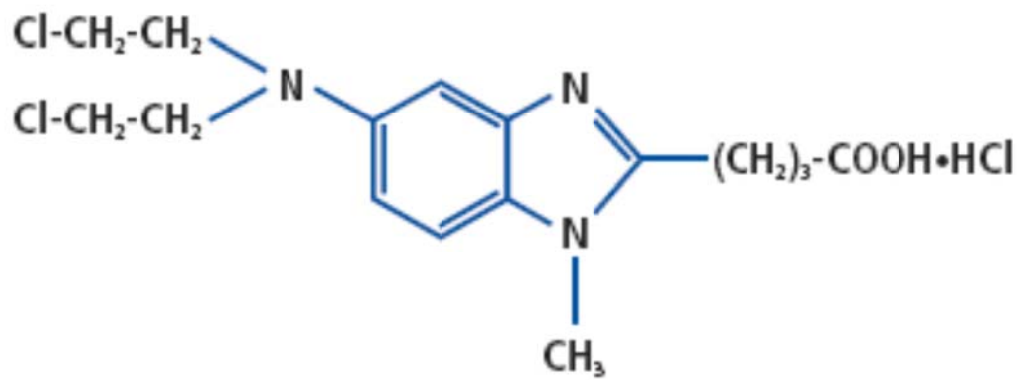
Figure 4. Chemical structure of alkylating agent, bendamustine hydrochloride.

Figure obtained from FDA website,
http://www.accessdata.fda.gov/drugsatfda_docs/label/2008/022303lbl.pdf.

CHAPTER 2: Material and methods

Cell lines

MCL cell lines JeKo-1, Mino, Granta 519 and SP-53 were obtained from Dr. Hesham Amin at MD Anderson Cancer Center. JeKo-1, Mino, and SP-53 were maintained in RPMI-1640 medium (Corning Cellgro for JeKo-1 and SP-53, American Type Culture Collection for Mino) supplemented with 10% fetal bovine serum (FBS; Invitrogen) for JeKo-1 or 20% FBS for Mino and SP-53 cells. Granta 519 was maintained in Dulbecco modified Eagle medium with high glucose (DMEM, Corning Cellgro) with 20% FBS. Characterization of these cell lines showed high levels of cyclin D1, c-Myc, and B-cell lymphoma 2 (Bcl-2) family members such as induced myeloid leukemia cell differentiation protein (Mcl-1), Bcl-2 and B-cell lymphoma-extra large (Bcl-X$_L$) (Amin 2003). These cell lines were authenticated using an AmpF/STR Identification Kit (Applied Biosystems) and routinely tested for *Mycoplasma* contamination using a MycoTect kit (Invitrogen). Experiments were conducted in cells with less than 20 passages, and maintained at logarithmic growth concentration between 10^5 cells/mL and 10^6 cells/mL determined by a Coulter channelyzer (Beckman Culter, Inc.) with less than 10% endogenous cell death confirmed by flow cytometry.

Primary cells from MCL and other B-cell lymphoma patients

Samples were obtained from lymphoma tissue bank at MD Anderson Cancer Center or healthy donors after informed consents through institutional review board–approved protocols that were in agreement with the Declaration of Helsinki. Peripheral blood mononuclear cells (PBMCs) were isolated from fresh aphesis or whole blood samples using the standard Ficoll-Hypaque (Invitrogen) density gradient centrifugation. A Coulter chanelyzer was used to determine cell count and size for each experiment. Primary cells were cultured in RPMI-1640 medium with 10% FBS, at densities between 10^7 cells/mL and 10^8 cells/mL during experiments. Endogenous cell death levels

were determined before each experiment using flow cytometry, and only samples with less than 40%

inherent cell death were used for experiments.

Drugs

SGI-1776 was provided by SuperGen (now Astex Pharmaceuticals, Inc.). Bendamustine

hydrochloride was originally obtained from Cephalon (now Teva Pharmaceuticals Industries, Ltd.)

and later purchased from Selleckchem, USA. SGI-1776 was shipped in powder form and they were

stored in a desiccator at room temperature. Powders were dissolved in dimethyl sulfoxide (DMSO)

immediately before use and stored at -20°C. Bendamustine hydrochloride was dissolved in DMSO

and stock solutions were made and stored in -80°C.

In our investigations, micromolar concentrations of SGI-1776 and bendamustine were used,

and for both drugs, the highest concentration was 10μM. These concentrations were chosen based on

previous publications. For SGI-1776, high percentage (>85%) of the drug bound to human plasma

proteins and FBS in the cell media, that micromolar concentrations of SGI-1776 are needed to reach

nanomolar concentrations of free drug (Chen 2009).

Apoptosis assays

Cells were treated with DMSO alone or drugs, then cells (10^6 cells per experiment) were

washed with PBS and then incubated with annexin V (BD Pharmingen) followed by propidium

iodine (PI) in annexin binding buffer. After 15min of incubation, annexin V/PI positivity for cell

death was measured using FACSCalibur flow cytometer (BD Biosciences).

Cell cycle assays

DMSO or drug-treated cells (>10^6 cells per experiment) were washed with PBS, and then

cells were fixed overnight at 4°C using 70% ethanol. Cells were then removed from ethanol by

centrifugation and washed twice with PBS, followed by 15min co-incubation with 25μg/mL PI and

2.5µg/mL DNAse-free RNAse (Roche Diagnostics) at room temperature. PI positivity was then

measured by flow cytometry for cell cycle profiling.

Immunostaining of γ-H2AX

Post-treatment MCL cell lines (10^6 or more cells) were washed twice with PBS, and then

fixed with ice-cold 70% ethanol overnight at 4°C. Ethanol was removed by centrifugation and then

cells were washed once with PBS and twice with PBS with 1% bovine serum albumin (BSA) to

avoid cell loss. After washing, cells were incubated with primary phospho-Histone 2AX (Ser139) or

γ-H2AX antibody (EMD Millipore) for 2hr at room temperature with gentle shaking, and then were

washed three times with PBS with 1% BSA plus 0.1% NP-40 (Sigma-Aldrich Corp). Cells were then

incubated with Alexa Fluor mouse IgG secondary antibody (488 goat, Invitrogen Corp) for 1hr at

room temperature protected from light, followed by three washes with PBS with 1% BSA and 0.1%

NP-40. Finally, cells were co-incubated with 10µg/mL PI and 2.5µg/mL DNAse-free RNAse for

30min at room temperature, and then they were analyzed by flow cytometry. The cells showed

upward shift of florescent signals compared to baseline were marked as percent positive for DNA

damage.

Immunohistochemistry

Formalin-fixed, paraffin-embedded MCL tissue sections were used for immunohistochemical

analysis. Heat-induced antigen retrieval (Dako target retrieval pH6) was used following a manual

procedure. Pim-1, Pim-2 and Pim-3 antibodies (all rabbit; Abcam plc) were used to stain the tissue

for Pim kinase protein expression. Detection of Pim kinase expression was performed with

biotinylated secondary antibody, horseradish peroxidase, and 3,3′-diaminobenzidine as a chromogen

(Abcam), then tissue slides were counterstained with hematoxylin. Meanwhile, appropriate negative

and positive control slides were run in parallel. Photographs of the results were taken using an

Olympus U-TV0 camera (Olympus Corporation) mounted on an Olympus BX41 microscope.

Hematoxylin staining image was obtained at 100× magnification (objective Plan N 10×) while Pim kinases staining images were obtained at 400× magnification (objective Plan N 40×). Images were processed using CellSens software (Olympus).

Macromolecule synthesis assays

MCL cell lines or B-cell lymphoma primary samples were incubated with [methyl-^{3}H]-thymidine, [5,6-^{3}H]-uridine or [4,5-^{3}H]-L-leucine (1.0mCi/mL stock; Moravek Biochemicals) for 30-45min of each experiment. Cells from cell lines (10^6) or primary samples (10^7) were seeded in each well of a 12-welled plate, respectively, and each treatment was done in triplicate. Various concentrations of radioactive nucleosides were used in cell lines (0.8mCi/mL) and in primary samples (4mCi/mL). The incorporated radioactivity was used to measure DNA, RNA and protein synthesis, using a Packard Tri-Carb liquid scintillation analyzer (GMI, Inc) as previously described (Balakrishnan 2005).

Gene expression assays

Total RNA from MCL cell lines and B-cell lymphoma primary cells was extracted using the RNAeasy mini kit manually or QIAcube automated system (Qiagen N.V.). NanoDrop ND 1000 spectrophotometer (Thermo Fisher Scinetific) was used to quantify RNA. RNA extract was diluted to a desirable concentration (30-50ng/mL for target genes, and 5ng/mL for *18S* control), and then mixed with a 1-step TaqMan reverse transcription polymerase chain reaction (RT-PCR) master mix (Applied Biosystems). Gene expression levels were measured with an ABI prism 7900 sequence detection system (Applied Biosystems). Primers and probes for *PIM1* (Hs01065498_m1), *PIM2* (Hs00179139_m1), *PIM3* (Hs00420511_g1), *MCL1* (Hs00172036_m1), *MYC* (Hs00153408_m1), *CCDN1* (Hs00765553_m1), and *18S* (4333760) (Applied Biosystems) were used to detect expression levels of the corresponding genes. Each experiment was performed in triplicate and relative gene expression levels were normalized to *18S*, an endogenous control.

Protein expression assays with immunoblots

Control and drug-treated MCL cell lines and B-cell lymphoma primary cells were lysed using radioimmunoprecipitation assay buffer (RIPA; Upstate Biotechnology) and sonication, and then protein concentration was measured using Bio-Rad DC protein assay (Bio-Rad Laboratories). Total protein lysates (30-50μg) were loaded into 10%, 12% or 4-12% bis-tris polyacrylamide gels (Bio-Rad Laboratories) and transferred to nitrocellulose membranes (GE Osmonics Labstore), then probed with targeted primary antibodies at 4°C overnight (Table 1). Membranes were then washed and incubated with infrared-labeled secondary antibodies for 1hr at room temperature, and then the protein bands were visualized using an Odyssey infrared imager (LI-COR Biosciences).

siRNA transfection

PIM1, PIM2 genes were knocked down individually or in combination by corresponding human siRNAs for *PIM1* (S10527) and *PIM2* (S21749) (Ambion/Invitrogen). Negative control siRNA #1 (AM4611; Ambion/Invitrogen) was also used for each set of experiments. siRNA transfection was performed using Amaxa Nuceofector I device (Lonza Group) with Amaxa cell line nucleofector kit V (Lonza Group) for electroporation. After transfection, cells were placed back to 37°C incubator for 24hr, and then they were harvested and tested for viability and. For each experiment, 150μM of siRNA (both negative control and treatment) was used to knockdown each gene and 150μM of siGLO red transfection indicator (Dharmacon Inc) was used to detect transfection efficiency. Cell type-specific protocols were optimized for transfection efficiency (>60%) and cell viability (>30%).

Table 1.

	Primary Antibodies	Companies		Primary Antibodies	Companies
1	Phospho-Bad (Ser112)	Cell Signaling Technology, Beverly, MA	10	GAPDH	Cell Signaling Technology, Beverly, MA
2	Total Bad	Cell Signaling Technology, Beverly, MA	11	Phospho-H2AX (Ser139)	EMD Millipore, Billerica, MA
3	Bcl-2	Dako, Carpinteria, CA	12	Phospho-Histone H3 (Ser10)	EMD Millipore, Billerica, MA
4	Bcl-X$_L$	BD Transduction Laboratories, Lexington, KY	13	Total Histone H3	Cell Signaling Technology, Beverly, MA
5	Phospho-c-Myc (Ser62)	Abcam, Cambridge, MA	14	Mcl-1	Santa Cruz Biotechnology, Santa Cruz, CA
6	Total c-Myc (clone C33)	Santa Cruz Biotechnology, Santa Cruz, CA	15	PARP	BD Biosciences, Franklin Lakes, NJ
7	Cyclin D1	Santa Cruz Biotechnology, Santa Cruz, CA	16	Cleaved PARP (Asp214)	Cell Signaling Technology, Beverly, MA
8	Phospho-Cdc25C (Ser216)	Cell Signaling Technology, Beverly, MA	17	Pim-1 (clone 12H8)	Santa Cruz Biotechnology, Santa Cruz, CA
	Cdc25C	Upstate/Millipore, Billeria, MA	18	Pim-2	Sigmal-Aldrich, St. Louis, MO
8	Phospho-4E-BP1 (Thr37/46)	Cell Signaling Technology, Beverly, MA	19	Pim-3	Abgent, San Diego, CA
9	Total 4E-BP1	Santa Cruz Biotechnology, Santa Cruz, CA	20	XIAP	BD Biosciences, Franklin Lakes, NJ

Table 1. Primary antibodies used in immunoblot analyses and their sources.

Data analyses

All plots were prepared and analyzed using GraphPad Prism software version 5 (GraphPad Software, Inc). All cell line data were performed in triplicates and were presented as mean value ± standard error of the mean (SEM). DMSO was used as vehicle control for all drug treatments. For single drug treatment experiments, most data were analyzed by the Student paired, 2-tailed t-test. For combination drug treatments, fractional analysis was used to determine if the combination methods lead to less than, equal to or more than additive effect on induction of apoptosis, or similarly on increase of γ-H2AX phosphorylation, or thymidine, uridine and leucine incorporation inhibition. Phosphorylated and total protein expression levels detected by immunoblots were quantified using Odyssey software for the Odyssey Infrered Imaging System (LI-COR Biosciences), and then normalized to DMSO control using GraphPad Prism software. For immunoblot analyses, a ratio of phosphorylated protein to total protein level was calculated for the phosphorylated proteins, whereas a ratio of protein to GAPDH level was carried out for total protein only targets.

CHAPTER 3. SGI-1776 single agent therapy in MCL

It has been demonstrated that Pim kinases are overexpressed in MCL and that Pim kinases are involved with regulation of transcription, translation, cell death and cell cycle regulation (Figure 2). Importantly, Pim-1 overexpression is negatively related to MCL patient outcome during therapy (Hsi 2008). In addition, Pim kinases are proven to be druggable targets as mice lacking all three Pim kinases were viable and fertile (Mikkers 2004; Swords 2011). Based on this background we aim to evaluate the potential utility of SGI-1776 in MCL and that inhibition of phosphorylation of downstream substrates will disrupt transcriptional, translational, and cell cycle processes and while promoting cell death.

To test these hypotheses, we propose the following two aims:

Aim 1) Analyze the biological consequences of SGI-1776 in MCL cells.

Aim 2) Identify the biological function of Pim kinases in their signaling pathways and primary biomarkers impacted by SGI-1776 in MCL cells.

Aim 1. Analyze the biological consequences of SGI-1776 in MCL cells.

Aim 1.1. Expression of Pim kinases in MCL cell lines and primary tissue samples.

Expression of Pim kinases in MCL cell lines.

Immunoblots of untreated or DMSO-treated JeKo-1 and Mino cells were performed to determine the expression levels of Pim-1, -2 and -3 (Figure 5). At least 10^6 log-phased cells of both cell lines were harvested to extract protein lysates, and GAPDH control was used for each Pim kinase detected. For both Pim-1 and Pim-2, multiple bands were detected and for Pim-3, one band was detected. These results are consistent with reports of alternative translation start sites of Pim-1 and Pim-2 (Nawijn 2011).

Figure 5.

Cell lines
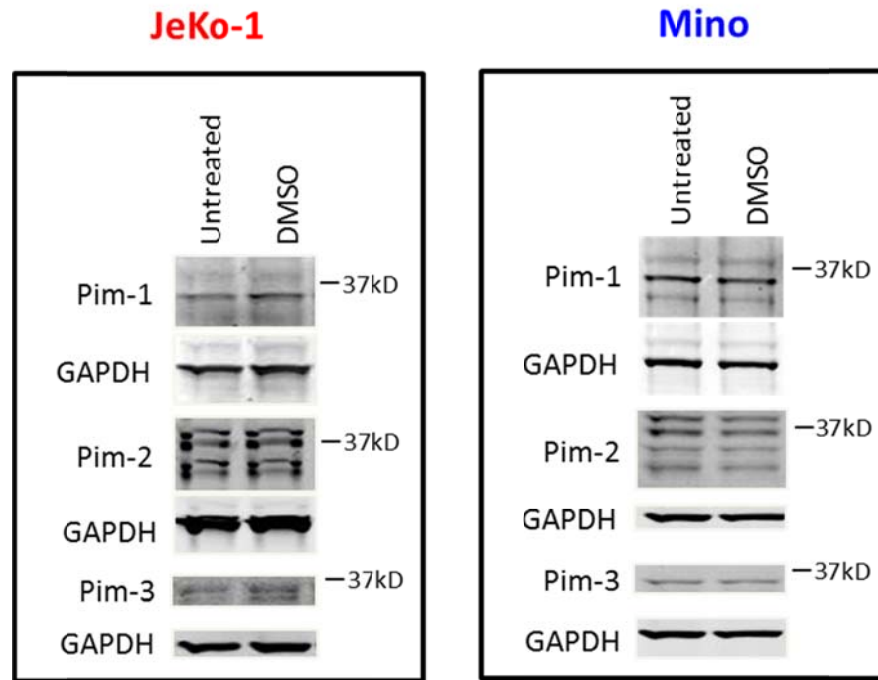
Figure 5. Expression of all three Pim kinases in JeKo-1 and Mino cell lines.

JeKo-1 and Mino cells were either untreated or treated with DMSO, and then protein lysates were analyzed by immunoblot analysis with antibodies against Pim-1, -2 and -3 to detect expression of Pim-1, Pim-2, and Pim-3 kinases.

Expression of Pim kinases in MCL primary tissue samples.

A series of MCL patient paraffin-embedded tissue sections were obtained for immunohistochemical analysis to detect Pim kinase expression (Figure 6). These tissues were stained with Pim kinase antibodies and both negative and positive controls are used in parallel. Reactivity for all three Pim kinases was detected in 92% of the cases, with variable intensities for different Pim kinases (Table 2). Data showed that Pim-1 and Pim-2 expressed stronger intensity than Pim-3; meanwhile, Pim-1 was mostly nuclear and cytoplasmic, whereas Pim-2 was mostly cytoplasmic and Pim-3 was mostly nuclear (Table 2).

In addition, it was noticeable that in our Pim kinases expression study using paraffin-embedded MCL lymph node tissue samples, we detected a higher-than-usual incidence of Pim kinase expression compared to the literature (Hogan 2008; Gomez-Abad 2011).

Aim 1.2. Detection of SGI-1776 induced dose- and time-dependent apoptosis in MCL cell lines.

Induction of dose-dependent apoptosis by SGI-1776 in MCL cell lines.

Effect of SGI-1776 in apoptosis was evaluated using MCL cell lines JeKo-1, Mino, Granta 519 and SP-53. All four cell lines were either untreated, or treated with DMSO or increasing concentrations of SGI-1776 (0.1, 1, 3, 5 10μM) for 24hr.

Following treatment, MCL cells were harvested and were washed with PBS and then stained with Annexin V/PI, and levels of apoptosis were measured by flow cytometry. Dose-dependent induction of apoptosis in JeKo-1 (Figure 7), Mino (Figure 8), Granta 519 (Figure 9) and SP-53 (Figure 10) are indicated by the increasing number of cells in the lower and upper right quadrants paired with decreasing number of cells in the lower left quadrants. Percentages of apoptotic cells resulting from each drug concentration in each of the four cell lines indicated a dose-dependent increase of apoptosis levels (Figure 11A).

Figure 6.

MCL primary tissue samples
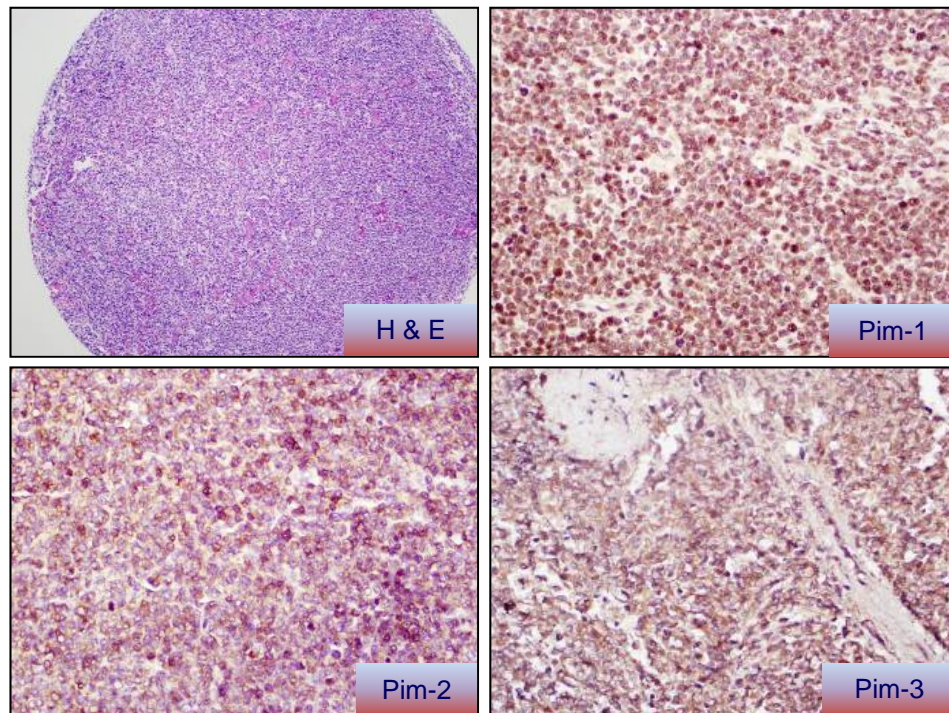
Figure 6. Expression of three Pim kinases in MCL primary tissue samples.

Histologic sections of paraffin-embedded MCL tissue sample were immunohistochemically stained with Hematoxylin and eosin, and were then stained with anti-Pim-1, -2, and -3 antibodies and counterstained with hematoxylin. The tissue sample slides were visualized using an Olympus U-TV0 camera.

Table 2.

MCL samples, Number positive for kinase/number analyzed	
Pim-1	11/12
Pim-2	11/12
Pim-3	11/12

Table 2. Incidence of Pim kinases expressions in immunohistochemically stained MCL primary tissue samples.

Data presented as number positive for kinase/total number analyzed.

Reactivity:

PIM1: Faint to moderate staining; mostly *nuclear and cytoplasmic*

PIM2: Strong; mostly *cytoplasmic*

PIM3: Very faint staining, mostly *nuclear*

Figure 7. Increase of apoptosis by SGI-1776 treatment in JeKo-1 cells measured by Annexin V/PI assay.

JeKo-1 cells were either untreated, or treated with DMSO, or different doses of SGI-1776 (0.1, 1, 3, 5 or 10μM) for 24hr. Cells were harvested and then stained with Annexin V for 15mins followed by 5mins of PI. Levels of apoptosis for each treatment was detected using flow cytometry, where apoptotic cells were indicated by the cell population present in lower right, upper left, as well as upper right quadrants. Experiments were performed in triplicate and the panel graphs shown are representative of cell death at different concentrations of SGI-1776.

Figure 7.
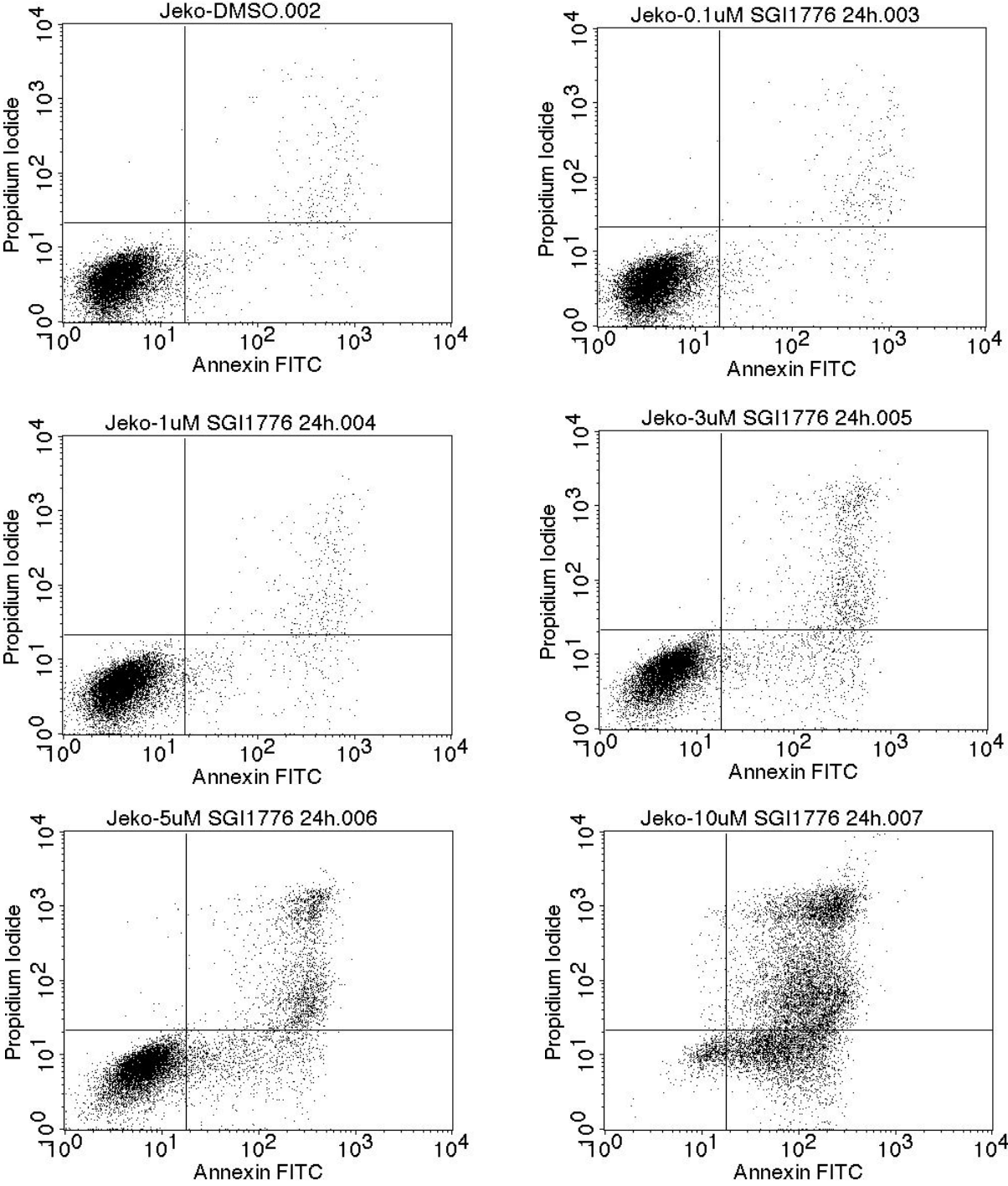
Figure 8. Increase of apoptosis by SGI-1776 treatment in Mino cells measured by Annexin

V/PI assay.

Mino cells were either untreated, or treated with DMSO, or different doses of SGI-1776 (0.1, 1, 3, 5 or 10μM) for 24hr. Cells were harvested and then stained with Annexin V for 15mins followed by 5mins of PI. Levels of apoptosis for each treatment was detected using flow cytometry, where apoptotic cells were indicated by the cell population present in lower right, upper left, as well as upper right quadrants. Experiments were performed in triplicate and the panel graphs shown are representative of cell death at different concentrations of SGI-1776.

Figure 8.
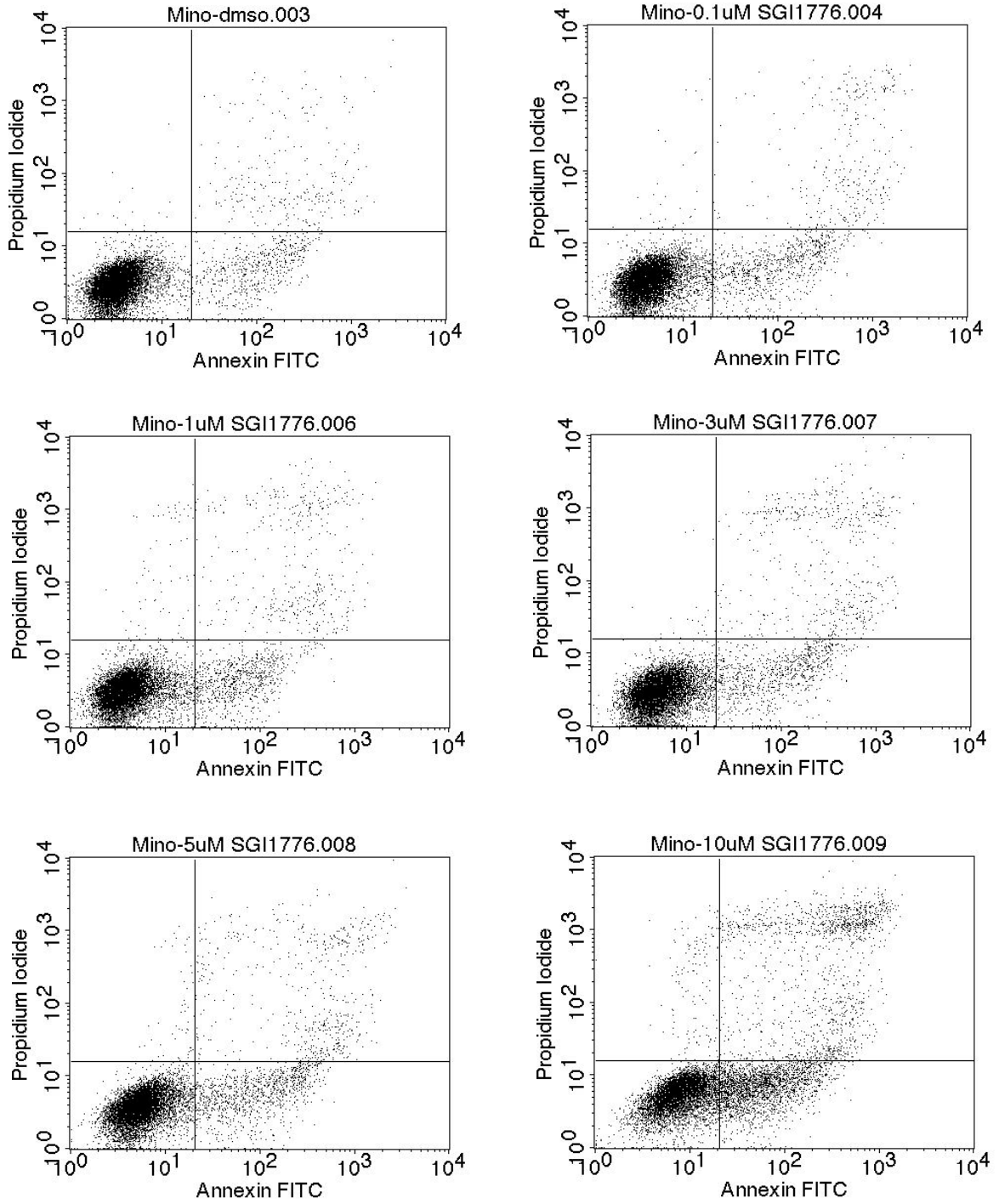
Figure 9. Increase of apoptosis by SGI-1776 treatment in Granta-519 cells measured by

Annexin V/PI assay.

Granta-519 cells were either untreated, or treated with DMSO, or different doses of SGI-1776 (0.1, 1, 3, 5 or 10µM) for 24hr. Cells were harvested and then stained with Annexin V for 15mins followed by 5mins of PI. Levels of apoptosis for each treatment was detected using flow cytometry, where apoptotic cells were indicated by the cell population present in lower right, upper left, as well as upper right quadrants. Experiments were performed in triplicate and the panel graphs shown are representative of cell death at different concentrations of SGI-1776.

Figure 9.
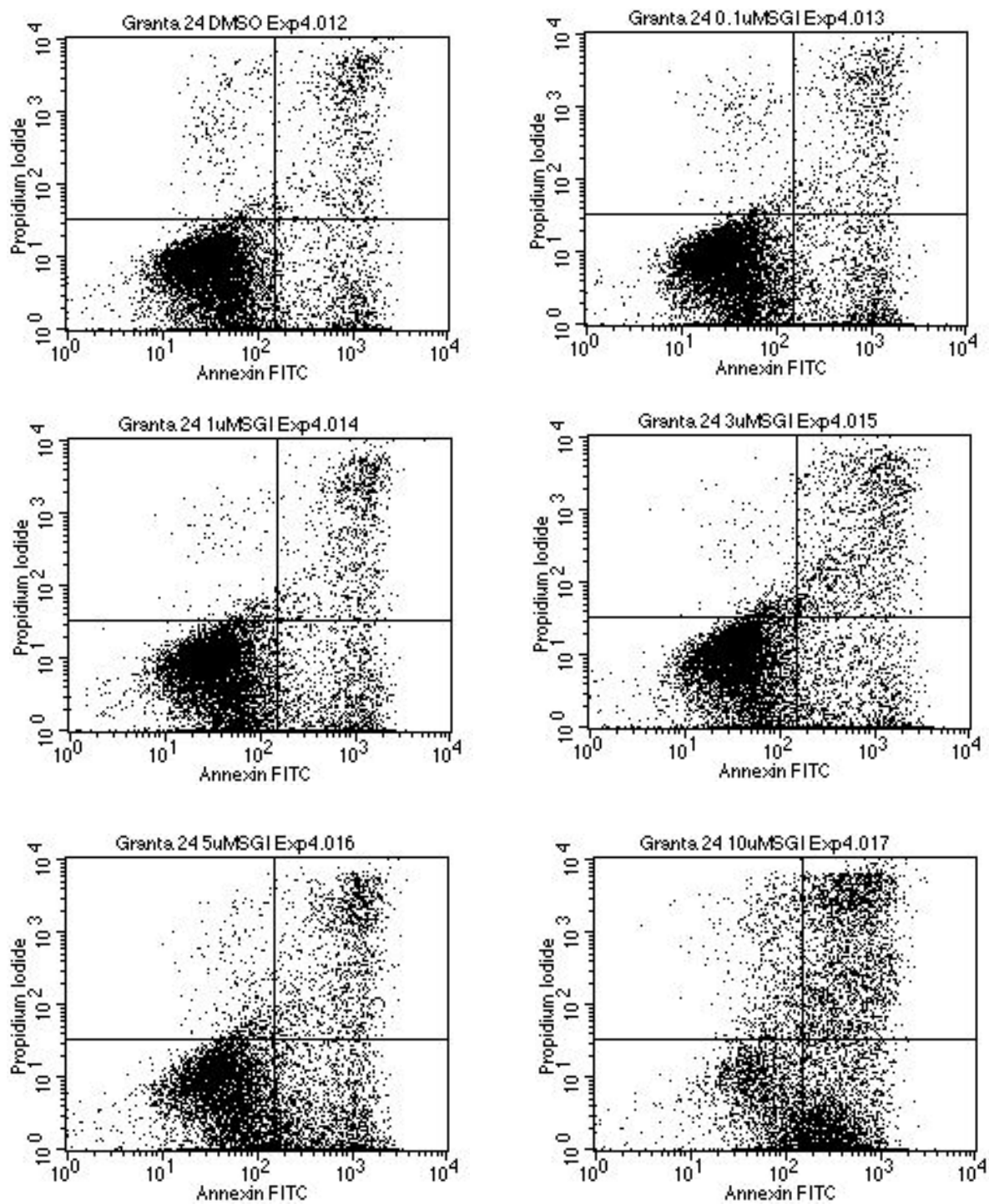
Figure 10. Increase of apoptosis by SGI-1776 treatment in SP-53 cells measured by Annexin V/PI assay.

SP-53 cells were either untreated, or treated with DMSO, or different doses of SGI-1776 (0.1, 1, 3, 5 or 10μM) for 24hr. Cells were harvested and then stained with Annexin V for 15mins followed by 5mins of PI. Levels of apoptosis for each treatment was detected using flow cytometry, where apoptotic cells were indicated by the cell population present in lower right, upper left, as well as upper right quadrants. Experiments were performed in triplicate and the panel graphs shown are representative of cell death at different concentrations of SGI-1776.

Figure 10.
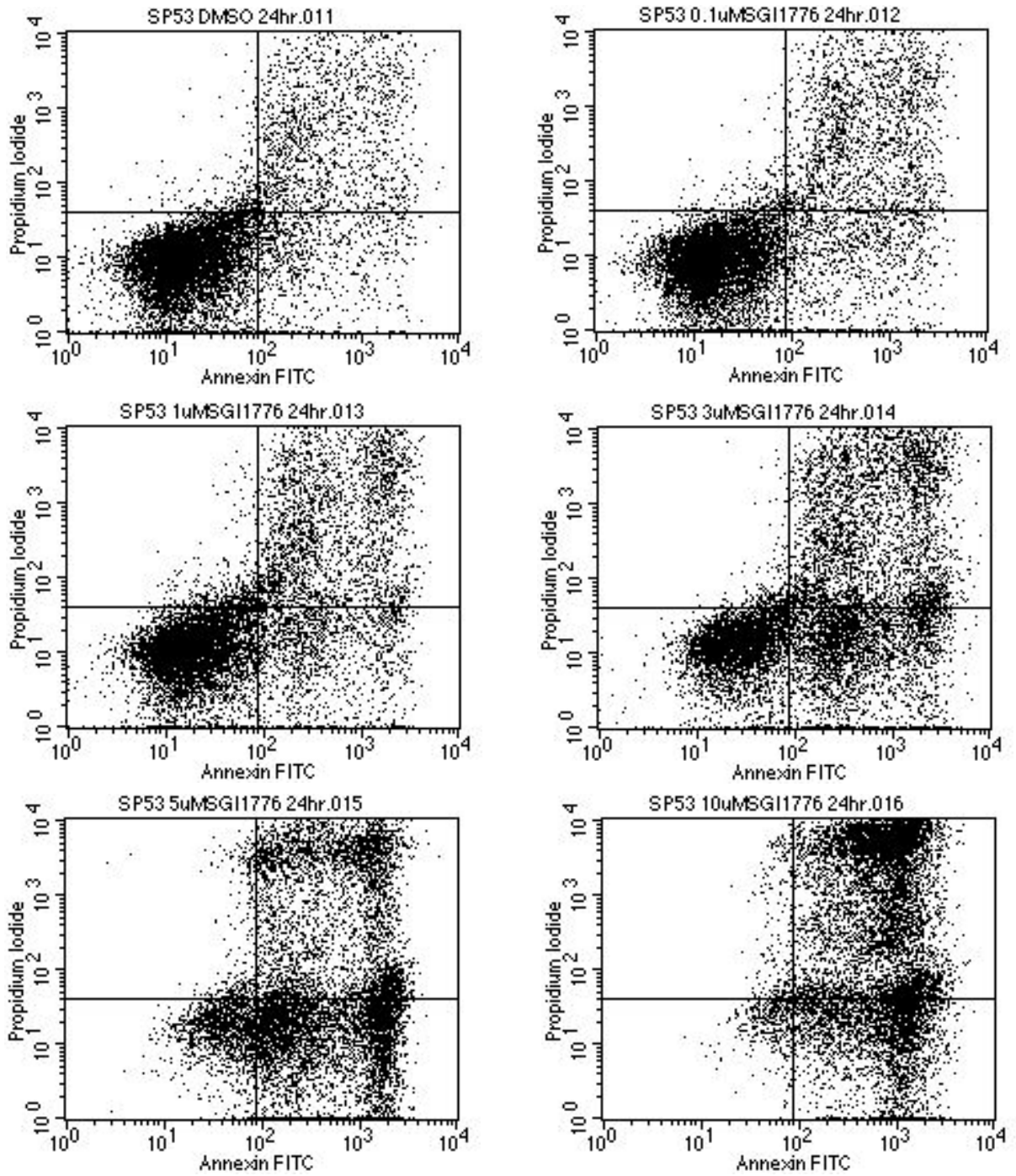
Figure 11. Induction of dose-dependent apoptosis by SGI-1776 in MCL cell lines.

(A) Dose-dependent annexin-V/PI positivity induced by SGI-1776 in MCL cell lines. Four MCL cell lines (JeKo-1, Mino, Granta 519 and SP-53) were treated with DMSO alone or with a range of doses (0.1, 1, 3, 5 or 10μM) of SGI-1776 for 24hr, and then stained with annexin-V/PI. Apoptosis level, indicated by annexin-V/PI positivity was determined by flow cytometry. (B) Apoptosis level in JeKo-1 and Mino was confirmed by the presence and intensity of cleaved PARP on an immunoblot assay. SGI-1776 was used to treat JeKo-1 and Mino for 24hr in the concentrations mentioned above, the protein lysates extracted were used for immunoblot analysis. Experiments were performed in triplicate and results shown are average cell death ± SEM.

Figure 11.

A
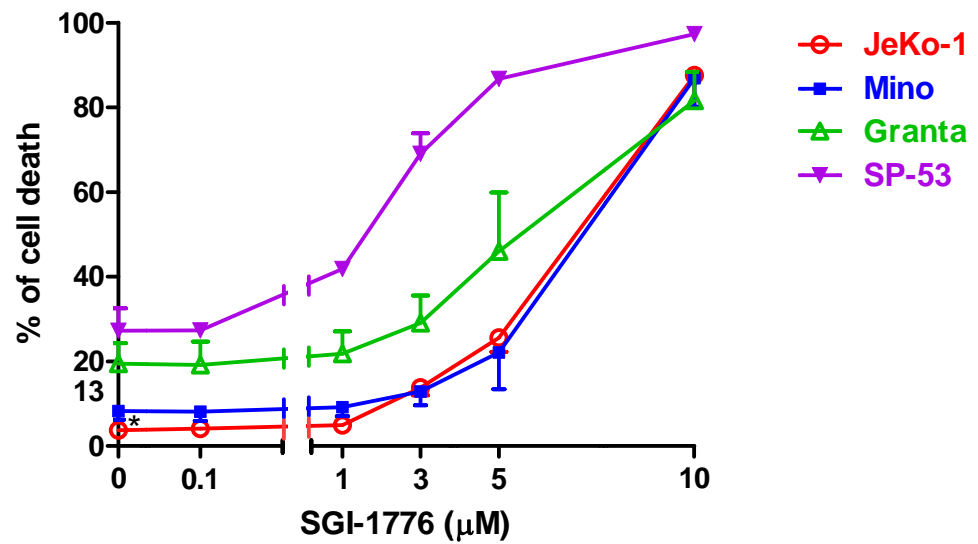
B
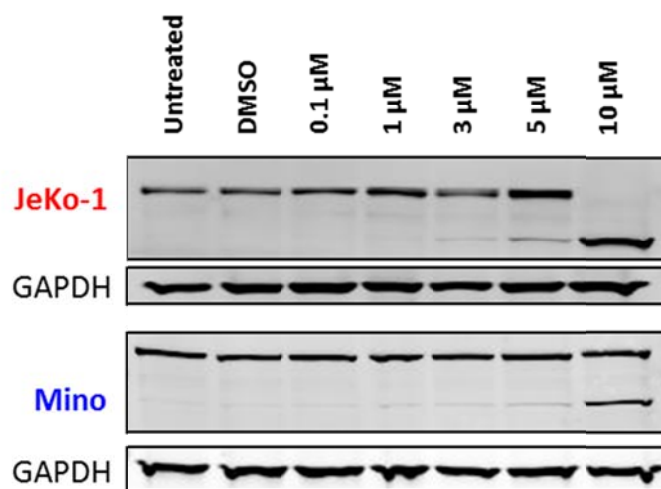
Treatment with 0.1μM SGI-1776 for 24hr resulted in low levels of apoptosis, whereas an average of 1%-15% Annexin V/PI positivity was detected at 1μM, 5%-40% at 3μM, 15%-60% at 5μM and 60%-80% at 10μM of SGI-1776 treatments.

Induction of apoptosis was also confirmed by immunoblot analysis of PAPR cleavage following dose-dependent SGI-1776 treatments in JeKo-1 and Mino (Figure 11B). In both cell lines, cleaved PARP was detected with 5μM and with greater intensity with10μM SGI-1776 treatments.

Induction of time-dependent apoptosis by SGI-1776 in MCL cell lines.

JeKo-1 and Mino cell lines were treated with 10μM of SGI-1776 for various times then cell death levels were measured using flow cytometry (Figure 12A). Average apoptosis levels in JeKo-1 were 5%, 17%, 33%, 50% and 89% for 2, 4, 8, 16, and 24hr of SGI-1776 treatment, respectively; whereas in Mino, 2%, 3%, 5%, 10% and 38% of apoptosis were measured.

To confirm the occurrence of apoptosis induction, PARP cleavage was measured using immunoblots and in both cell lines, visible cleaved PARP band was detected as early as 4hr of SGI-1776 treatment (Figure 12B).

Aim 2. Identify the biological function of Pim kinases in their signaling pathways and primary biomarkers impacted by SGI-1776 in MCL cells.

Aim 2.1. Effect of SGI-1776 on Pim kinase phosphorylation targets in MCL cell lines.

In order to confirm whether SGI-1776 act on Pim kinases and inhibit their kinase function, and also to identify the specific pathways inhibited by this drug, we investigated the effect of SGI-1776 on known Pim kinase phosphorylation targets –c-Myc, Histone H3, 4E-BP1 and Bad, and analyzed the changes of their phosphorylation levels. MCL cell lines JeKo-1 and Mino were treated with SGI-1776 in dose-dependent fashion, and immunoblot analyses were performed to detect both phospho- and total protein expression levels.

Figure 12. Induction of time-dependent apoptosis by SGI-1776 in MCL cell lines.

(A) Time-dependent annexin-V/PI positivity induced by SGI-1776 in MCL cell lines. JeKo-1 and Mino cells were treated with DMSO alone or with 10μM SGI-1776 for different time points (0.5, 1, 2, 4, 8, 16, or 24hr), stained with annexin-V/PI, and then apoptosis levels were measured by flow cytometry. (B) Apoptosis levels in JeKo-1 and Mino was confirmed by immunoblot analysis of cleaved PARP. Both MCL cell lines were treated with 10μM SGI-1776 for times indicated above, and protein lysates extracted from cells were used for immunoblot analysis. Experiments were performed in triplicate and results shown are average cell death ± SEM.

Figure 12.

A

B
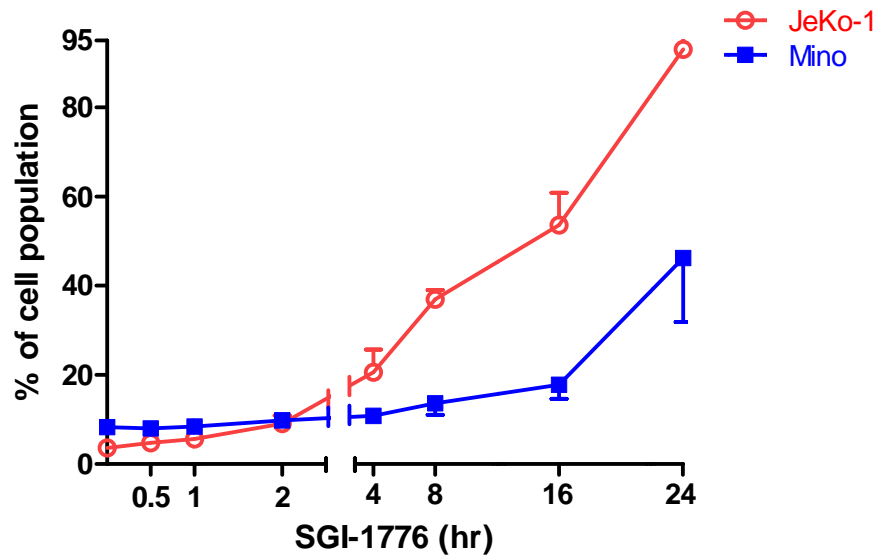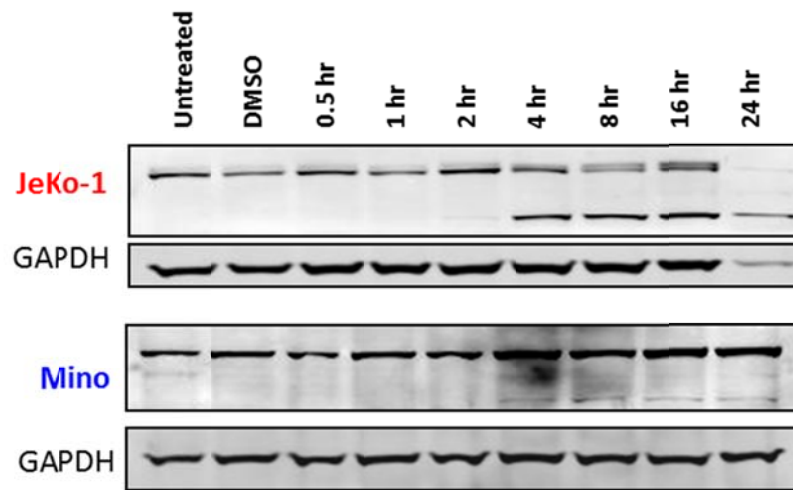
Effect of SGI-1776 on Pim kinase target and transcription regulator c-Myc in MCL cell lines.

JeKo-1 and Mino cells were either untreated, or treated with DMSO, or with various doses of SGI-1776 (0.1, 1, 3, 5, 10μM) for 24hr, then $2x10^6$ cells were harvested and total protein lysates were extracted for immunoblot analysis. In cell lines, c-Myc (Ser62) and total c-Myc levels were detected, and each protein band was quantitated (Figure 13A). GAPDH was measured as loading control and the levels were relatively even except for JeKo-1 with 10μM SGI-1776 treatment, where extensive apoptosis was observed (Figures 13, 14).

Ratios of c-Myc (Ser62) to total c-Myc levels were calculated and results were normalized to DMSO control (Figure 13B). A dose-dependent decrease of phospho- to total c-Myc ratio was observed in both cell lines, whereas JeKo-1 demonstrated greater decrease compared to Mino.

Effect of SGI-1776 on Pim kinase target and transcription regulator Histone H3 in MCL cell lines.

JeKo-1 and Mino cells were untreated, or treated with DMSO or SGI-1776 in above concentrations for 24hr, and then cells were harvested and total protein lysates were extracted for immunoblot analysis. Histone H3 (Ser10) and total Histone H3 proteins were detected and quantitated (Figure 14A). Normalized ratios of Histone H3 (Ser10) to total Histone H3 levels indicated a dose-dependent decrease only occurred in JeKo-1 but not in Mino (Figure 14B).

Effect of SGI-1776 on Pim kinase target and translation regulator 4E-BP1 in MCL cell lines.

Untreated, or DMSO-treated, along with dose-dependent SGI-1776-treated JeKo-1 and Mino cells were harvested after 24hr, and then total protein lysates were extracted for 4E-BP1 immunoblot analysis. 4E-BP1 (Thr37/46) and total 4E-BP1 proteins were both detected and quantitated (Figure 15A). Normalized ratios of 4E-BP1 (Thr37/46) to total 4E-BP1 levels indicated a dose-dependent decrease in both JeKo-1 and Mino cell lines (Figure 15B).

Figure 13. Effect of SGI-1776 on Pim kinase target, c-Myc, in MCL cell lines.

JeKo-1 and Mino cells were untreated or treated with DMSO alone or with different doses of SGI-1776 (0.1, 1, 4, 5, 10µM) for 24hr. (A) Protein lysates were analyzed using immunoblot to detect the expression levels of c-Myc (Ser62) and total c-Myc. (B) Quantitation of immunoblots for each cell line was performed by measuring ratios of phospho-c-Myc to total c-Myc for each SGI-1776 treatment, and then ratios from each treatment were normalized to the result of DMSO-treated cells. Experiments were performed in triplicate and results were shown as average ratios ± SEM.

Figure 13.

A

B

45
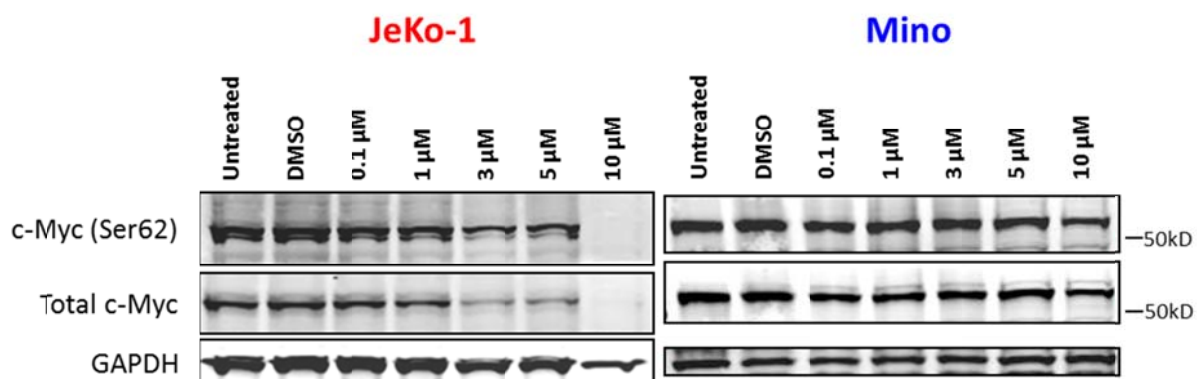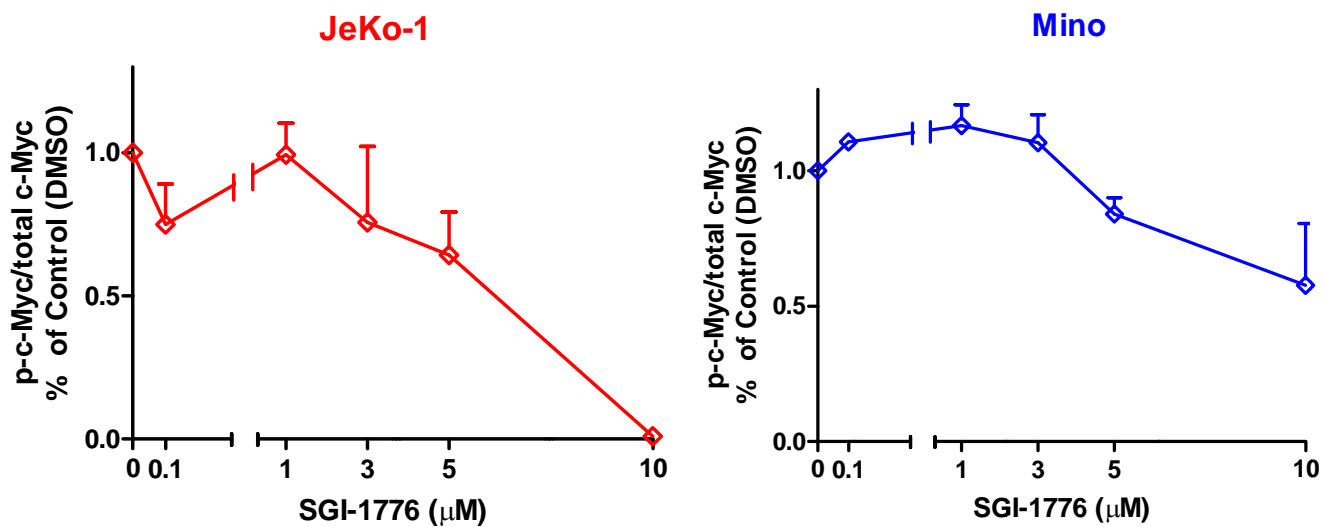
Figure 14. Effect of SGI-1776 on Pim kinase target, Histone H3, in MCL cell lines.

JeKo-1 and Mino cells were untreated or treated with DMSO alone or with different doses of SGI-1776 (0.1, 1, 4, 5, 10μM) for 24hr. (A) Protein lysates were analyzed using immunoblot to detect the expression levels of Histone H3 (Ser10) and total Histone H3. (B) Quantitation of immunoblots for each cell line was performed by measuring ratios of phospho-Histone H3 to total Histone H3 for each SGI-1776 treatment, and then ratios from each treatment were normalized to the result of DMSO-treated cells. Experiments were performed in triplicate and results were shown as average ratios ± SEM.

Figure 14.

A
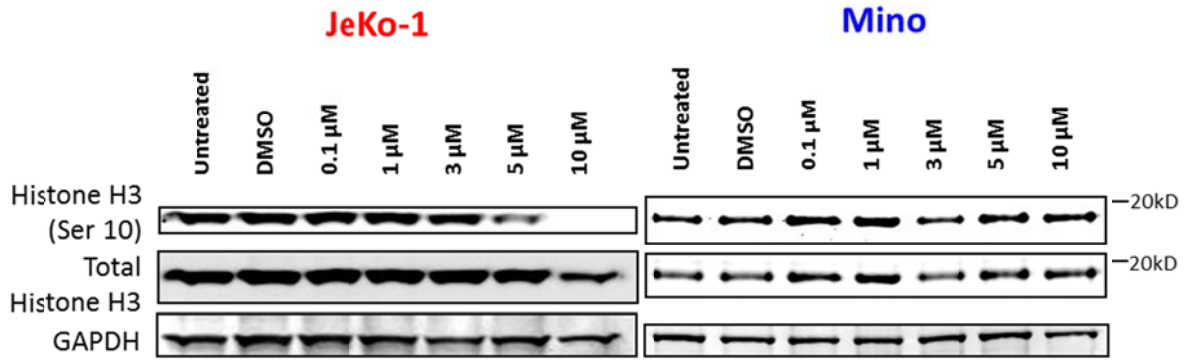
B
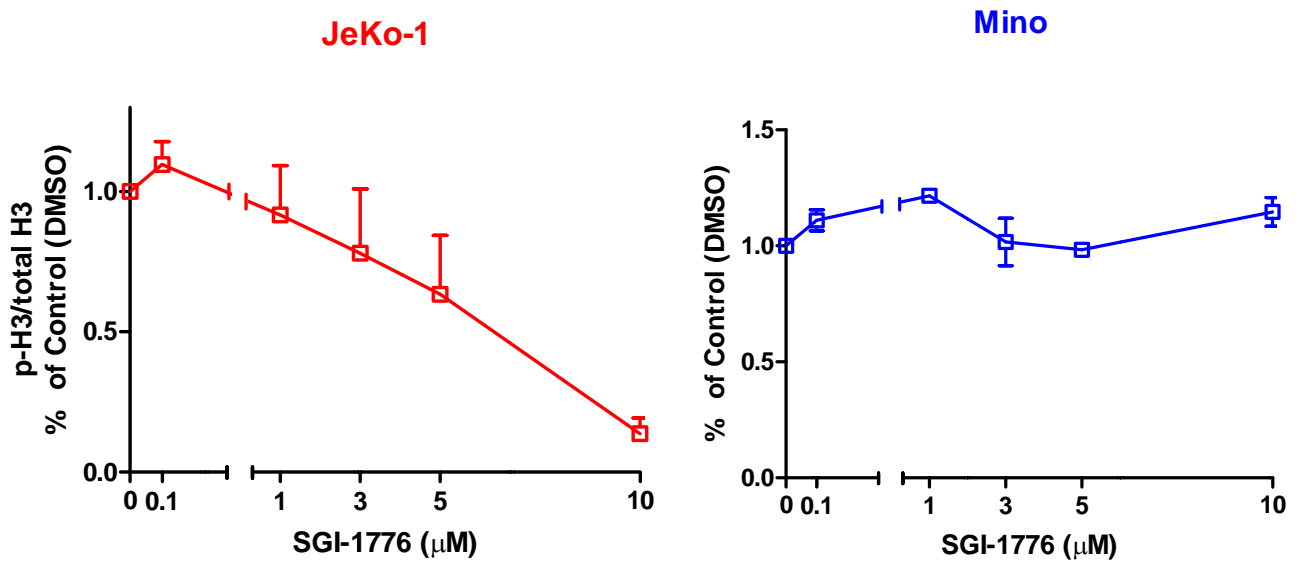
Figure 15. Effect of SGI-1776 on Pim kinase target, 4E-BP1, in MCL cell lines.

JeKo-1 and Mino cells were untreated or treated with DMSO alone or with different doses of SGI-1776 (0.1, 1, 4, 5, 10µM) for 24hr. (A) Protein lysates were analyzed using immunoblot to detect the expression levels of 4E-BP1 (Thr37/46) and total 4E-BP1. (B) Quantitation of immunoblots for each cell line was performed by measuring ratios of phospho-4E-BP1 to total 4E-BP1 for each SGI-1776 treatment, and then ratios from each treatment were normalized to the result of DMSO-treated cells. Experiments were performed in triplicate and results were shown as average ratios ± SEM.

Figure 15.

A

B
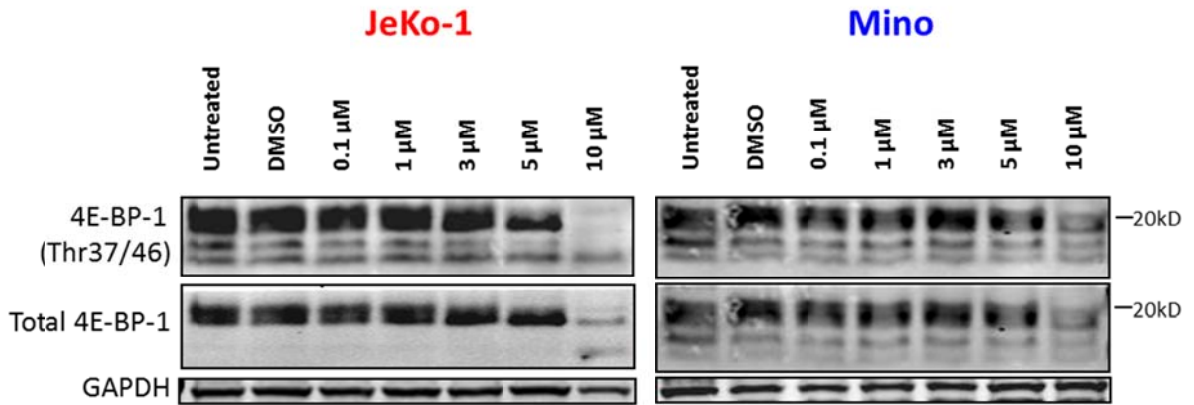
<u>Effect of SGI-1776 on Pim kinase target and cell survival regulator Bad in MCL cell lines.</u>

JeKo-1 and Mino cells were untreated or treated with DMSO or SGI-1776 in varies concentrations mentioned above, or remain untreated for 24hr, cells were then harvested and total protein lysates were extracted for immunoblot analysis of Bad protein (Figure 16A). Bad (Ser112) and total Bad proteins levels indicated a dose-dependent decrease in JeKo-1 but not in Mino (Figure 16B).

<u>Aim 2.2. Effect of SGI-1776 on RNA synthesis and of *MCL1* gene expression levels in MCL cell lines.</u>

c-Myc phosphorylation was decreased in both JeKo-1 and Mino cell lines, which suggest a possible role in repressing c-Myc-driven transcription process in MCL cells by SGI-1776. Based on this evidence, we hypothesized that RNA synthesis along with short-lived mRNAs expression levels would also be affected.

<u>Effect of SGI-1776 on global RNA synthesis in MCL cell lines.</u>

MCL cell lines JeKo-1, Mino, Granta 519 and SP-53 were treated with DMSO or increasing concentrations of SGI-1776 (0.1, 1, 3, 5, 10μM) for 24hr, while JeKo-1 and Mino cells were treated with DMSO or 10μM of SGI-1776 for various time points (0.5, 1, 2, 4, 8 16, 24hr). In the last 30min prior to harvesting, radioactively-labeled uridine was added for incorporation into the newly synthesized RNA. The incorporated radioactivity was measured using scintillation counter, and results were measured as DPM/cell normalized to DMSO control (Figure 17).

In the dose-dependent experiments with various concentrations of SGI-1776 over a 24hr period, a steady decrease of RNA synthesis levels compared to DMSO control was detected in all three cell lines except for Mino. In Mino cells, the RNA synthesis level increased under low doses (0.1 and 1μM) of SGI-1776 treatment and then started to decrease at higher doses, and eventually

Figure 16. Effect of SGI-1776 on Pim kinase target, Bad, in MCL cell lines.

JeKo-1 and Mino cells were untreated or treated with DMSO alone or with different doses of SGI-1776 (0.1, 1, 4, 5, 10µM) for 24hr. (A) Protein lysates were analyzed using immunoblot to detect the expression levels of Bad (Ser112) and total Bad. (B) Quantitation of immunoblots for each cell line was performed by measuring ratios of phospho-Bad to total Bad for each SGI-1776 treatment, and then ratios from each treatment were normalized to the result of DMSO-treated cells. Experiments were performed in triplicate and results were shown as average ratios ± SEM.

Figure 16.

A
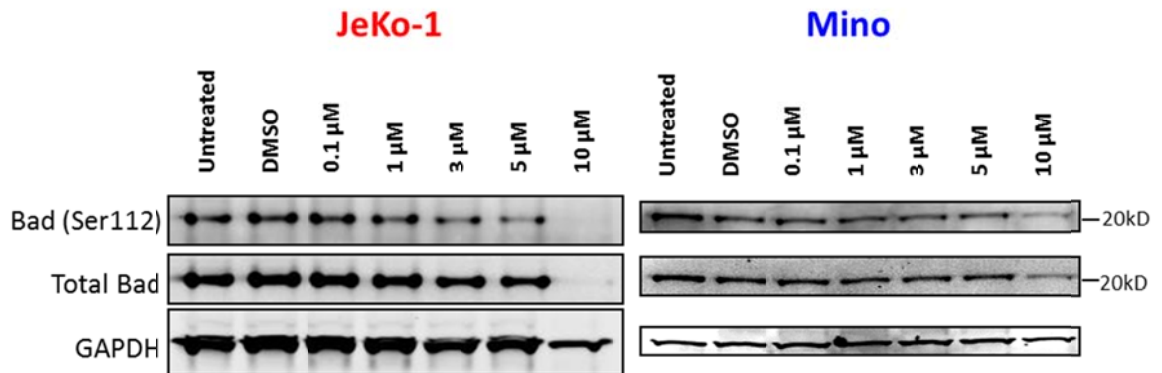
B

Figure 17. Inhibition of global RNA synthesis by SGI-1776 in MCL cell lines.

(A)MCL cell lines JeKo-1, Mino, Granta 519 and SP-53 cells were treated with DMSO or with different doses of SGI-1776 (0.1, 1, 4, 5, 10µM) for 24hr. (B)JeKo-1 and Mino cells were treated with DMSO or 10µM of SGI-1776 for different time periods (0.5, 1, 2, 4, 8, 16, 24hr). For both sets of experiments, MCL cells were co-incubated with [5,6-^{3}H]-uridine for 30min before harvesting, then radioactivity incorporated into the cells were measured using scintillation counter. DPM/cell was calculated and normalized to DMSO-treated cells. Experiments were done in triplicates and results were shown as average percentages ± SEM.

Figure 17.

A

B

went down to 40% of DMSO control at 10μM (Figure 17A). Very similar decrease patterns were detected in JeKo-1 and Granta 519 cells, with slow decrease at lower doses of SGI-1776 (less than 3μM), and faster decrease at higher doses, showing 60%-75%, 45%-57% and 22%-28% of DMSO control at 3, 5 and 10μM of SGI-1776, respectively. Meanwhile, in SP-53, the highest sensitivity that dramatic decrease (>20%) was observed at 0.1μM of SGI-1776 and then leveled with other cell lines, showing about 28% of DMSO control by 10μM of SGI-1776.

In the time-dependent experiments with various times with 10μM of SGI-1776 over a 24hr period, there was a significant decrease of RNA synthesis in both JeKo-1 and Mino cells at short time points, reaching almost 50% of DMSO by 1hr (Figure 17B). However, RNA synthesis in both cell lines recovered to 60%-75% of control by the 2nd hour, and slowly decreased after that. By 24hr, both went down to 40% of DMSO control.

Effect of SGI-1776 on *MCL1* gene expression levels in MCL cell lines.

To test the effect of SGI-1776 in short-lived mRNAs expression levels, we carried out experiments to analyze the change of *MCL1* level, an short-lived oncogene known to be overexpressed and play a role in anti-apoptosis in MCL cell lines (Amin 2003; Khoury 2003).

JeKo-1 and Mino cells were treated with DMSO or dose- or time-dependent SGI-1776 for 24hr, using the concentrations and time points mentioned above (Figure 18A, B). Upon treatments of SGI-1776, cells were harvested and total RNA was extracted for RT-PCR experiment. SGI-1776 treatment resulted in both dose- and time-dependent decrease of *MCL1* mRNA levels in JeKo-1 and Mino cells, with more prominent results shown in JeKo-1.

In the dose-dependent experiments with various concentrations of SGI-1776 over a 24hr period, *MCL1* mRNA level in JeKo-1 cells decreased by 35% and 38% compared to DMSO control at 3 and 5μM of SGI-1776 treatment, respectively.

Figure 18. Reduction of *MCL1* mRNA expression levels by SGI-1776 treatment in MCL cell lines.

(A)MCL cell lines JeKo-1, Mino cells were treated with DMSO or with increasing doses of SGI-1776 (0.1, 1, 4, 5, 10μM) for 24hr. (B)JeKo-1 and Mino cells were treated with DMSO or 10μM of SGI-1776 for different time periods (0.5, 1, 2, 4, 8, 16, 24hr). Total RNA was extracted and quantified. Isolated RNA was analyzed by real-time RT-PCR with primers and probes for *MCL1* mRNA. Each *MCL1* gene expression level measured was normalized to *18s* endogenous control and each set of experiment was normalized to DMSO experiment control. All experiments were done in triplicate results were shown as average ratios ± SEM.

Figure 18.

A
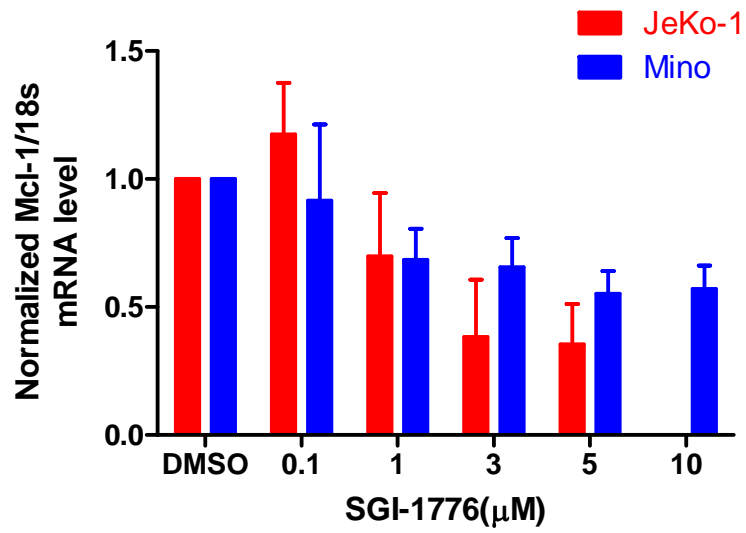
B
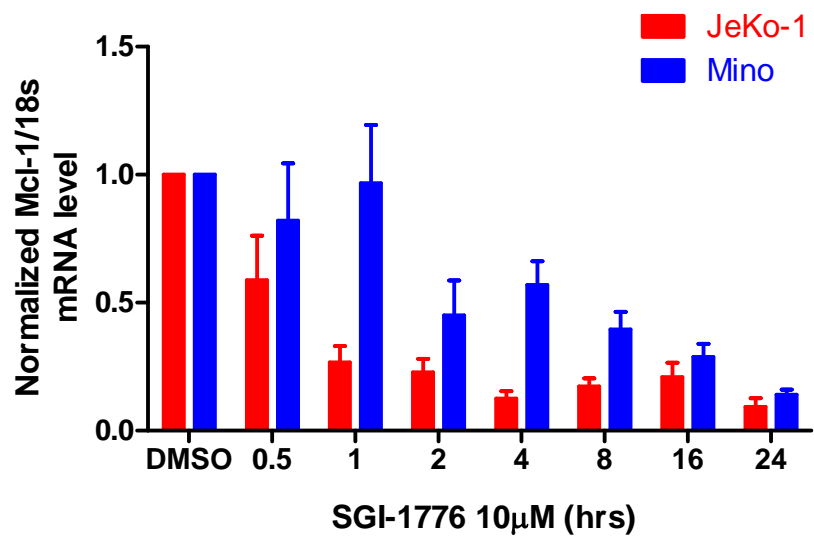
The 24hr treatment of 10μM SGI-1776 lead to apoptosis level that is too extensive that there were not enough cells to be harvested for this particular experiment. In Mino cells, less extensive yet gradual decrease of *MCL1* mRNA level was detected, and the *MCL1* expression levels reached 65% and 55% of control at 3 and 5μM, respectively (Figure 18A).

In the time-dependent experiments with various times of 10μM SGI-1776 over a 24hr period, a rapid and dramatic decrease of *MCL1* mRNA expression levels were detected in JeKo-1 cells, showing a reduction by 42% of control within 30min, and then further decreased by 73% of control in 1hr. The *MCL1* expression levels continued to decrease after 3hr, and after 4 and 24hr, only 12% of *MCL1* mRNA remained. In Mino cells, there was an initial increase of *MCL1* mRNA expression during the first hour of treatment, which then started to decrease to about 50% of control after 5hr and finally decreased to 14% of control after 24hr (Figure 18B).

Aim 2.3. Effect of SGI-1776 on anti-apoptotic protein expression levels in MCL cell lines.

Our observation of decrease of 4E-BP1 phosphorylation in both JeKo-1 and Mino cells indicated that cap-dependent translation is negatively affected by SGI-1776 (Richter 2005). We also detected both dose- and time-dependent decrease of *MCL1* mRNA levels in these MCL cell lines (Figure 18). Hence, we hypothesize that the expression levels of short-lived anti-apoptotic Mcl-1 protein would be decrease due to SGI-1776 treatment.

Effect of SGI-1776 on Mcl-1 protein expression levels in MCL cell lines.

To test this hypothesis, we evaluated the changes of short-lived Mcl-1 protein level, a known onco-protein in MCL (Khoury 2003). JeKo-1 and Mino cells were treated with various doses of SGI-1776 described and Mcl-1 protein were measured using immunoblots (Figure 19A), and normalized using GAPDH compared to DMSO control (Figure 19B).

Figure 19. Dose-dependent reduction of Mcl-1 protein expression levels by SGI-1776 treatment in MCL cell lines.

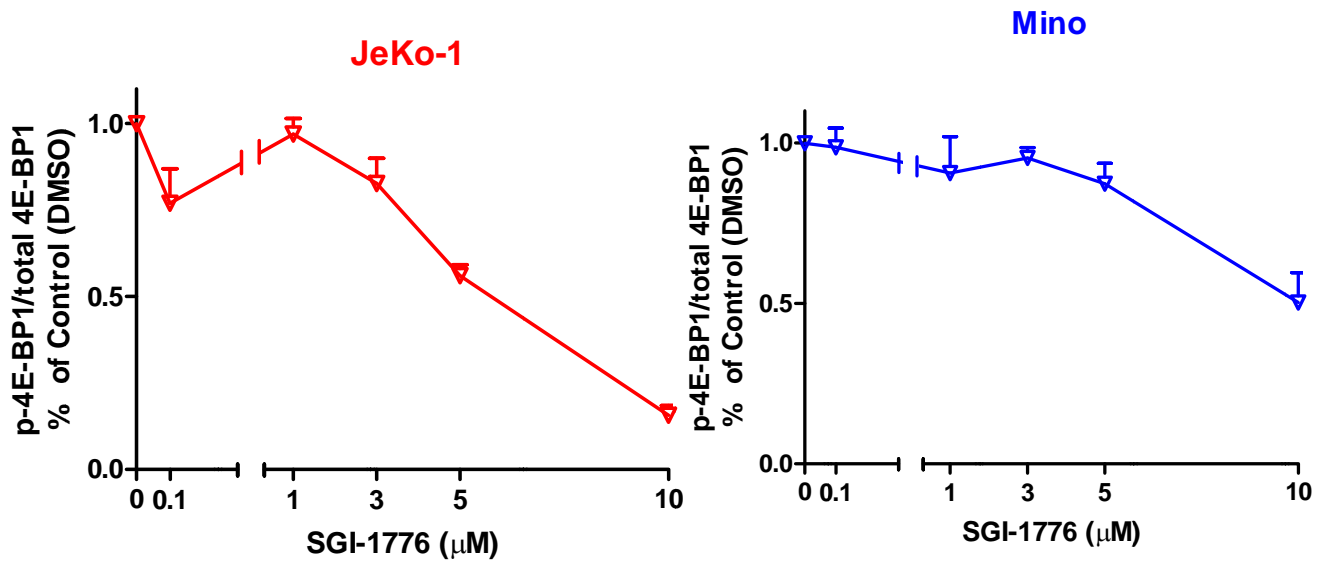(A)MCL cell lines JeKo-1, Mino cells were treated with DMSO or with different doses of SGI-1776 (0.1, 1, 4, 5, 10μM) for 24hr. Protein lysates were analyzed using immunoblot to detect the expression levels of Mcl-1. (B)Quantitation of immunoblots for each cell line was performed by measuring ratios of Mcl-1 to GAPDH for each SGI-1776 treatment, and normalized to DMSO control. Experiments were performed in triplicate and results were shown as average ratios ± SEM.

Figure 19.

A

Mcl-1 protein

| | Untreated | DMSO | 0.1 μM | 1 μM | 3 μM | 5 μM | 10 μM |

JeKo-1 — 37kD

GAPDH

Mino — 37kD
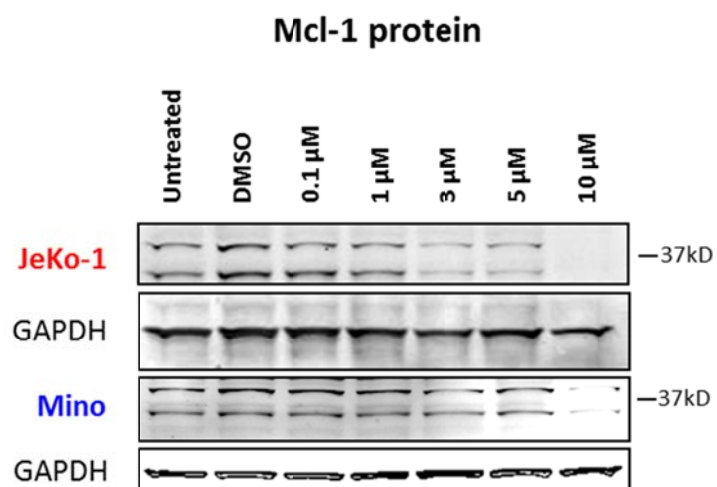
GAPDH

B

Results indicated a dose-dependent decrease of Mcl-1/GAPDH in both cell lines following SGI-1776 treatment at concentrations greater than 3μM in both cell lines. Again, of the two cell lines, there was a more dramatic decrease of Mcl-1 levels in JeKo-1 compared to Mino.

JeKo-1 and Mino cells were also treated with 10μM of SGI-1776 for increasing times, and Mcl-1 and GAPDH protein expression levels were detected (Figure 20A), and ratios of Mcl-1/GAPDH were normalized to DMSO control (Figure 20B). Notably, only JeKo-1 cells, there was a clear time-dependent decrease of Mcl-1 expression, whereas in Mino, although moderate decrease (up to 25%) was observed by 2hr, there is an increase of Mcl-1 level at 4hr followed by further decrease of this protein.

Effect of SGI-1776 on other anti-apoptotic proteins in MCL cell lines.

Due to lack of consistent decrease of cell-death-inducing phospho-Bad levels in MCL cell lines, and the limited degree of inhibition of both Mcl-1 mRNA and protein levels, we hypothesize that anti-apoptosis proteins other than Mcl-1 may play a role in apoptosis induction in MCL. We investigated the effect of SGI-1776 in other Bcl-2 family proteins (Bcl-2, Bcl-X_L) and XIAP, which are all anti-apoptosis proteins known to play a role in NHL (Akyurek 2006; Perez-Galan 2011).

JeKo-1 and Mino cells were treated with SGI-1776 for different doses for 24hr, and cells were harvested for immunoblot analysis (Figure 21A, B). Interestingly, we did not see any decrease of these protein expression levels in either cell line. In JeKo-1, only 10μM treatment of SGI-1776 lead to decrease of Bcl-X_L and XIAP levels, and this could be due to the extensive cell death as shown by the decrease of GAPDH protein levels.

Aim 2.4. Effect of SGI-1776 on cell cycle profile and cell cycle regulators in MCL cell lines.

Effect of SGI-1776 on cell cycle profiles in MCL cell lines.

Figure 20. Time-dependent reduction of Mcl-1 protein expression levels by SGI-1776 treatment in MCL cell lines.

(A)MCL cell lines JeKo-1, Mino cells were treated with DMSO or with 10μM of SGI-1776 for different time points (0.5, 1, 2, 4, 8, 16 and 24hr). Protein lysates were analyzed using immunoblot to detect the expression levels of Mcl-1. (B)Quantitation of immunoblots for each cell line was performed by acquiring ratios of Mcl-1 to GAPDH for each SGI-1776 treatment, and then ratios from each treatment were normalized to the result of DMSO-treated experiment. Experiments were performed in triplicate and results were shown as average ratios ± SEM.
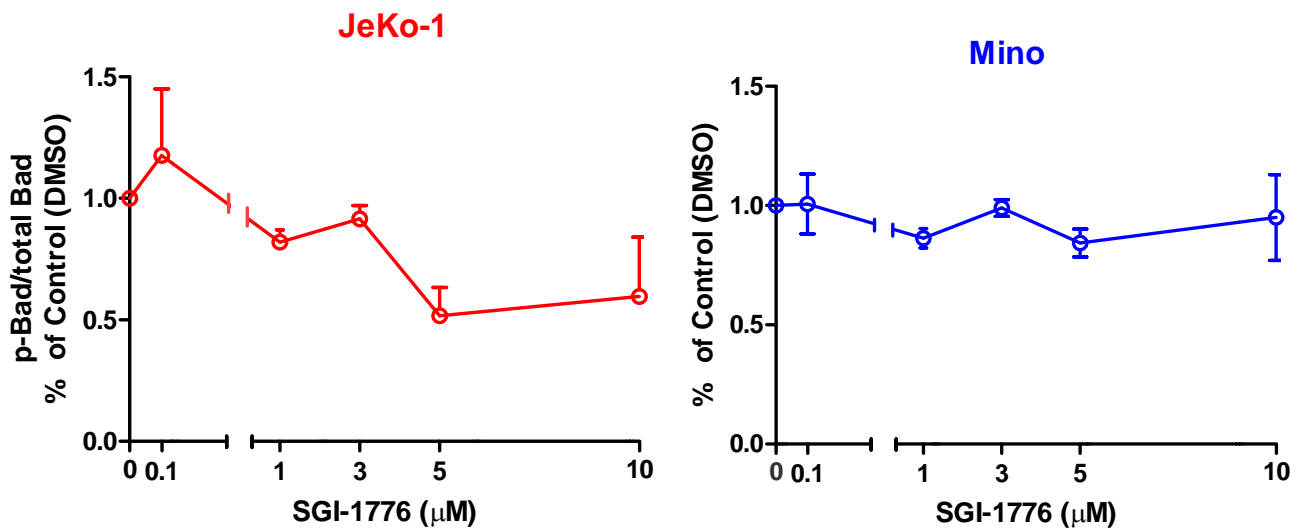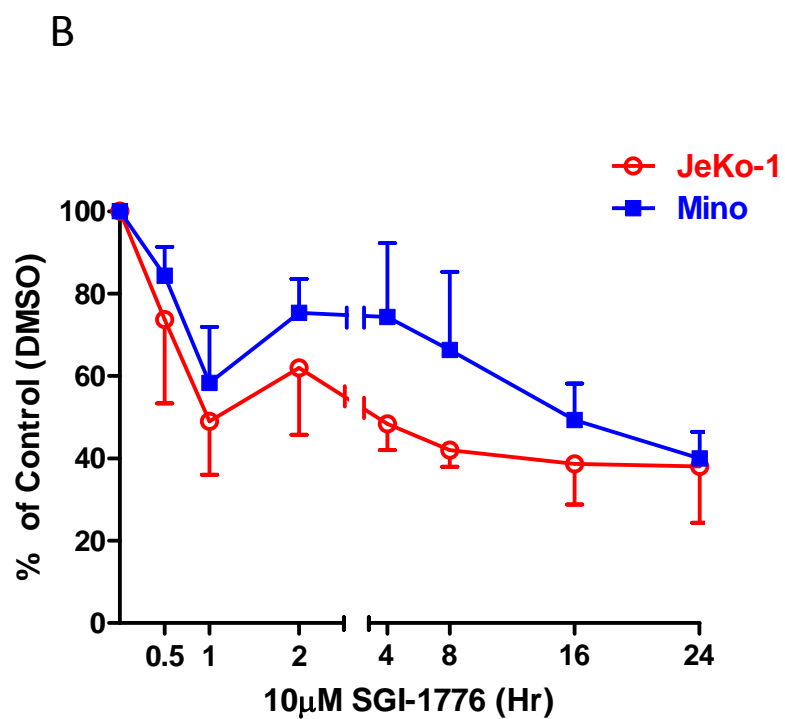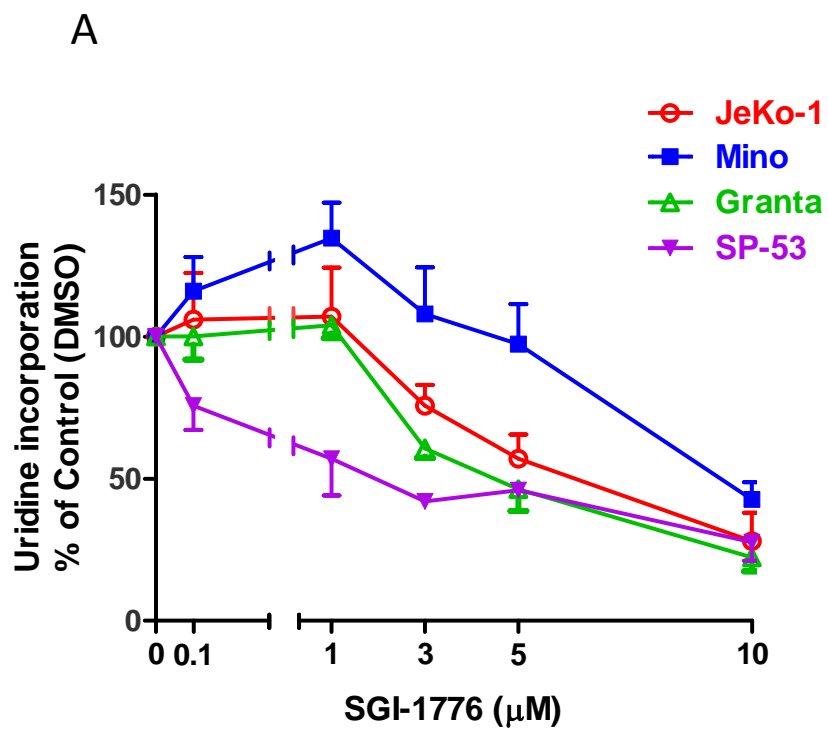
Figure 20.

A

B
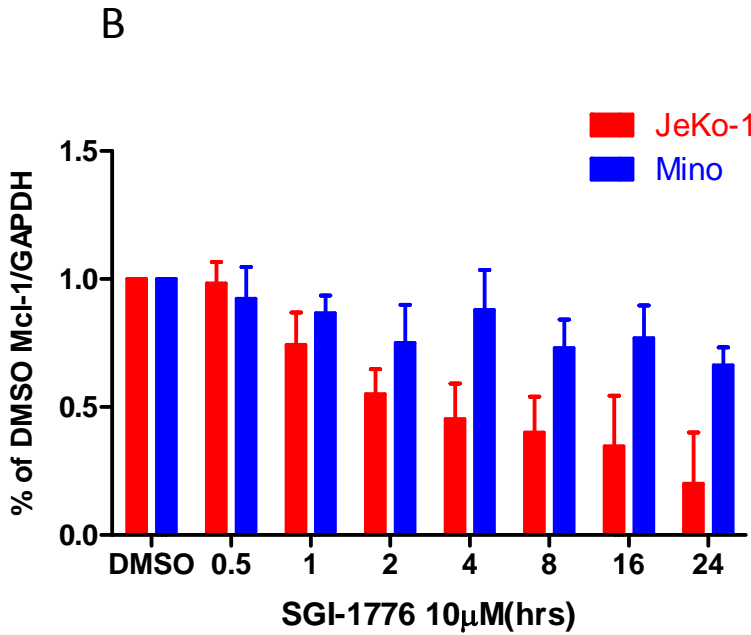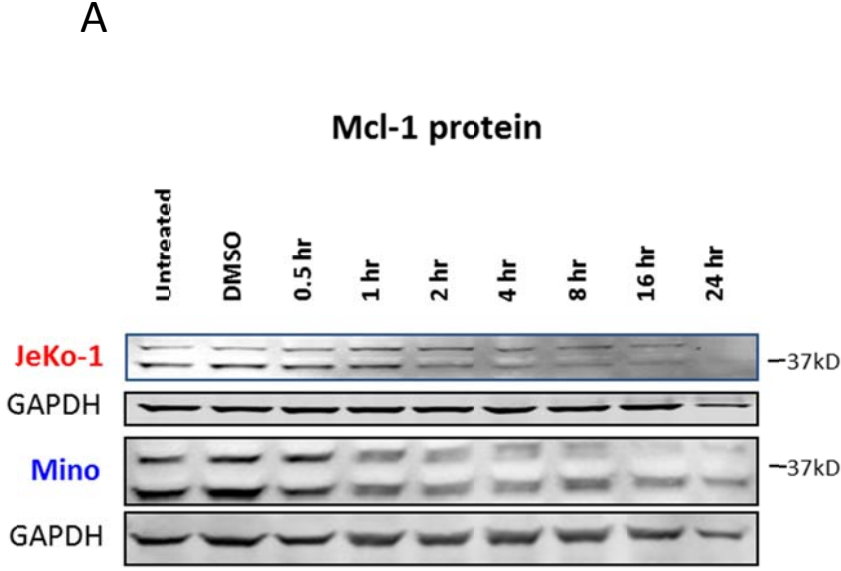
Figure 21. Effect on other Bcl-2 family proteins and XIAP by SGI-1776 treatment in MCL cell lines.

MCL cell lines (A)JeKo-1 and (B)Mino cells were treated with DMSO or with 10μM of SGI-1776 for different time points (0.5, 1, 2, 4, 8, 16 and 24hr). Protein lysates were analyzed using immunoblot to detect the expression levels of Bcl-2 family proteins Bcl-2, Bcl-X$_L$ and XIAP. Experiments were performed in duplicate.

Figure 21.

A

JeKo-1

	Untreated	DMSO	0.1 μM	1 μM	3 μM	5 μM	10 μM

Bcl-2

Bcl-X$_L$

XIAP

GAPDH

B

Mino

	Untreated	DMSO	0.1 μM	1 μM	3 μM	5 μM	10 μM

Bcl-2

XIAP

GAPDH

Bcl-X$_L$

GAPDH
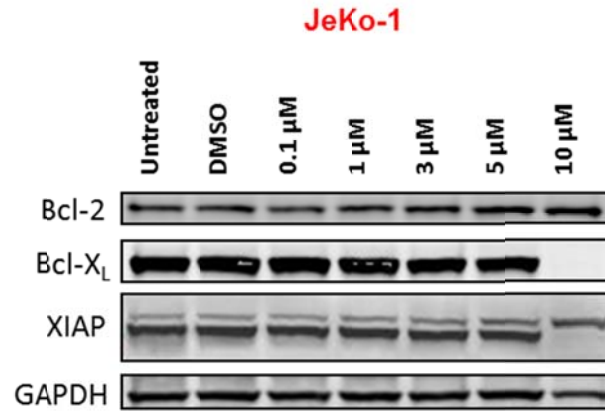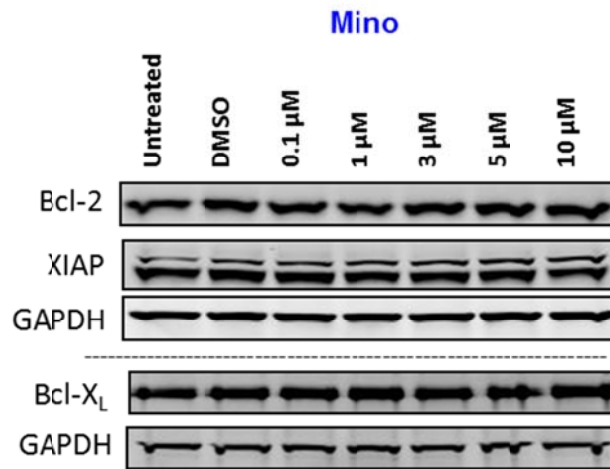
Pim kinases are known to regulate cell cycle regulators such as p27 and cdc25C (Chen 2010), therefore, we hypothesize that cell cycle profile would be affected by SGI-1776 treatment. We treated JeKo-1 and Mino cells with different doses of SGI-1776 for 24hr, and then cells cycle profiles were measured and analyzed using flow cytometry; percentages of cells in each cell cycle phase were measured (Figure 22).

In JeKo-1 cells, little change was observed in cell cycle profile, and with 10μM SGI-1776, there was only a slight increase of G1-staged cells compared to DMSO-treated cells (<5%, Figure 22A). However, in Mino cells, there was a clear dose-dependent increase of G1 population accompanied with decrease of S and G1 population compared to DMSO control, with 3%, 12% and 37% increase in G1-phased cells in 3, 5 and 10μM SGI-1776, respectively (Figure 22B).

Effect of SGI-1776 on cdc25C phosphorylation in MCL cell lines.

To further investigate Pim kinases' role in cell cycle regulation, we analyzed the changes of phosphorylation levels of a known Pim kinase substrate, cdc25C (Bachmann 2006).

As mentioned above, JeKo-1 and Mino cells were treated with SGI-1776 for 24hr and then cells were harvested for immunoblot analysis of phospho- and total cdc25C protein expression levels (Figure 23).

Although in JeKo-1 cells, phospho-cdc25C (Ser216) levels decreased with increasing SGI-1776, there was an even more significant dose-dependent decrease of total cdc25C levels, making it difficult to draw a conclusion for changes of phospho-cdc25C levels. In Mino cells, neither phospho- nor total protein levels decreased, also suggesting an inconclusive result.

Effect of SGI-1776 on cyclin D1 levels in MCL cell lines.

Figure 22. Cell line-specific differential effect on cell cycle by SGI-1776 treatment in MCL cell lines.

MCL cell lines (A)JeKo-1 and (B)Mino cells were treated with DMSO or with different doses of SGI-1776 (0.1, 1, 3, 5, 10μM) for 24hr, then cells were fixed with ice cold 70% ethanol and then incubated with propidium iodine. Cell cycle profiles were analyzed using flow cytometry, where G1, S, G2/M cell cycle stages were shown as percent population. Experiments were performed in triplicate and results were shown as average percentages ± SEM.

Figure 22.

A

JeKo-1

B
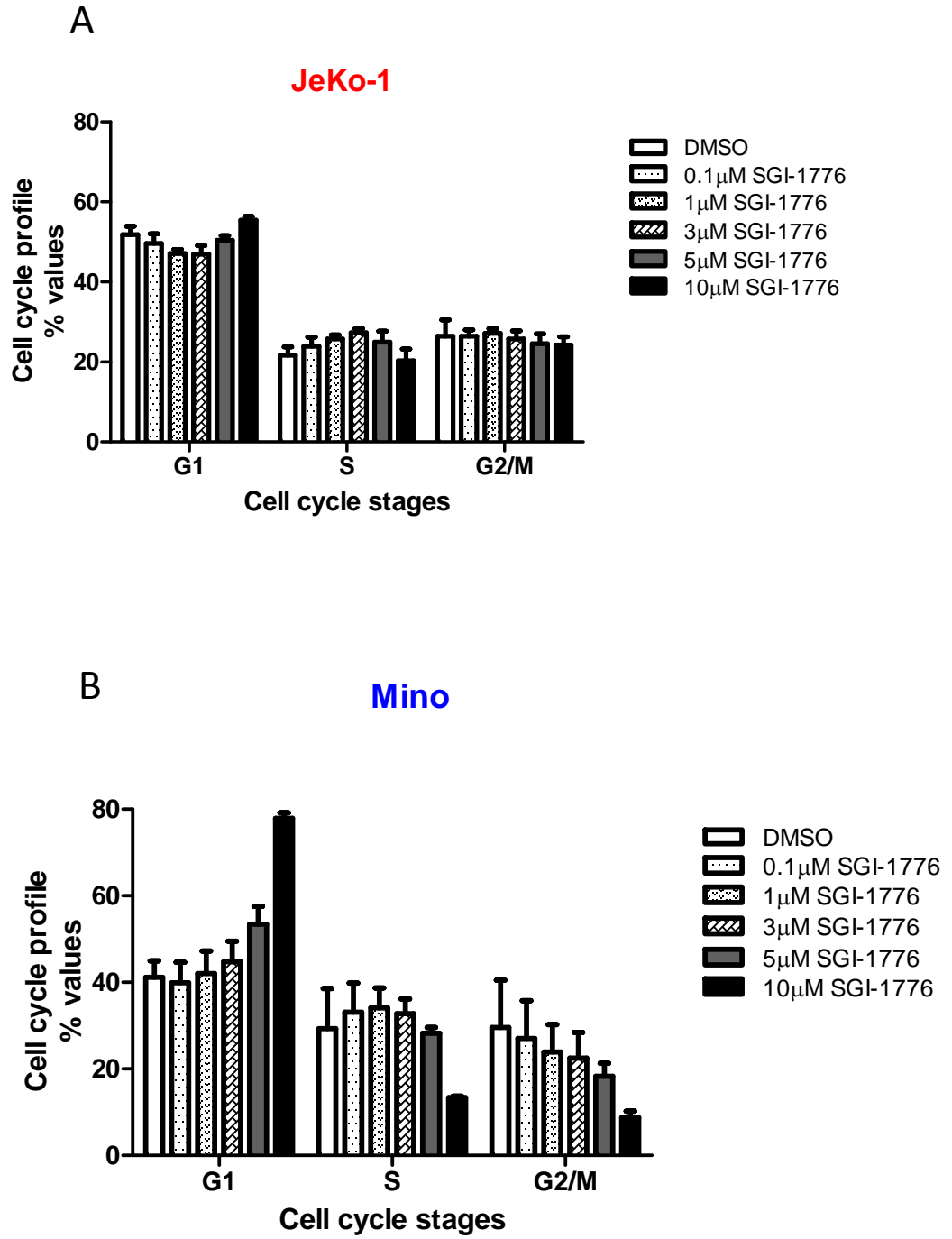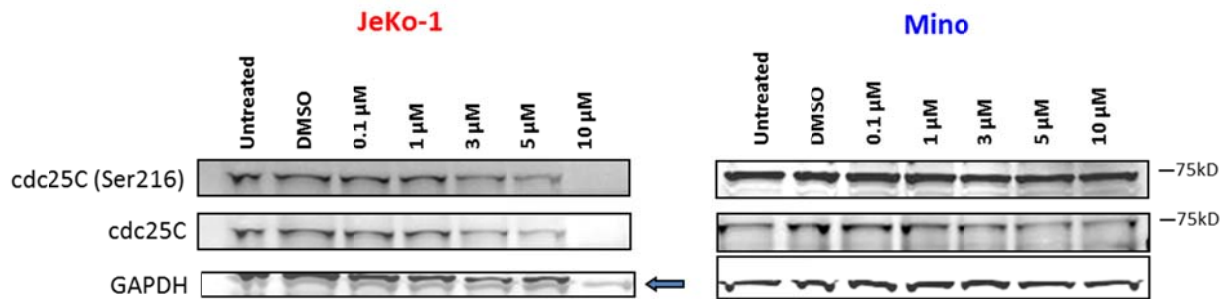
Mino

Figure 23.

Figure 23. Cell line-specific effect of cdc25C phosphorylation by SGI-1776 treatment in MCL cell lines.

MCL cell lines JeKo-1 and Mino cells were treated with DMSO or with different doses of SGI-1776 (0.1, 1, 3, 5, 10μM) for 24hr. Protein lysates were extracted from the cells and then analyzed using immunoblot to detect the expression levels of phospho- and total cdc25C protein. Experiments were performed in duplicate.

Cyclin D1 is a cell cycle regulator protein with oncogenic feature when overexpressed due to t(11;14) (q13;q32), it is also the molecular hallmark of MCL disease (Vasef 1997). It has been shown that MCL cell lines JeKo-1 and Mino are cyclin D1 positive (Amin 2003). Pim kinases are reportedly known to regulate cell cycle proteins, but their relationship with cyclin D1 is unknown (Mochizuki 1999). Therefore, we hypothesize that cyclin D1 level would be affected by SGI-1776, and carried out immunoblot analysis to test this hypothesis.

JeKo-1 and Mino cells were treated with SGI-1776 in various doses for 24hr and 10μM dose for different time points, then cells were harvested, and protein lysates were extracted for immunoblot analysis (Figure 24A, B). In JeKo-1 cells, there was a clear decrease of cyclin D1 in both dose- and time-dependent fashions. Notably, significant decrease of cyclin D1 was detected at 3μM or higher concentrations of SGI-1776 for 24hr, or 4hr or longer for 10μM SGI-1776 treatments. However, in Mino cells, we observed dose- and time-dependent increase of cyclin D1 levels with SGI-1776 treatments, which was in contract with the results in JeKo-1.

Aim 2.5. Effects of *PIM1, PIM2* and *PIM1/2* siRNAs in MCL cell lines.

To confirm the findings of SGI-1776 on Pim kinase phosphorylation substrates and Mcl-1 mRNA and protein levels are on-target effects, we conducted siRNA knockdown studies using single siRNAs *PIM1, PIM2*, and combination of *PIM1* and *PIM2* (denoted as *PIM1/2*) in MCL cell lines JeKo-1 and Mino, and performed immunoblots, RT-PCR experiments to evaluate the changes of Pim kinase substrate phosphorylation levels and Mcl-1 protein and mRNA levels.

Effects of *PIM1, PIM2*, and *PIM1/2* siRNA on *PIM1, PIM2* and *MCL1* mRNA levels.

JeKo-1 and Mino cells were transfected with *PIM1, PIM2*, and *PIM1/2* siRNA using electrophoresis method, and then cells were placed back in cell culture and harvested after 24hr. Total RNA was extracted for RT-PCR experiment to detected *PIM1* and *PIM2* and *MCL1* mRNA levels (Figure 25).

Figure 24. Cell line-specific differential effect on cyclin D1 by SGI-1776 treatment in MCL cell lines.
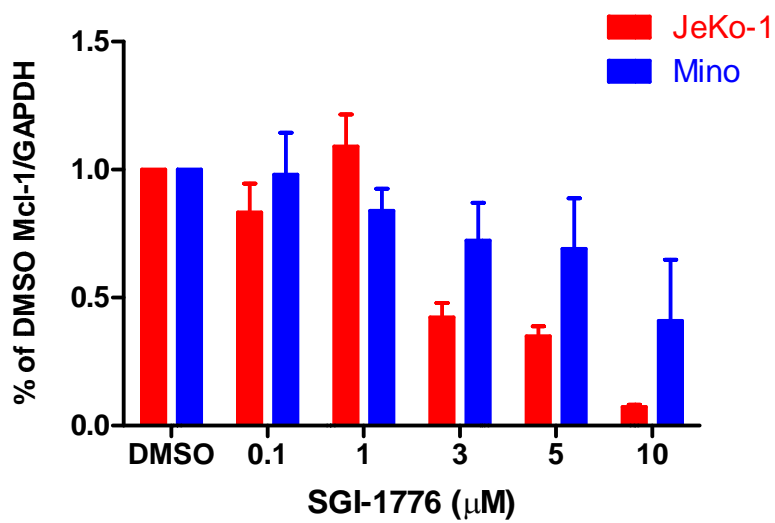
MCL cell lines (A)JeKo-1 and (B)Mino cells were treated with DMSO or with different doses of SGI-1776 (0.1, 1, 3, 5, 10μM) for 24hr, or with 10μM of SGI-1776 for different time points (0.5, 1, 2, 4, 8, 16 and 24hr). Protein lysates were extracted from the cells and then analyzed using immunoblot to detect the expression levels of cyclin D1 protein. Experiments were performed twice.

Figure 24.

A
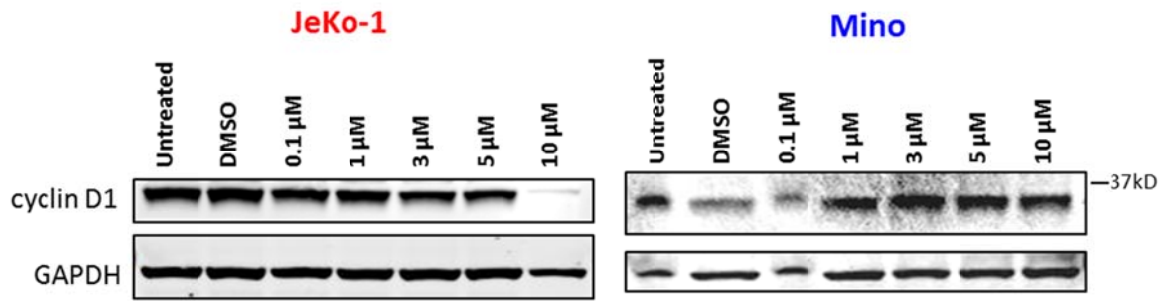
B
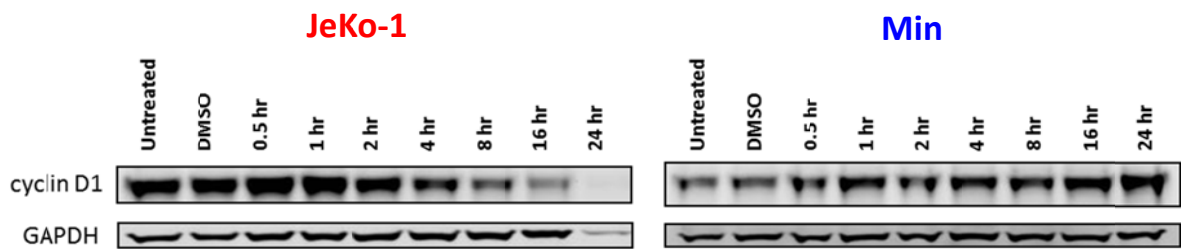
Figure 25. Effect on PIM1, PIM2 and MCL1 mRNA expression levels by PIM1, PIM2 siRNA

treatments in MCL cell lines.

(A)JeKo-1 and (B)Mino cells were transfected with 150nM of scramble siRNA, transfection indicator siGLO, either *PIM1* or *PIM2* siRNA alone or with combination of *PIM1* and *PIM2* siRNA using electroporation method. After 24hr post-transfection incubation, cell viability and transfection efficiency were tested using flow cytometry, and cells were harvested for RT-PCR study. Short-lived *PIM1*, *PIM2* and *MCL1* mRNA expression levels were detected and results were normalized to scramble control. Experiments were performed in triplicate and results were shown as average ratios ± SEM.

Figure 25.

A

B
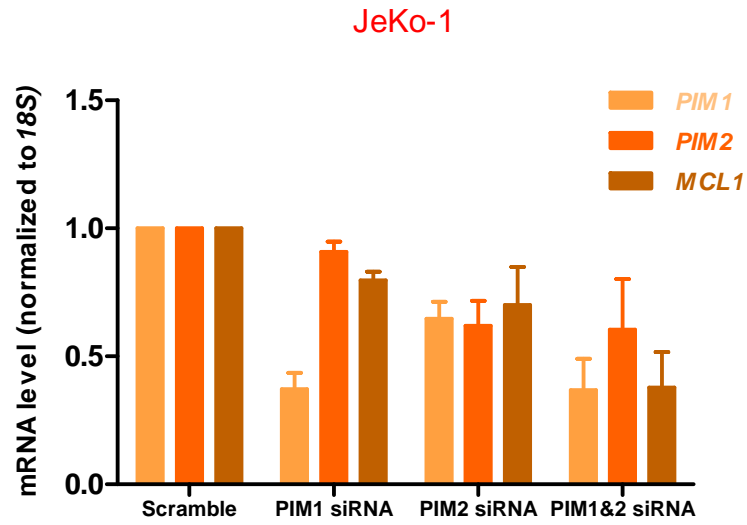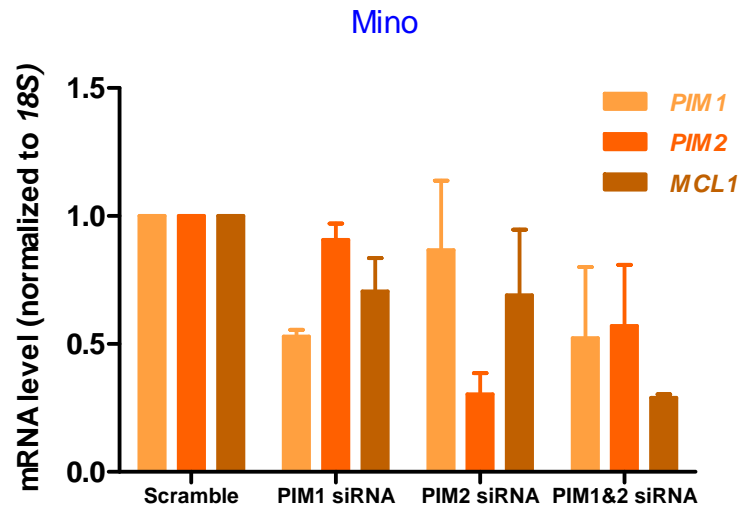
In JeKo-1 cells, *PIM1* siRNA lead to significant decrease of *PIM1* mRNA expression (>60%), but much smaller effect was observed on *MCL1* mRNA level (~20%) and even less for *PIM2* mRNA (~10%). Meanwhile, *PIM2* siRNA treatment equally reduced both *PIM1* and *PIM2* mRNA levels to around 60% of scramble control, while reducing *MCL1* mRNA level by 30%. For *PIM1/2* knockouts, reduction of *PIM1* and *PIM2* mRNA levels were compatible to those of *PIM1* or *PIM2* single knockouts, however, *MCL1* mRNA level was reduced much more than *PIM1, PIM2* single knockouts, reaching more than 60% reduction, which is more than *PIM1* and *PIM2* single knockouts combined (Figure 25A).

In Mino cells, similar trends were observed (Figure 25B). *PIM1* single knockout lead to 50%, 10% and 30% reduction in *PIM1*, *PIM2* and *MCL1* mRNA levels, respectively. Meanwhile, *PIM2* single knockout caused 14%, 70% and 30% reduction of *PIM1, PIM2* and *MCL1* levels. *PIM1/2* double knockout resulted in 50% reduction in *PIM1*, which is comparable to single *PIM1* knockout. However, less reduction in *PIM2* was observed (43%) compared to *PIM2* single knockout which was 70% reduction. We also observed synergistic effect in decreasing *MCL1* in *PIM1/2* double knockout study, which was a robust 72% decrease, compared to 30% in both *PIM1*and *PIM2* single knockout studies.

Effect of *PIM1, PIM2, PIM1/2* siRNA on Mcl-1 protein levels in JeKo-1.

Based on the results of *PIM1, PIM2* and *PIM1/2* siRNA knockouts on *MCL1* mRNA, we hypothesized that similar results will be observed in Mcl-1 protein in JeKo-1. JeKo-1 cells were treated with *PIM1, PIM2* and *PIM1/2* siRNAs, and then cells were harvested and protein lysates were used to perform immunoblots (Figure 26A). Mcl-1 and GAPDH proteins were detected and quantitated; Mcl-1/GAPDH levels were calculated and normalized to scramble control (Figure 26B).

As shown in Figure 26B, *PIM1/2* double knockout lead to the most amount of decrease in *MCL1* compared to the single knockouts, and *PIM2* knockout was more effective in reducing *MCL1*

Figure 26. Effect on Mcl-1 protein expression levels by *PIM1, PIM2* siRNA treatments in JeKo-1 cells.

(A)JeKo-1 cells were transfected with 150nM of scramble siRNA, transfection indicator siGLO, either *PIM1* or *PIM2* siRNA alone or with combination of *PIM1* and *PIM2* siRNA using electroporation method. After 24hr post-transfection incubation, cell viability and transfection rate were tested using flow cytometry, and cells were harvested for immunoblot study. Levels of Mcl-1 and GAPDH protein expression were measured. (B)Quantitation of the immunoblot with siRNA-treated JeKo-1 cells. Mcl-1 to GAPDH ratios were calculated and results were normalized to scramble control. Annexin V/PI positivity values indicating apoptosis level were marked under each lane of western blot. All experiments were performed in triplicate and results were shown as average ratios ± SEM.

Figure 26.

A

B
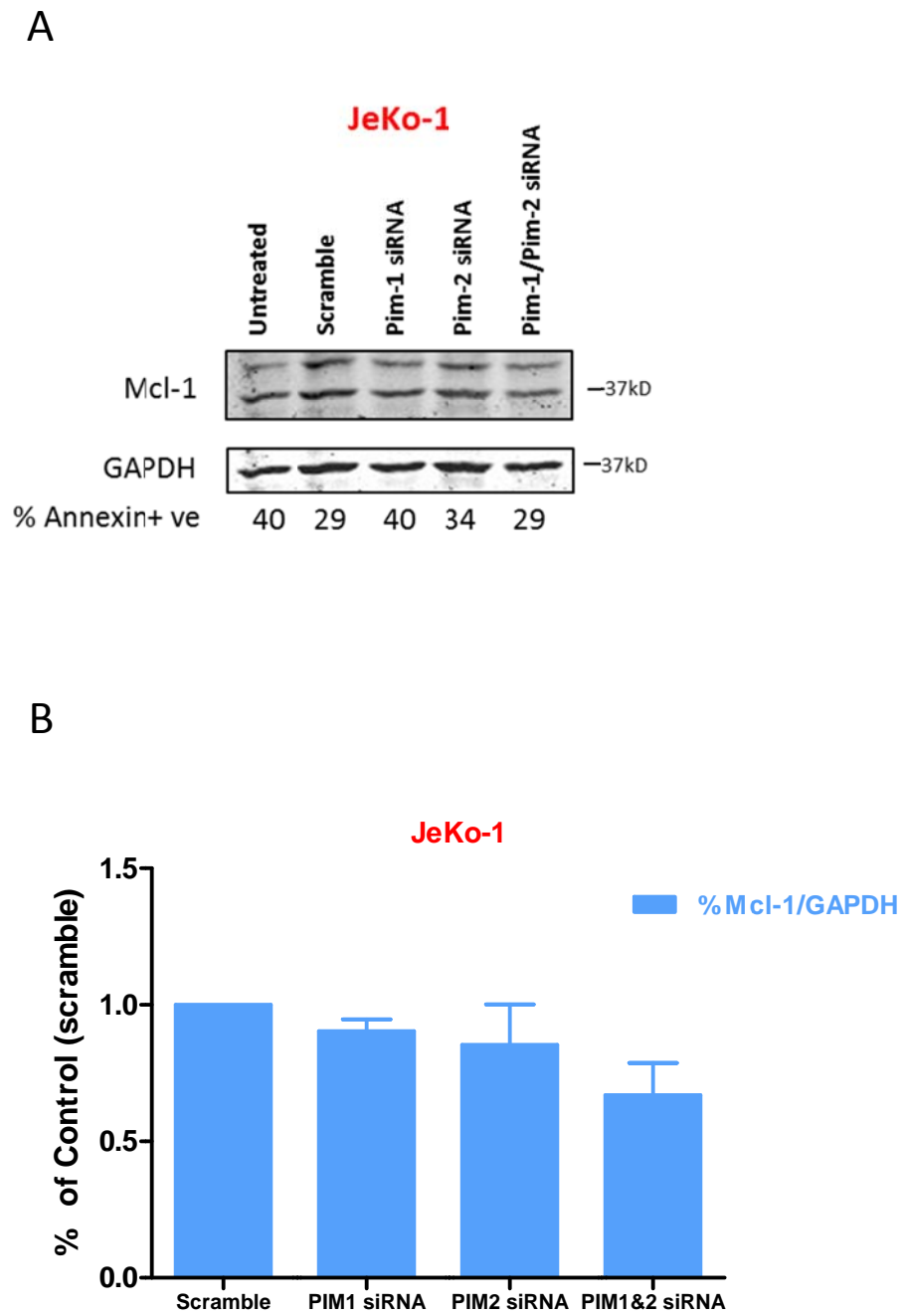
than *PIM1* knockout. However, for each siRNA treatment, the reduction of *MCL* mRNA was less extensive compared to their equivalent mRNA level.

Effect of *PIM1, PIM2, PIM1/2* siRNA on Mcl-1 protein levels in Mino.

Mino cells were also treated with *PIM1, PIM2* and *PIM1/2* siRNA and their effect on Mcl-1 protein levels were measured (Figure 27). It appears that *PIM1* single knockout did not result in a decrease of Mcl-1level in Mino. However, *PIM2* single knockout and *PIM1/2* double knockout lead to reduction of Mcl-1 levels by 5%, and 16%, respectively.

Effects of *PIM1, PIM2* and *PIM1/2* siRNA on Pim kinase phosphorylation targets in JeKo-1.

c-Myc and 4E-BP1 phosphorylation was consistently decreased in SGI-1776-treated JeKo-1 and Mino cells, therefore, we investigated whether the effect on these Pim kinase phospho-targets are consistent with *PIM1, PIM2* and *PIM1/2* siRNA-treated cells. Both JeKo-1 and Mino cell lines were treated with these siRNAs, and then cells were harvested and protein lysates were extracted for immunoblot analysis. Both phospho- and total c-Myc and 4E-BP1 were detected and quantitated (Figure 28A), and ratios of phospho- to total protein levels were calculated, normalized to scramble control, and then plotted (Figure 28B).

In JeKo-1 cells, *PIM1* single knockout lead to a decrease in both phospho-c-Myc and 4E-BP1 at 20% compared to control, however, *PIM2* single knockout neither reduced phospho-c-Myc by 5% nor phospho-4E-BP1 levels. *PIM1/2* double knockout caused around 20% reduction of both phospho-c-Myc and 4E-BP1, compatible to that of *PIM1* single knockout.

Effects of *PIM1, PIM2* and *PIM1/2* siRNA on Pim kinase phosphorylation targets in Mino.

Mino cells were also treated with *PIM1, PIM2* and *PIM1/2* siRNAs, and immunoblots of phospho- and total c-Myc and 4E-BP1 were measured and quantitated (Figure 29A). Plotted ratios of phospho- to total protein levels indicated that phospho-c-Myc levels were decreased in all three

Figure 27. Effect on Mcl-1 protein expression levels by *PIM1, PIM2* siRNA treatments in Mino cells.

(A)Mino cells were transfected with 150nM of scramble siRNA, transfection indicator siGLO, either *PIM1* or *PIM2* siRNA alone or with combination of *PIM1* and *PIM2* siRNA using electroporation method. After 24hr post-transfection incubation, cell viability and transfection rate were tested using flow cytometry, and cells were harvested for immunoblot study. Levels Mcl-1 and GAPDH protein expression were measured. (B)Quantitation of the immunoblot with siRNA-treated Mino cells. Mcl-1 to GAPDH ratios were calculated and results were normalized to scramble control. Annexin V/PI positivity values indicating apoptosis levels were marked under each lane of western blot. All experiments were performed in triplicate and results were shown as average ratios ± SEM.

Figure 27.

A
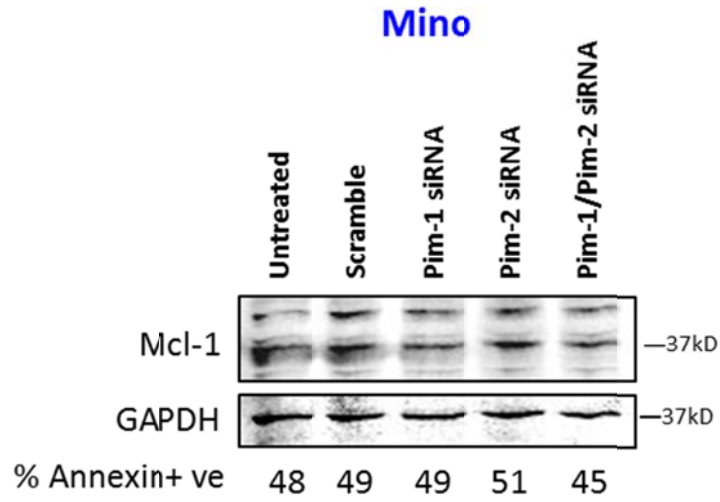
B
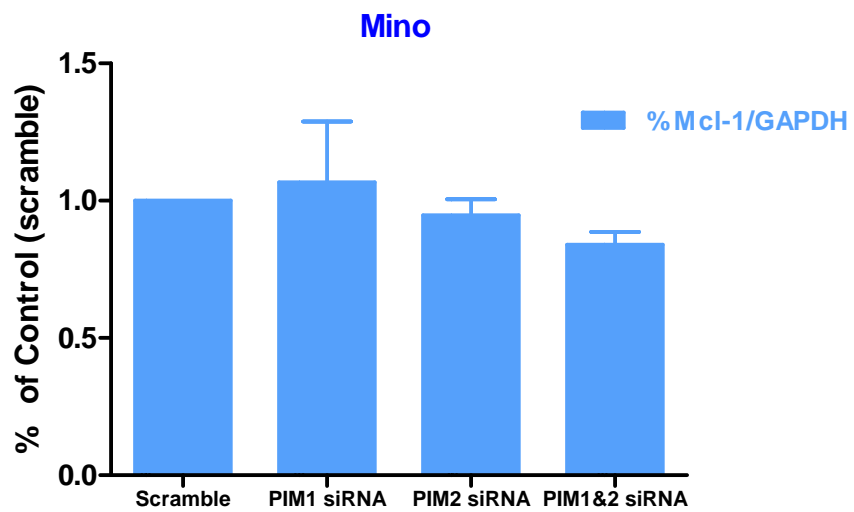
Figure 28. Effect on Pim kinase phosphorylation targets by *PIM1, PIM2* siRNA treatments in

JeKo-1 cells.

(A)JeKo-1 cells were transfected with 150nM of scramble siRNA, transfection indicator siGLO, either *PIM1* or *PIM2* siRNA alone or with combination of *PIM1* and *PIM2* siRNA using electroporation method. After 24hr post-transfection incubation, cell viability and transfection rate were tested using flow cytometry, and cells were harvested for immunoblot study. Levels of phospho-c-Myc (Ser62), total c-Myc, phospho-4E-BP1 (Thr37/46), total 4E-BP1, and GAPDH protein expression were measured. (B)Quantitation of the immunoblot with siRNA-treated JeKo-1 cells. Ratios of phospho- to total proteins were calculated and results were normalized to scramble control. Annexin V/PI positivity values indicating apoptosis level were marked under each lane of western blot. All experiments were performed in triplicate and results were shown as average ratios ± SEM.

Figure 28.
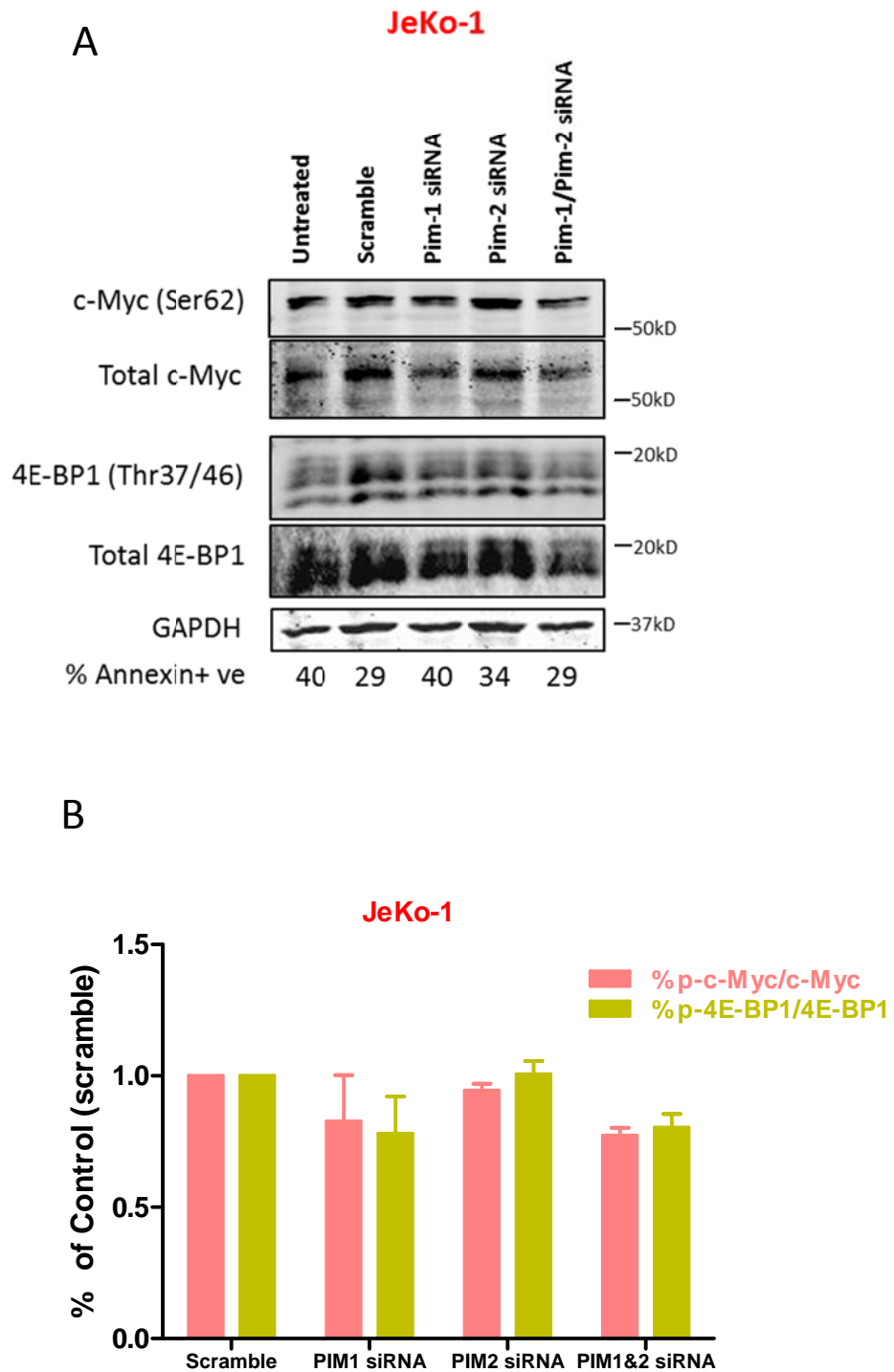
Figure 29. Effect on Pim kinase phosphorylation targets by *PIM1, PIM2* siRNA treatments in Mino cells.

(A)Mino cells were transfected with 150nM of scramble siRNA, transfection indicator siGLO, either *PIM1* or *PIM2* siRNA alone or with combination of *PIM1* and *PIM2* siRNA using electroporation method. After 24hr post-transfection incubation, cell viability and transfection rate were tested using flow cytometry, and cells were harvested for immunoblot study. Levels of phospho-c-Myc (Ser62), total c-Myc, phospho-4E-BP1 (Thr37/46), total 4E-BP1, and GAPDH protein expression were measured. (B)Quantitation of the immunoblot with siRNA-treated Mino cells. Ratios of phospho- to total proteins were calculated and results were normalized to scramble control. Annexin V/PI positivity values indicating apoptosis levels were marked under each lane of western blot. All experiments were performed in triplicate and results were shown as average ratios ± SEM.

Figure 29.

A
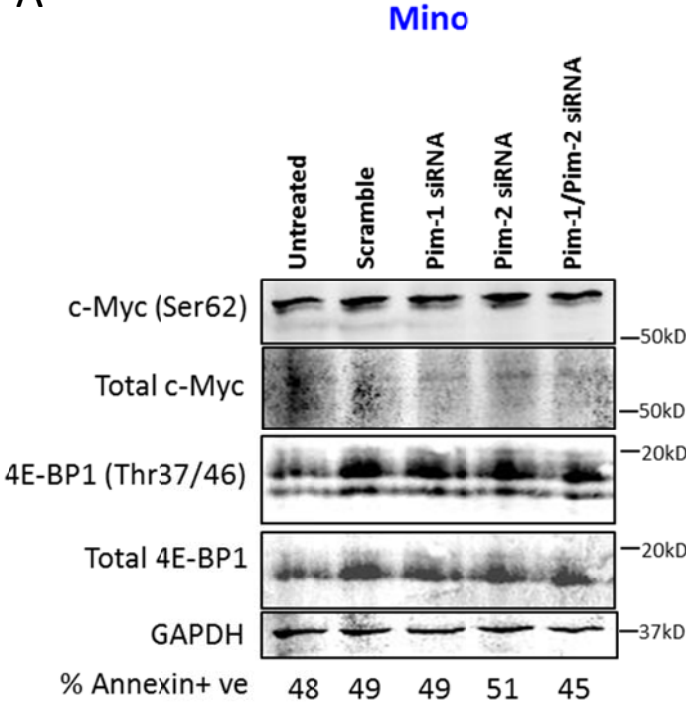
B
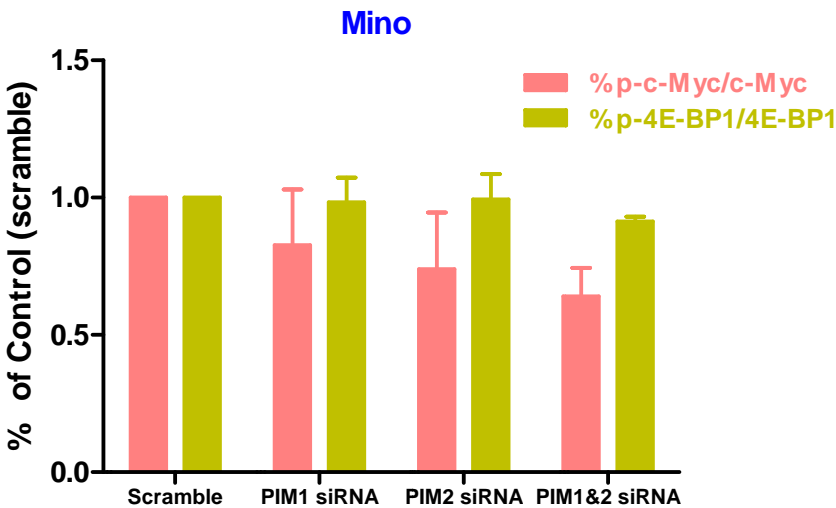
siRNA treatment conditions, with 20%, 25% and 35% decrease in *PIM1, PIM2* and *PIM1/2* siRNA-treated cells, respectively (Figure 29B). However, only slight decrease (~10%) decrease in phoshpo-4E-BP1 level was observed in *PIM1/2* double knockout studies but not the single knockout studies.

Aim 2.6. Effect of SGI-1776 on MCL primary samples.

To determine if SGI-1776's effect of reducing phospho-c-Myc (Ser62) and phospho-4E-BP1 (Thr37/46) levels in MCL cell lines is also observed in MCL primary cells, we investigated the effects of this drug on Pim kinase phosphorylation targets and oncoprotein Mcl-1 and cyclin D1 using malignant PBMCs isolated from MCL primary patient samples (Table 3).

Effect of SGI-1776 on Pim kinase phosphorylation targets in MCL primary samples.

PBMCs were isolated from late-staged MCL patients, and the SGI-1776 treatment was started on the same day of isolation (Table 2). Primary MCL cells were treated with increasing doses of SGI-1776 (0.1, 1, 3, 5, 10μM) for 24hr and then cells were harvested for flow cytometry and immunoblot analyses (Figure 30).

Phospho- and total c-Myc and 4E-BP1 protein levels were evaluated, and for both phospho-c-Myc and phospho-4E-BP1, there was a dose-dependent decrease with the SGI-1776 treatment. In addition, there was also a dose-dependent increase of apoptosis (n=3), with about 30% increase in cell death was observed by 10μM SGI-1776 among all samples.

Effect of SGI-1776 on Mcl-1 and cyclin D1 levels in MCL primary patent samples.

We then tested the effect of SGI-1776 on short-lived oncoproteins cyclin D1 and Mcl-1 in MCL primary samples; as both are known to be over expressed in MCL patients and play a role in worsen patient prognosis and treatment outcomes (Vasef 1997; Khoury 2003).

Table 3.

Patient numbers	1	[§]2	[§]3	*4	5
Dx	MCL	MCL	MCL	MCL	MCL
Sample type	AS	PB	PB	PB	AS
Tumor cells % of lymphocytes	90	80	80	0	0
Patient age, yrs	74	54	54	53	75
White blood count, per µL	213,000	79,000	53,000	58,000	67,700
Lymphocytes%	99	75	77	1	94
Neutrophils%	1	21	22	86	6
Metaphase%	0	0	0	0	7
Blasts%	0	0	0	1	0
Monocytes%	0	4	1	1	0
Growth Factor	No	No	No	Neopogen	No

Table 3. MCL patient characteristics.

[§]Samples 2 and 3 are from the sample patient but obtained on different days.

*This patient had stage IV disease but was in remission when the blood samples were collected. Therefore, these samples served as normal PBMCs.

AS, apheresis sample; PB, peripheral blood.

Figure 30. Dose-dependent reduction of Pim kinase phosphorylation targets by SGI-1776 treatment in primary MCL patient samples.

(A)Malignant PBMCs isolated from blood samples of MCL patients were either untreated, or treated with DMSO or different doses of SGI-1776 (0.1, 1, 3, 5, 10μM) for 24hr. Then cells were harvested and viability of cells with or without SGI-1776 treatment was tested using flow cytometry. Protein lysates were extracted and immunoblots were performed to analyze changes of phospho-c-Myc (Ser62), 4E-BP1 (Th37/46). Expression levels of phospho-c-Myc (Ser62) and total c-Myc, phospho-4E-BP1 (Thr37/46) and total 4E-BP1 as well as GAPDH protein expression were measured. Annexin V/PI positivity values were marked under each lane of immunoblot.

Figure 30.

MCL#2

SGI-1776 (µM) — columns: Untreated, DMSO, 0.1 µM, 1 µM, 3 µM, 5 µM, 10 µM

	Untreated	DMSO	0.1 µM	1 µM	3 µM	5 µM	10 µM	
c-Myc (Ser62)								50kD
Total c-Myc								50kD
4E-BP1 (Thr37/46)								20kD
Total 4E-BP1								20kD
GAPDH								
% Annexin+ ve	58	60	62	71	90	90	92	

MCL#3

SGI-1776 (µM) — columns: Untreated, DMSO, 0.1 µM, 1 µM, 3 µM, 5 µM, 10 µM

	Untreated	DMSO	0.1 µM	1 µM	3 µM	5 µM	10 µM	
c-Myc (Ser62)								50kD
Total c-Myc								50kD
4E-BP1 (Thr37/46)								20kD
Total 4E-BP1								20kD
GAPD								
% Annexin+ ve	60	61	62	73	91	92	92	

MCL#5

SGI-1776 (µM) — columns: Untreated, DMSO, 0.1 µM, 1 µM, 3 µM, 5 µM, 10 µM

	Untreated	DMSO	0.1 µM	1 µM	3 µM	5 µM	10 µM	
c-Myc (Ser62)								50kD
Total c-Myc								50kD
4E-BP1 (Thr37/46)								20kD
Total 4E-BP1								20kD
GAPD								
% Annexin+ ve	52	56	58	59	74	81	86	

Patient samples were treated with various doses of SGI-1776 for 24hr, then cells were harvested and analyzed for their Mcl-1 and cyclin D1 protein expression levels by immunoblots (Figure 31). In the three MCL patient samples, both Mcl-1 and cyclin D1 were detected by immunoblots and SGI-1776 treatment lead to a dose-dependent decrease of both proteins, that at 3μM or higher doses, the levels of expression almost diminished for all three samples.

Effect of SGI-1776 on Pim kinase phosphorylation targets in normal PBMCs.

There should be a good therapeutic window for anti-cancer drugs in clinical use, which requires the drug to be specifically cytotoxic towards malignant cancer cells but not healthy cells in patients.

To compare the effect of SGI-1776 in normal PBMCs, we obtained PBMCs from three healthy donors and a MCL patient who is in remission, indicated by the very low levels of lymphocyte count (Table 2). Normal PBMCs were treated with SGI-1776 for 24hr with different doses (1, 3 and 10μM), and then Pim kinase phosphorylation targets c-Myc and 4E-BP1 were evaluated using immunoblots (Figure 32).

Notably, cells from the patient in remission (MCL#4) expressed a higher level of phospho- and total c-Myc levels compared to the healthy donors, but all four samples showed much lower expression levels of phospho- and total c-Myc and 4E-BP1 compared to the positive control, untreated Mino cells. Importantly, there was no obvious trend of decrease in phosphorylation levels of c-Myc or 4E-BP1 in any of these samples. In addition, in all four samples tested, apoptosis levels were very low compared to the malignant samples tested, even high SGI-1776 doses did not kill the cells.

Figure 31. Dose-dependent reduction of short-lived Mcl-1 and cyclin D1 protein expression levels by SGI-1776 treatment in primary MCL patient samples.

(A)Malignant PBMCs isolated from blood samples of MCL patients were either untreated, or treated with DMSO or different doses of SGI-1776 (0.1, 1, 3, 5, 10µM) for 24hr. Then cells were harvested and viability of cells with or without SGI-1776 treatment was tested using flow cytometry. Protein lysates were extracted and immunoblots were performed to analyze changes of short-lived oncoproteins Mcl-1 and cyclin D1 levels. Expression levels of Mcl-1, cyclin D1 and GAPDH protein expression were measured. Annexin V/PI positivity values indicating apoptosis levels were marked under each lane of western blot.

Figure 31.

MCL#2

SGI-1776 (µM)	Untreated	DMSO	0.1 µM	1 µM	3 µM	5 µM	10 µM	
Mcl-1								—37kD
cyclin-D1								—37kD
GAPDH								
% Annexin+ ve	58	60	62	71	90	90	92	

MCL#3

SGI-1776 (µM)	Untreated	DMSO	0.1 µM	1 µM	3 µM	5 µM	10 µM	
Mcl-1								—37kD
cyclin-D1								—37kD
GAPDH								
% Annexin+ ve	60	61	62	73	91	92	92	

MCL#5

SGI-1776 (µM)	Untreated	DMSO	0.1 µM	1 µM	3 µM	5 µM	10 µM	
Mcl-1								—37kD
cyclin-D1								—37kD
GAPDH								
% Annexin+ ve	52	56	58	59	74	81	86	
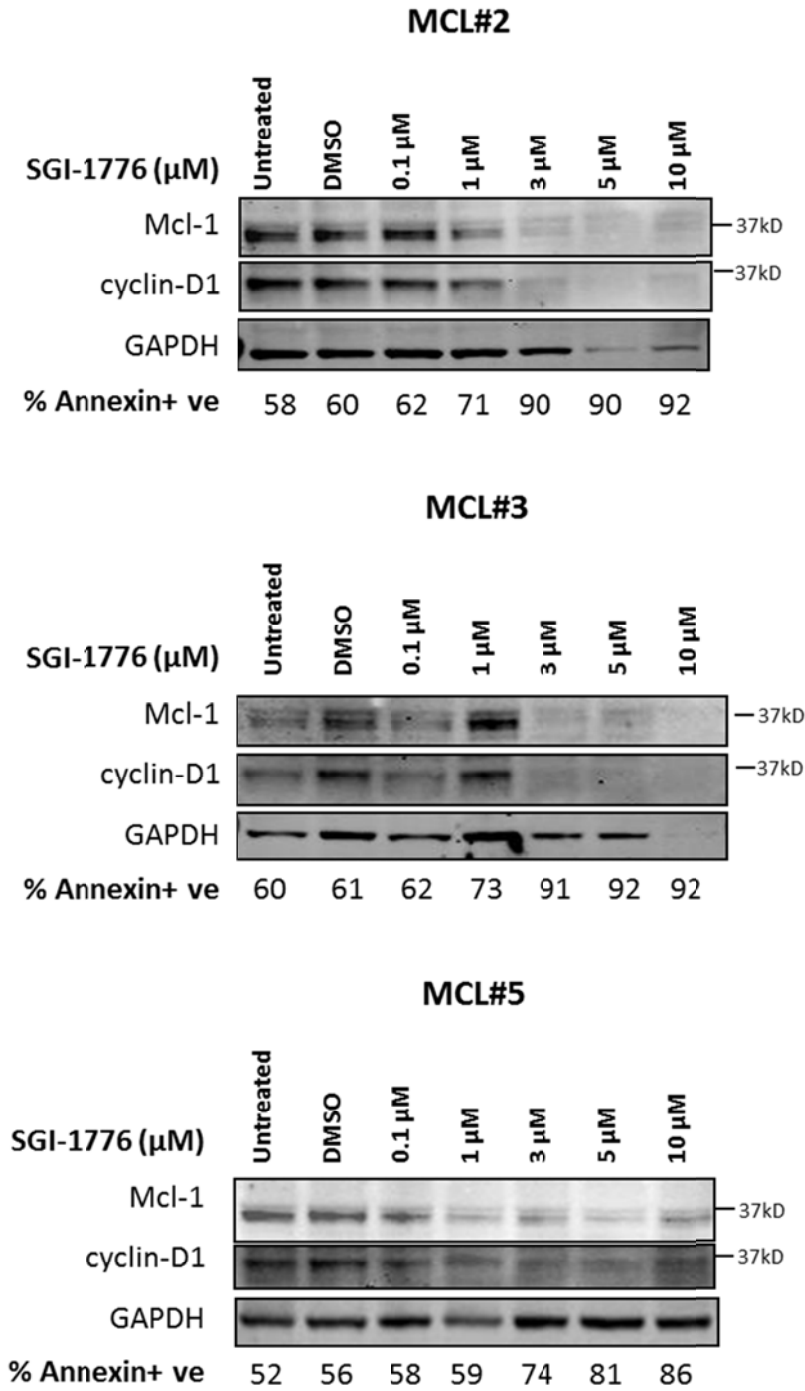
Figure 32. Effect on Pim kinase phosphorylation targets by SGI-1776 treatment in normal PBMCs.

Normal PBMCs isolated from a patient in remission, and three healthy donors' blood samples were either untreated or treated with DMSO or different doses of SGI-1776 (1, 3, 10μM) for 24hr. Cells were harvested and protein lysate was extracted for immunoblot analysis. Expression levels of phospho- and total c-Myc, phospho- and total 4E-BP1, and GAPDH proteins were measured. Annexin V/PI positivity values were marked under each lane of the immunoblots. Untreated Mino cells were used as positive control displayed on the far right panel.

Figure 32.
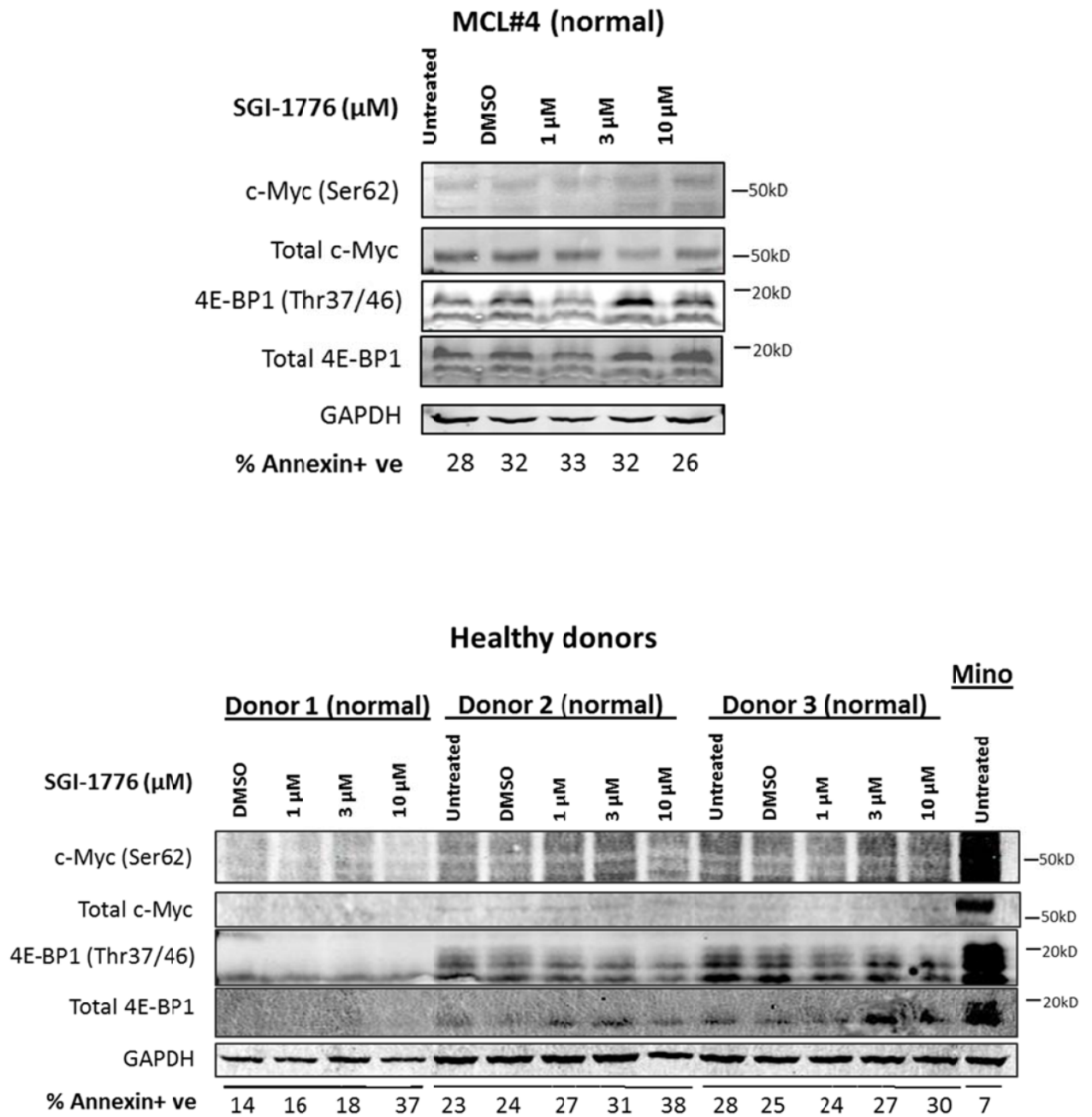
Effect of SGI-1776 on MCl-1 and cyclin D1 levels in normal PBMCs.

We also tested the effect of SGI-1776 on Mcl-1 and cyclin D1 in normal PBMCs, and found that although some normal PBMCs express high levels of Mcl-1, but SGI-1776 failed to reduce their levels even at high doses (Figure 33).

Effect of SGI-1776 on *MCL1* mRNA levels in MCL primary patent samples.

To further validate the effect of SGI-1776 on transcription regulation, we tested its effect on short-lived *MCL1* mRNA levels, in malignant PBMCs (Figure 34). Two late-staged MCL samples were used to isolate malignant PBMCs for this study. Cells were treated with DMSO, or 1, 3, and 5μM of SGI-1776 for 24hr, then they were harvested and total RNA was extracted for RT-PCR studies.

In both samples, there was a dose-dependent decrease of *MCL1* mRNA levels, started at 1μM concentration. MCL#1 had a greater than 40% decrease of *MCL1* by 10μM whereas in MCL#5, this level dropped to 44% of DMSO control.

Effect of SGI-1776 on *MCL1* mRNA levels in normal PBMCs.

We also tested the effect of SGI-1776 on *MCL1* levels in normal PBMCs, where cells were also treated with SGI-1776 (1, 3, 10μM) for 24hr as mentioned above (Figure 35).

Interestingly, we did not observe a consistent trend of decrease of *MCL1* levels in these samples –in MCL#4, *MCL1* level first increased and then dropped to 80% of DMSO control, whereas in Lymph# 2 and 3, the *MCL1* levels decreased by 3μM but increased at 10μM.

Figure 33. Dose-dependent reduction of short-lived Mcl-1 and cyclin D1 protein expression levels by SGI-1776 treatment in normal PBMCs.

Normal PBMCs isolated from a patient in remission, and three healthy donors' blood samples were either untreated or treated with DMSO or different doses of SGI-1776 (1, 3, 10μM) for 24hr. Cells were harvested and protein lysate was extracted for immunoblot analysis. Expression levels of Mcl-1, cyclin D1 and GAPDH proteins were measured. Annexin V/PI positivity values were marked under each lane of the immunoblots. Untreated Mino cells were used as positive control displayed on the far right panel.

Figure 33.

MCL#4 (normal)

SGI-1776 (μM)	Untreated	DMSO	1 μM	3 μM	10 μM	
Mcl-1						—37kD
cyclin-D1						—37kD
GAPDH						
% Annexin+ ve	28	32	33	32	26	

Healthy donors

	Donor 1 (normal)				Donor 2 (normal)					Donor 3 (normal)					**Mino**	
SGI-1776 (μM)	DMSO	1 μM	3 μM	10 μM	Untreated	DMSO	1 μM	3 μM	10 μM	Untreated	DMSO	1 μM	3 μM	10 μM	Untreated	
Mcl-1																—37kD
cyclin-D1																—37kD
GAPDH																
% Annexin+ ve	14	16	18	37	23	24	27	31	38	28	25	24	27	30	7	
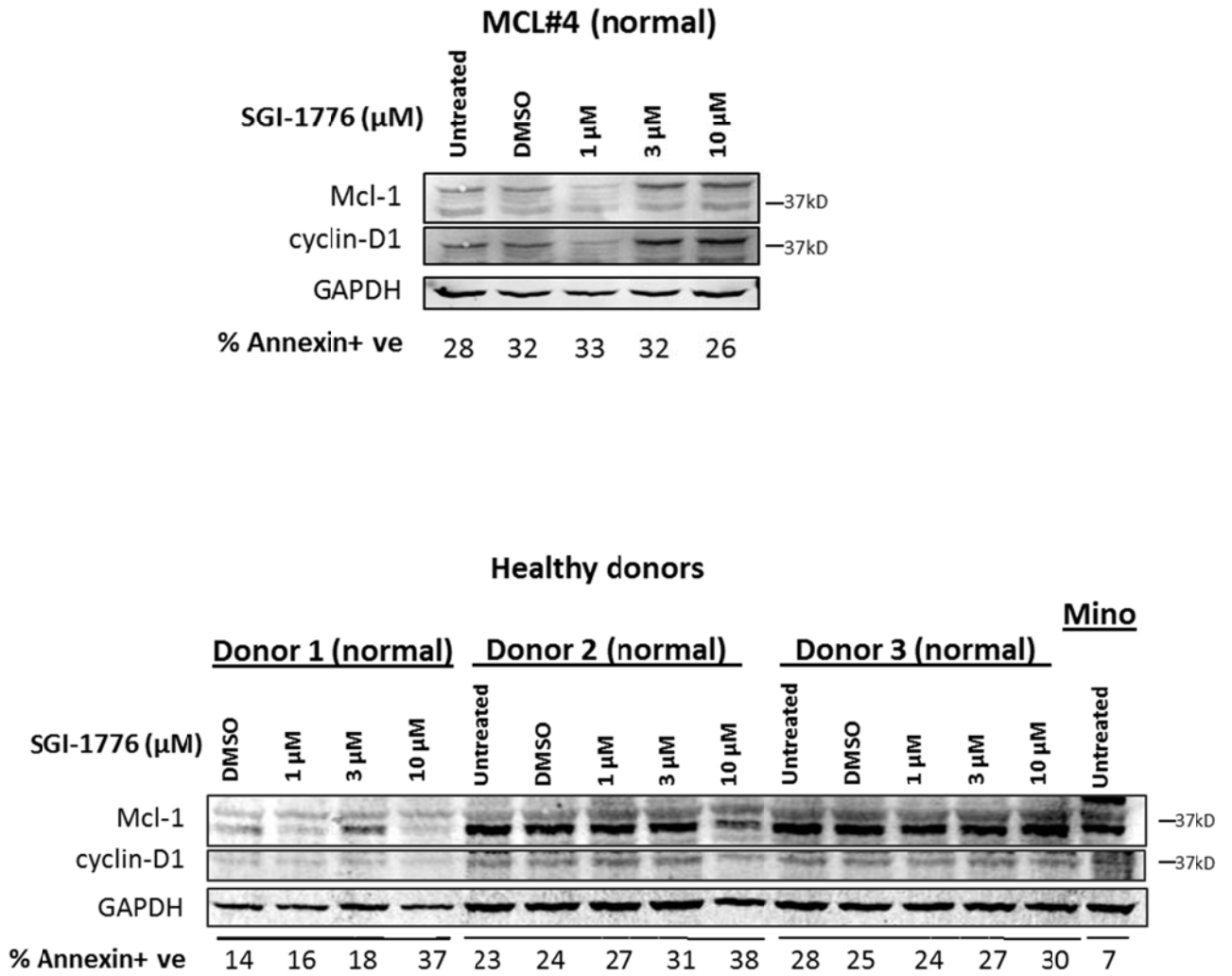
Figure 34. Reduction of *MCL1* mRNA levels in MCL primary cells.

Malignant PBMCs isolated from two blood samples of MCL patients were either untreated or treated with DMSO or different doses of SGI-1776 (1, 3, 10µM) for 24hr. Cells were then harvested and total RNA was extracted and purified. Expression levels of *MCL1* mRNA were measured using RT-PCR, and results were normalized to *18S* and also DMSO control.

Figure 34.
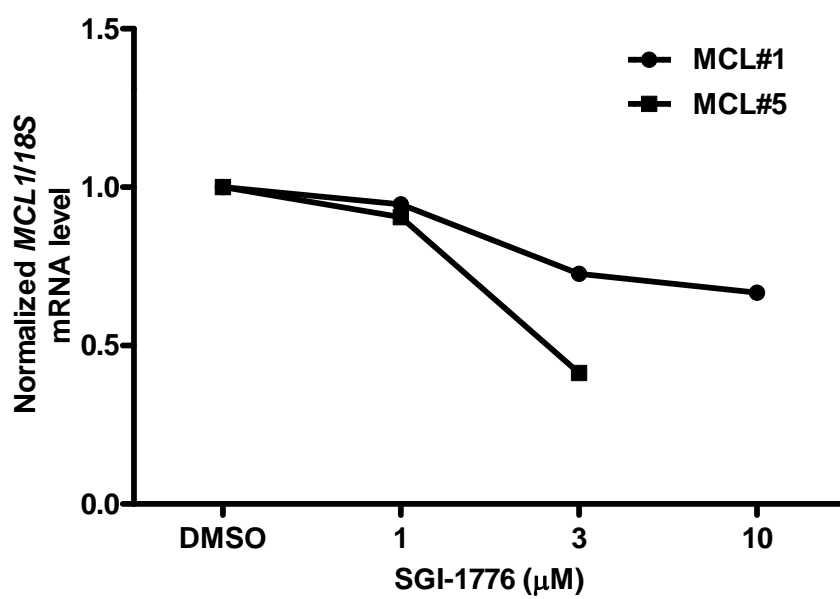
Figure 35. Effect on *MCL1* mRNA levels by SGI-1776 treatment in normal PBMCs.

Normal PBMCs isolated from a patient in remission, and three healthy donors' blood samples of were either untreated or treated with DMSO or different doses of SGI-1776 (1, 3, 10μM) for 24hr. Cells were then harvested and total RNA was extracted and purified. Expression levels of *MCL1* mRNA were measured using RT-PCR, and results were normalized to *18S* and DMSO control.

Figure 35.
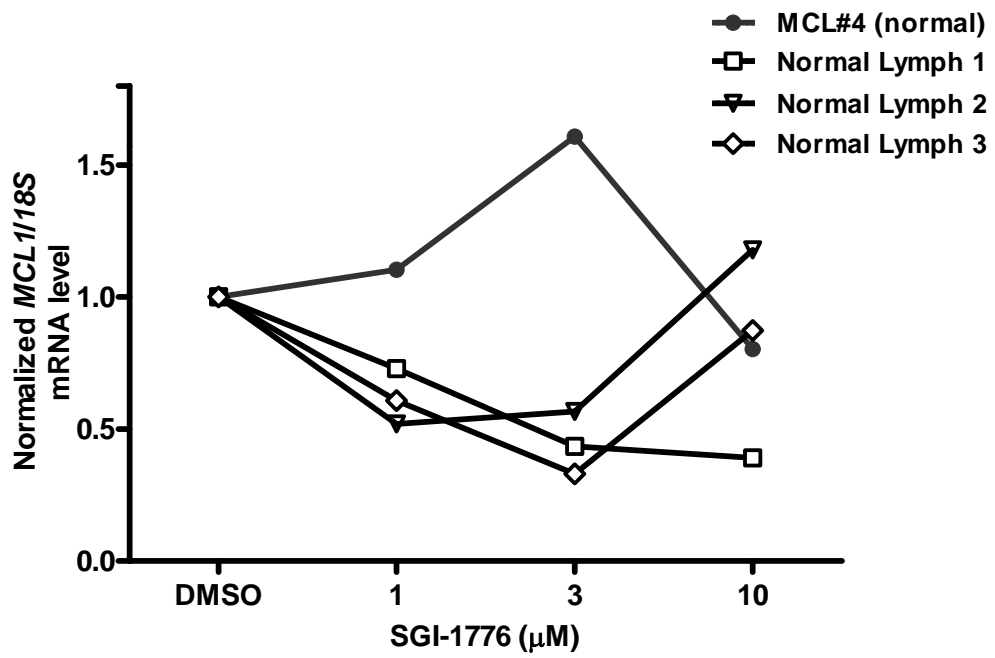
<u>Aim 2.7. Relationships among events of transcription, translation and cell death in MCL cell lines.</u>

In order to generate a clear picture among the relationships among the phenomenon observed on transcription, translation and cell death lead by SGI-1776 treatments in MCL cell lines, we drew correlations between specific events of each aspect.

<u>Relationship between global transcription inhibition and cell death in MCL cell lines.</u>

First, we began by evaluating the relationship between global transcription reduction and cell death. To establish the relationship, we chose the global RNA synthesis inhibition data of the dose-dependent SGI-1776 treatment in four MCL cell lines, calculated into percentages of total population and normalized to DMSO control, and then plotted them against cell death data, also in percentage and normalized to control (Figure 36).

Linear correlation was drawn and the calculated linear regression values were >0.9 for JeKo-1, Granta 519 and Mino, whereas in SP-53, $r^2 = 0.68$. Collectively of the four cell lines together, $r^2 = 0.8$ with p<0.0001. This indicated that RNA synthesis inhibition was directly correlated with cell death in four MCL cell lines.

<u>Relationship between reduction of c-Myc (Ser62) phosphorylation and inhibition of global transcription in MCL cell lines.</u>

We tested the relationship between reduction of c-Myc (Ser62) phosphorylation –a consistent event triggered by SGI-1776 treatment in both MCL cell lines and MCL primary samples, and global RNA synthesis in JeKo-1 and Mino cell lines. Ratios of c-Myc (Ser62)/total c-Myc were calculated from dose-dependent SGI-1776 treatments in both cell lines, normalized to DMSO control, and then plotted against global transcription inhibition (Figure 37).

Figure 36.
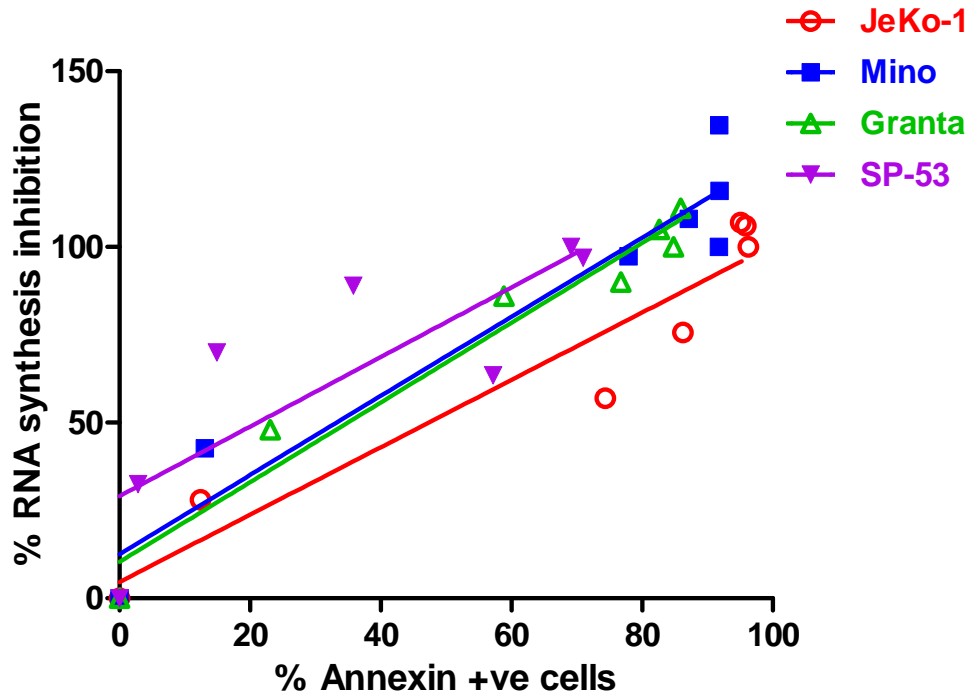
Figure 36. Strong correlation between global RNA synthesis inhibition and cell death lead by SGI-1776 treatment in MCL cell lines.

Both global RNA synthesis and cell death was measured in percentage of population, values were taken from dose-dependent SGI-1776 treatment for 24hr in JeKo-1, Mino, Granta 519 and SP-53 MCL cell lines. RNA synthesis inhibition was correlated with cell death by using linear regression, and r^2 and p values were calculated using the GraphPad Prism software.

Figure 37.
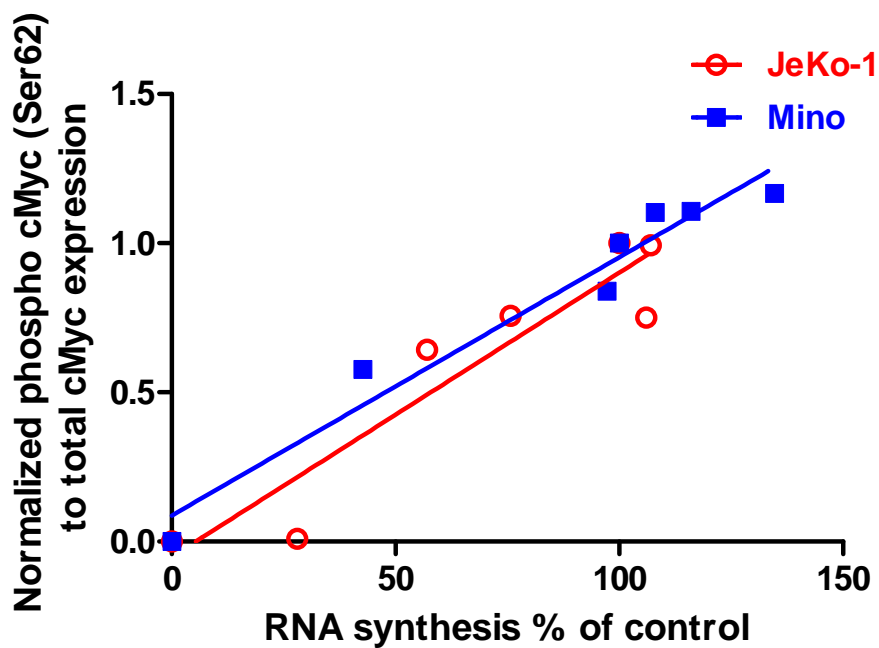
Figure 37. Strong correlation between decrease of c-Myc phosphorylation and RNA synthesis inhibition lead by SGI-1776 treatment in MCL cell lines.

Both decrease of c-Myc phosphorylation and cell death was measured in percentage of population, whereas ratios of phospho-c-Myc to total c-Myc was calculated then normalized to DMSO control. Values were taken from dose-dependent SGI-1776 treatment for 24hr in JeKo-1 and Mino cell lines. Phospho-c-Myc/total c-Myc was correlated with RNA synthesis inhibition using linear regression, and r^2 and p values were calculated using the GraphPad Prism software.

We observed a strong correlation between decrease of c-Myc phosphorylation and cell death in both cell lines, with linear regression value of >0.9, and p<0.02, suggesting the direct relationship of these two events.

Relationship between reduction of c-Myc (Ser62) phosphorylation and decrease of *MCL1* mRNA levels in MCL cell lines.

We tested the relationship within transcription regulation, between decrease of c-Myc phosphorylation and reduction of *MCL1* mRNA levels in JeKo-1 and Mino cells treated with SGI-1776. Data were extracted from immunoblots evaluating c-Myc phosphorylation and RT-PCR measuring changes of *MCL1* levels, calculated into c-Myc (Ser62)/total c-Myc and *MCL1/18s*, respectively, both normalized to DMSO control, and then plotted against each other (Figure 38).

We were also able to draw a strong association between the two events, with $r^2=0.7$ and p<0.03 with two cell lines taken together, which indicate a direct relationship of the two events.

Relationship between reduction of 4E-BP1 (Thr37/46) and cell death in MCL cell lines.

We also evaluated the relationship between translation and cell death, by drawing association between reduction of 4E-BP1 (Thr37/46) and increase in apoptosis levels in JeKo-1 and Mino cells treated with SGI-1776. Data were taken from immunoblots measuring the changes of phosphorylation of 4E-BP1 in dose-dependent SGI-1776 treatments in JeKo-1 and Mino cells, and ratios of phospho-/total protein levels were calculated, and plotted against apoptosis levels (Figure 39). Linear regression was performed and r^2 and p values were calculated using the GraphPad Prism software.

Figure 38.
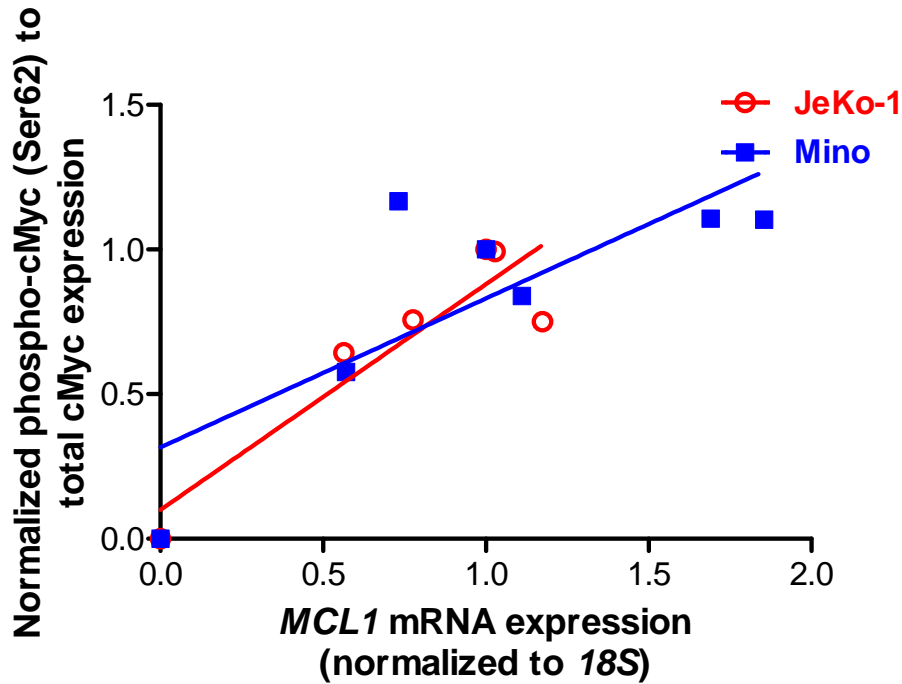
Figure 38. Strong correlation between decrease of c-Myc phosphorylation and decrease of

***MCL1* mRNA levels by SGI-1776 treatment in MCL cell lines.**

Both decrease of c-Myc phosphorylation and decrease in *MCL1* mRNA levels were measured in percentage of population, whereas ratios of phospho-c-Myc to total c-Myc was calculated then normalized to DMSO control, also ratios of *MCL1* to *18S* was calculated and also normalized to DMSO control. Values were taken from dose-dependent SGI-1776 treatment for 24hr in JeKo-1 and Mino cell lines. Phospho-c-Myc/total c-Myc was correlated with reduction of *MCL1* levels using linear regression, and r^2 and p values were calculated using the GraphPad Prism software.

Figure 39.
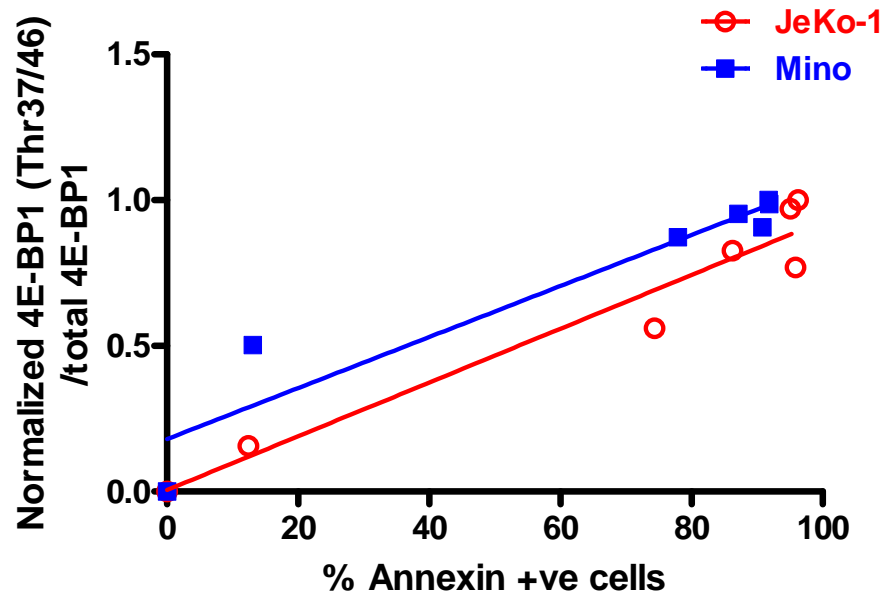
Figure 39. Strong correlation between decrease of 4E-BP1 phosphorylation and cell death by

SGI-1776 treatment in MCL cell lines.

Both decrease of 4E-BP1 phosphorylation and cell death levels were measured in percentage of population, whereas ratios of phospho-4E-BP1 to total 4E-BP1 was calculated then normalized to DMSO, cell death levels were also normalized to DMSO control. Values were taken from dose-dependent SGI-1776 treatment for 24hr in JeKo-1 and Mino cell lines. Phospho-4E-BP1/total 4E-BP1 was correlated with cell death levels using linear regression, and r^2 and p values were calculated using the GraphPad Prism software.

As expected, a strong correlation was detected between decrease of phospho-4E-BP1 and increase of apoptosis, with linear regression value of >0.9 and p<0.01. This also points to a direct relationship between translation inhibition and cell death.

Relationship between reduction of 4E-BP1 (Thr37/46) and Mcl-1 protein levels in MCL cell lines.

With regard to translation regulation, we looked at decrease of phospho-4E-BP1 and Mcl-1 protein levels in SGI-1776-treated JeKo-1 and Mino cells (Figure 40). Again, we found strong association between decrease of 4E-BP1 phosphorylation and Mcl-1 protein, with r^2>0.9 and p<0.004.

Figure 40.
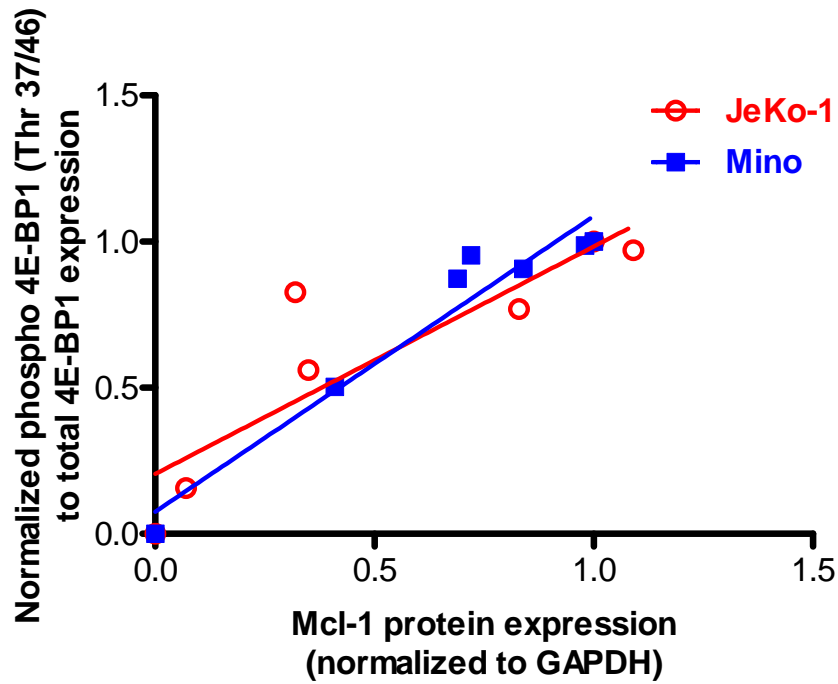
Figure 40. Strong correlation between decrease of 4E-BP1 phosphorylation and decrease of

MCL1 **mRNA levels by SGI-1776 treatment in MCL cell lines.**

Both decrease of 4E-BP1 phosphorylation and decrease in *MCL1* mRNA levels were measured in percentage of population, whereas ratios of phospho-4E-BP1 to total 4E-BP1 was calculated then normalized to DMSO, also ratios of *MCL1* to *18S* was calculated and also normalized to DMSO control. Phospho-4E-BP1/total 4E-BP1 was correlated with reduction of Mcl-1 levels using linear regression, and r^2 and p values were calculated using the GraphPad Prism software.

CHAPTER 4. Combination of bendamustine with SGI-1776 in B-cell lymphoma

Bendamustine is as an FDA-approved drug for NHL that disrupts DNA replication and transcription processes by inducing DNA damage in both replicating and quiescent cells (Leoni 2008; Gandhi 2009). Our studies in MCL have demonstrated that SGI-1776 is cytotoxic in MCL, and its primary mechanism of actions is through targeting transcription and translation, which leads to cell death. Based on the mechanism of actions of bendamustine and SGI-1776, we hypothesized that combination of bendamustine with SGI-1776 will enhance bendamustine-triggered DNA synthesis disruption, while promoting SGI-1776-induced transcription and translation inhibition, which will subsequently lead to more efficient growth inhibition and cell killing in B-cell lymphoma (Figure 41). We also hypothesized that such combination will result in additive to synergistic cytotoxicity in lymphoma cells, and propose the following aim.

Aim 3) Explore the combination strategy of SGI-1776 with bendamustine to identify the primary mechanism of actions to induce cytotoxicity in B-cell lymphoma.

To test this hypothesis, we used 5 and 10μM of bendamustine as this is easily achieved in plasma at maximum tolerated dose. Concentration of SGI-1776 (5μM) was selected based on single agent data in MCL cells described in Chapter 3.

Aim 3. Explore the combination strategy of SGI-1776 with bendamustine to identify the primary mechanism of actions to induce cytotoxicity in B-cell lymphoma.

Aim 3.1. Effect on apoptosis induction by bendamustine and SGI-1776 combination treatment in B-cell lymphoma cells.

Effect on apoptosis induction by bendamustine and SGI-1776 combination treatment in MCL cell lines.

Figure 41.
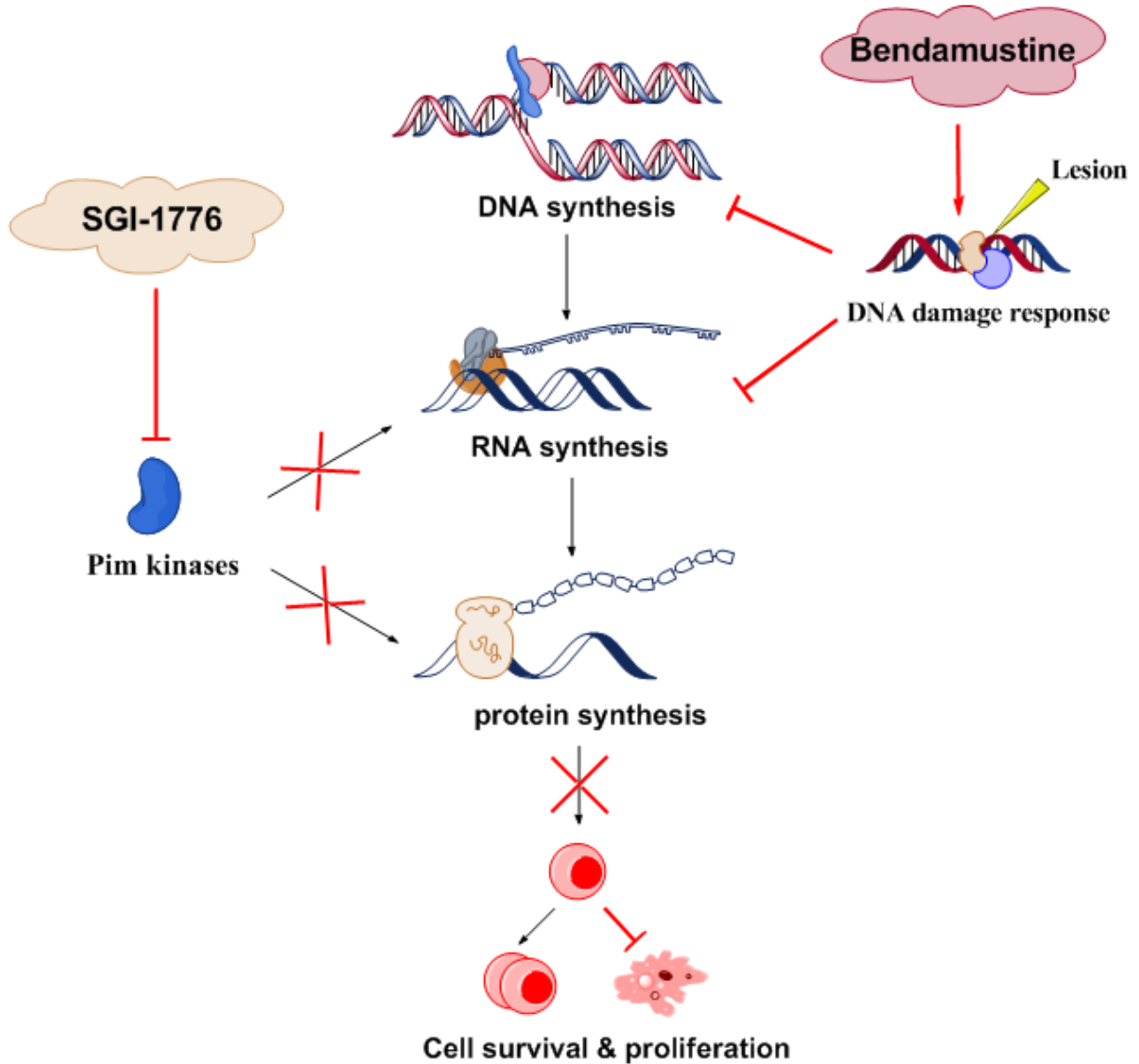
Figure 41. Rationale for combination strategy of bendamustine with SGI-1776 in MCL.

SGI-1776 has shown to sequester transcription and translation pathways whereas bendamustine inhibits DNA synthesis and transcription. Therefore, we hypothesize that combination of these two agents will lead to additive effect in causing apoptosis and disrupting cell proliferation processes.

MCL cell lines JeKo-1 and Mino were treated with DMSO, or selected concentrations of bendamustine (5, 10μM) and SGI-1776 (5μM), or combination of the two drugs (5μM of bendamustine +5μM SGI-1776, or 10μM bendamustine +5μM SGI-1776) for 24hr. Then cells were harvested and analyzed using flow cytometry for annexin V/PI positivity to measure induced apoptosis levels (Figure 42).

In JeKo-1 cells, an increase of 10% and 18% of apoptosis was measured in 5 and 10μM of bendamustine-treated cells, whereas 5μM SGI-1776 resulted in 13% cell death. In combination treatments, 5 or 10μM bendamustine +5μM SGI-1776 killed 24% and 34% of cells, respectively (Figure 42A). Using fractional analysis, the combination method showed more than additive to synergistic effect in cytotoxicity (Table 4).

In Mino cells, an increase of 10% and 22% of apoptosis was observed in 5 and 10μM of bendamustine treatments, while 5μM SGI-1776 killed 10% of the cells. Apoptosis levels in combination treatments were 15% and 25% for 5 or 10μM bendamustine +5μM SGI-1776, respectively (Figure 42B). Fractional analysis indicated more than additive effect in apoptosis induced by bendamustine and SGI-1776 combination in Mino cells (Table 4).

Effect in cell killing induced by bendamustine and SGI-1776 combination treatment in B-cell lymphoma primary samples.

To investigate the effect of bendamustine and SGI-1776 combination treatment in primary cells, we isolated malignant PBMCs from primary samples from patients diagnosed with MCL and splenic marginal zone lymphoma, also a B-cell lymphoma (Table 5). As with the cell lines, primary cells were treated with single agent SGI-1776 or bendamustine alone, or combination of the two drugs for 24hr, and apoptosis levels were analyzed using flow cytometry (Figure 43).

Figure 42. Cell death induced by bendamustine and SGI-1776 combination treatment in MCL cell lines.

MCL cell lines (A)JeKo-1 and (B)Mino were treated with DMSO, or different doses of bendamustine (5, 10µM) or 5µM SGI-1776, or combination of these two drugs are these concentrations (5 or 10µM bendamustine+ 5µM SGI-1776) for 24hr, then apoptosis levels were measured by annexin V/PI positivity measured by flow cytometry. Experiments were done in triplicate and results were shown as average cell death levels ± SEM.

B, bendamustine; S, SGI-1776.

Figure 42.

A
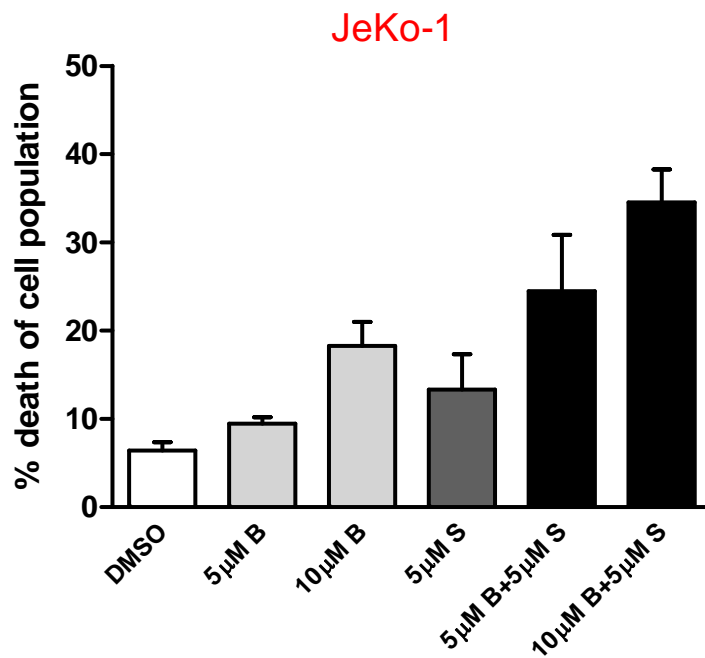
B
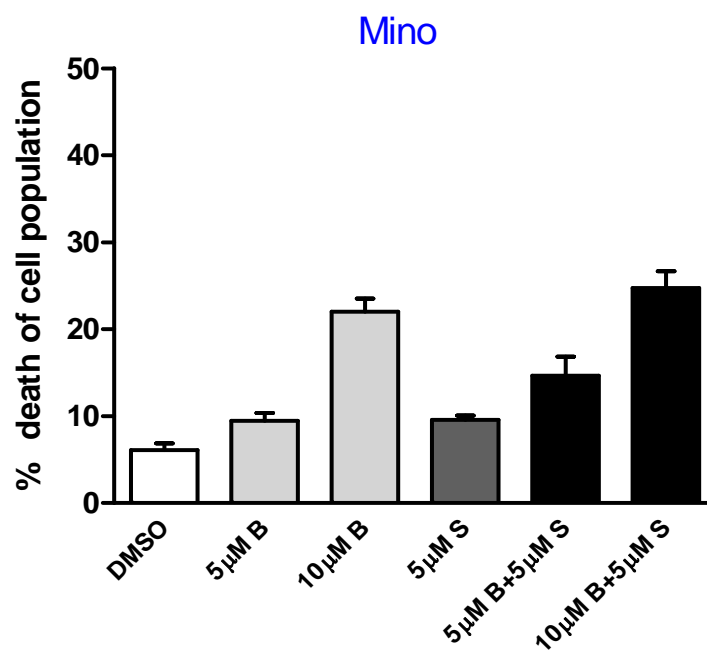
Table 4.

	Expected cell death		Observed cell death	
	5µM Bendamustine +5µM SGI-1776	10µM Bendamustine +5µM SGI-1776	5µM Bendamustine +5µM SGI-1776	10µM Bendamustine +5µM SGI-1776
JeKo-1	10%	18%	18%	28%
Mino	9%	26%	13%	31%
MCL	23%	24%	18%	21%
SMZL	34%	38%	35%	37%

Table 4. Factional analysis of combination of SGI-1776 with bendamustine in B-cell lymphoma.

Formula for fractional analysis:
%survival drug A X %survival drug B=Expected survival
1-%Expected survival rate=%Expected death

- Expected death>Observed death→ Less than additive to antagonistic
- Expected death=Observed death→ Additive
- Expected death<Observed death→ More than additive to synergistic

Table 5.

Patient numbers	6	7
Dx	MCL	SMZL
Sample type	PB	PB
Tumor cells % of lymphocytes	69	N/A
Patient age, yrs	57	75
White blood count, per μL	23,400	63,400
Lymphocytes%	71	87
Neutrophils%	24	10
Metaphase%	0	0
Blasts%	0	0
Monocytes%	2	2
Growth Factor	No	No

Table 5. B-cell lymphoma patient characteristics.

SMZL: splenic marginal zone lymphoma

PB, peripheral blood.

Figure 43. Cell death induced by bendamustine and SGI-1776 combination treatment in B-cell lymphoma primary cells.

Primary cells isolated from (A)MCL and (B)SMZL patients were treated with DMSO, or different doses of bendamustine (5, 10µM) or 5µM SGI-1776, or combination of these two drugs are these concentrations (5 or 10µM bendamustine+ 5µM SGI-1776) for 24hr, then apoptosis levels were measured by annexin V/PI positivity measured by flow cytometry.

B, bendamustine; S, SGI-1776.

Figure 43.

A

MCL#6

B

SMZL#7
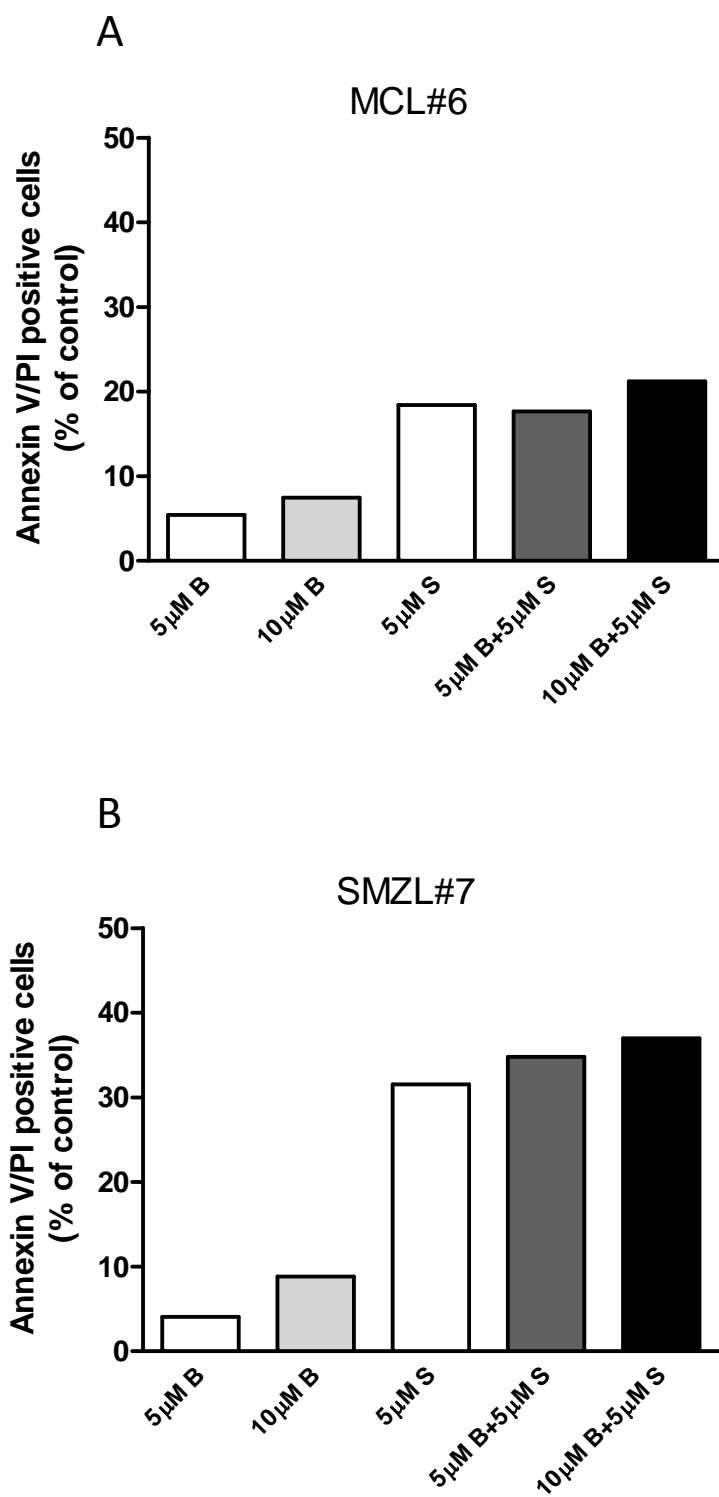
In the MCL primary patient sample, bendamustine single agent treatment resulted in low levels of apoptosis, 5% and 7% for 5 or 10μM bendamustine, respectively. However, single agent SGI-1776 was more effective in cell killing (18%). Combination treatments of 5 or 10μM bendamustine + 5μM SGI-1776 killed 18% and 22% of MCL cells, respectively (Figure 43A). Note that these numbers were pure cell kill induced by drug treatments –in order to prevent misunderstanding of the data, the endogenous cell deaths were subtracted from the total values. Fractional analysis indicated a less than additive effect in cell killing using this combination method in this particular MCL primary sample (Table 4).

In the SMZL samples, bendamustine single treatment resulted in less than 10% of cell death, whereas 5μM SGI-1776 induced 30% cell death. Combination treatments lead to 35%-37% of apoptosis (Figure 43B). Fractional analysis indicated additive effect in cell death in these specific SMZL primary cells.

Aim 3.2. Effect on DNA synthesis inhibition by bendamustine and SGI-1776 combination in JeKo-1.

To determine the effect of bendamustine and SGI-1776 on DNA synthesis, radioactive thymidine incorporation assay was performed in MCL cell line, JeKo-1. JeKo-1 cells were treated with bendamustine (5, 10μM) or SGI-1776 (5μM), or combination of the two drugs (5μM or 10μM bendamustine+5μM SGI-1776) for 24hr., Radioactively-labeled thymidine was added 45min before cell harvest, then incorporated radioactivity was measured using scintillation counter (Figure 44).

A reduction of 28% and 51% in DNA synthesis was detected by 5 and 10μM bendamustine treatment alone (p=0.04 and 0.03, respectively), whereas 5μM SGI-1776 decreased DNA synthesis by 24% of DMSO control. In combination studies, DNA synthesis was reduced to 57% and 40% of DMSO control, for 5 or 10μM bendamustine+5μM SGI-1776 treatments (p=0.03 and 0.04, respectively).

Figure 44.

Figure 44. Effect of bendamustine and SGI-1776 combination treatment on DNA synthesis

inhibition by in JeKo-1 cells.

JeKo-1 cells were treated with DMSO, bendamustine (5, 10µM) or SGI-1776 (5µM), or combination of these two drugs are these concentrations (5 or 10µM bendamustine+ 5µM SGI-1776) for 24hr, then cells were incubated with [methyl- ^{3}H]-thymidine at 0.8µCi/mL for 45min. Incorporated radioactivity was measured by scintillation counter and values were calculated into DPM/cell which was further normalized to DMSO control. Experiments were done in triplicate and results shown are average ratios ± SEM. Student t-test was perform to calculate statistical significance.

B, bendamustine; S, SGI-1776.

Compared to 5or 10μM of bendamustine treatment alone, 5 or 10μM bendamustine+5μM SGI-1776 combination treatments induced statistically significant decrease of DNA synthesis (p=0.02 and 0.1, respectively).

<u>Aim 3.3. Effect on RNA synthesis inhibition by bendamustine and SGI-1776 combination in MCL cell line and B-cell lymphoma primary cells.</u>

To examine the effect of bendamustine and SGI-1776 on global RNA synthesis, we performed uridine incorporation experiment where radioactively-labeled uridine was co-incubated with JeKo-1 cells after they were treated with single agent or combination of bendamustine and SGI-1776 using above concentrations (Figure 45).

Bendamustine treatment alone did not significantly reduce RNA synthesis levels, with only a 5% decrease with 10μM. However, consistent with our previous study, SGI-1776 inhibited RNA synthesis and a 24% decrease was detected with 5μM of SGI-1776 (Yang 2012). Around 20% decrease of global RNA levels were detected when bendamustine and SGI-1776 was combined. These changes in RNA synthesis showed a trend for a decrease when cells were treated with both drugs, but this was not statistically significant. To evaluate the inhibitory effect of bendamustine or SGI-1776 in primary patient cells, PBMCs from patients diagnosed with MCL or SMZL were isolated (Table 4), and treated with bendamustine or SGI-1766, or combination of the two drugs, and then uridine incorporation was carried out and measured using scintillation counter (Figure 46).

In MCL primary cells, bendamustine did not reduce the global RNA synthesis level, and SGI-1776 treatment alone lead to a moderate decreased of global RNA level (7%). However, when used in combination, the RNA synthesis levels were reduced to 76% and 60% of DMSO control, in respect of 5 or 10μM bendamustine + 5μM SGI-1776 treatments (Figure 46A).

In SMZL primary cells, 5 and 10μM of bendamustine caused 7% and 73% decrease in RNA synthesis, whereas SGI-1776 was ineffective in reducing RNA synthesis.

Figure 45.
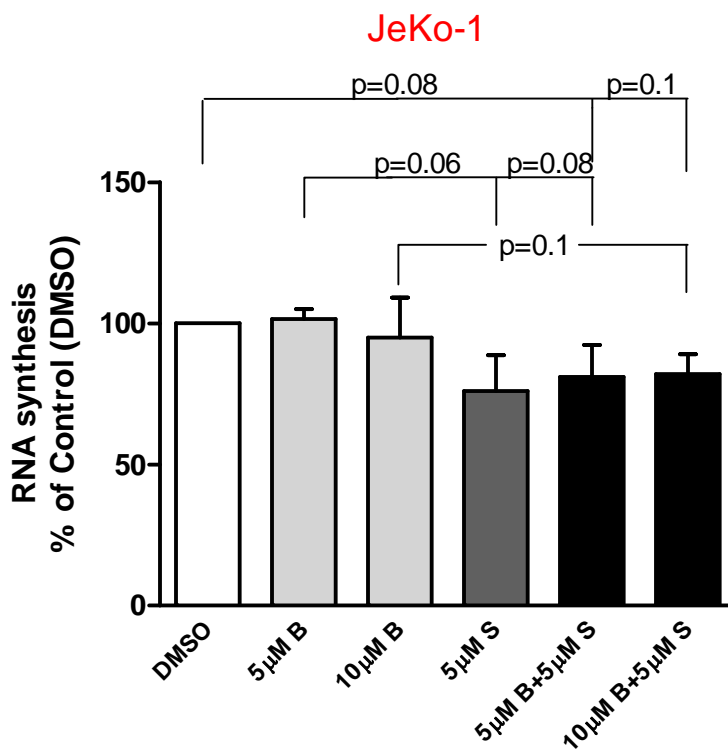
Figure 45. Effect of bendamustine and SGI-1776 combination treatment on RNA synthesis inhibition in JeKo-1 cells.

JeKo-1 cells were treated with DMSO, bendamustine (5, 10µM), SGI-1776 (5µM), or combination of these two drugs are these concentrations (5 or 10µM bendamustine+ 5µM SGI-1776) for 24hr, then cells were incubated with [5,6- ^{3}H]-uridine at 0.8µCi/mL for 45min. Incorporated radioactivity was measured by scintillation counter and values were calculated into DPM/cell which was further normalized to DMSO control. Experiments were performed in triplicate and results shown as average ratios ± SEM. Student t-test was perform to calculate statistical significance.

B, bendamustine; S, SGI-1776.

Figure 46. Effect of bendamustine and SGI-1776 combination treatment on RNA synthesis inhibition in B-cell lymphoma primary cells.

PBMCs isolated from (A)MCL and (B)SMZL patients were treated with DMSO, bendamustine (5, 10µM) , SGI-1776 (5µM), or combination of these two drugs are these concentrations (5 or 10µM bendamustine+ 5µM SGI-1776) for 24hr, then cells were incubated with [5,6-^{3}H]-uridine at 0.8µCi/mL for 45min. Incorporated radioactivity was measured by scintillation counter and values were calculated into as DPM/cell and were further normalized to DMSO control.

B, bendamustine; S, SGI-1776.

Figure 46.

A

MCL#6

B   SMZL#7

When used in combination, 5 or 10μM bendamustine + 5μM SGI-1776 lead to 4% and 79% of RNA synthesis decrease compared to DMSO control (Figure 46B).

These data suggest that SGI-1776 was more effective in reducing global RNA synthesis in replicating cell lines whereas bendamustine was more effective in quiescent primary B-cell lymphoma samples; combination of the two drugs was also effective in reducing global transcription levels.

Aim 3.4. Effect on protein synthesis inhibition by bendamustine and SGI-1776 combination in MCL cell line and B-cell lymphoma primary cells.

SGI-1776 is known to target protein synthesis in MCL cell lines and primary samples, as shown in our previous study (Yang 2012). It is also known that bendamustine lead to DNA damage which further causes disruption of DNA synthesis repair and transcription processes (Gandhi 2009; Rummel 2011). Hence, we hypothesize that SGI-1776-induced global translation inhibition is maintained or enhanced in the presence of bendamustine.

To investigate the effect of bendamustine and SGI-1776 treatment on protein synthesis, we treated JeKo-1 cells with bendamustine, SGI-1776, or combination of the two drugs, and then performed leucine incorporation experiments to analyze the reduction of protein synthesis caused by these treatments (Figure 47).

Bendamustine treatment (5, 10μM) reduced protein synthesis levels by 10%-13%, whereas SGI-1776 (5μM) brought it down to 60% of control. In combination studies, 5 or 10μM of bendamustine + 5μM of SGI-1776 reduced protein synthesis to 68% and 54% of DMSO control ($p<0.05$, respectively). Additionally, both 5μM bendamustine+5μM SGI-1776 lead to statistically significant decrease of protein synthesis compared to 5μM bendamustine alone ($p=0.06$).
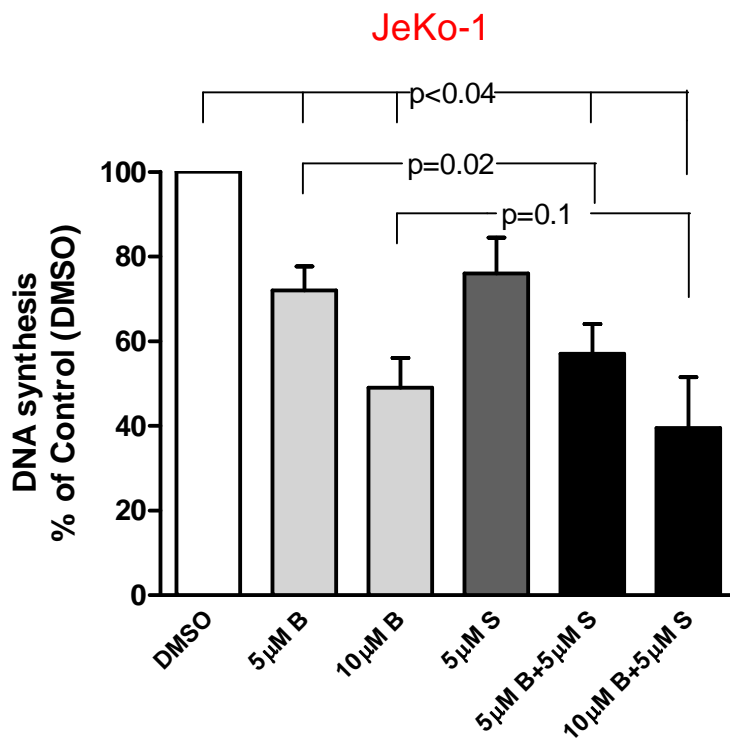
Figure 47.
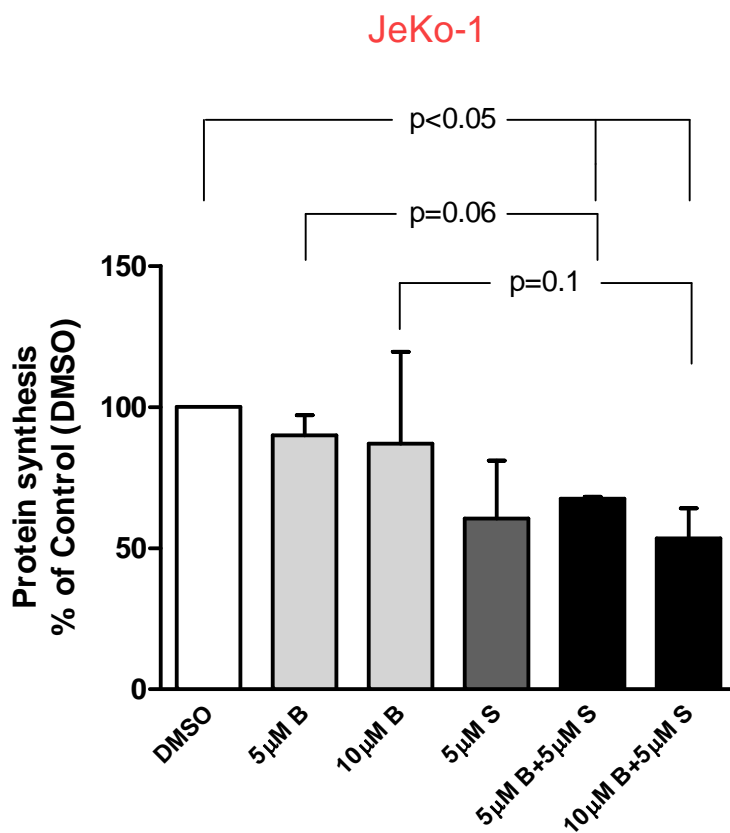
Figure 47. Effect of bendamustine and SGI-1776 combination treatment on protein synthesis inhibition in JeKo-1 cells.

JeKo-1 cells were treated with DMSO, bendamustine (5, 10µM), SGI-1776 (5µM), or combination of these two drugs are these concentrations (5 or 10µM bendamustine+ 5µM SGI-1776) for 24hr, then cells were incubated with [4,5- ^{3}H]-L-leucine at 0.8µCi/mL for 45min. Incorporated radioactivity was measured by scintillation counter and values were calculated into DPM/cell and were further normalized to DMSO control. Experiments were done in triplicate and results shown as average ratios ± SEM. Student t-test was perform to calculate statistical significance.

B, bendamustine; S, SGI-1776.

To confirm the effect of bendamustine and SGI-1776 on protein synthesis, we used the PBMCs isolated from MCL or SMZL patient samples and conducted leucine incorporation experiments to measure the decrease of protein synthesis in these model systems (Figure 48).

In MCL sample, 5 and 10μM of bendamustine reduced protein synthesis to around 50% of DMSO control, whereas 5μM SGI-1776 decrease this level to 42% of control. In combination treatment, protein synthesis levels were reduced to 28% and 42% of DMSO control, in respect of 5 or 10μM of bendamustine + 5μM of SGI-1776 treatment, respectively (Figure 48A).

In SMZL sample, interestingly, only 5μM of bendamustine treatment decreased protein synthesis level (85% of control), but not 10μM treatment. 5μM of SGI-1776 reduced protein synthesis by 5%. When used together, protein synthesis decreased to 63% and 75% of DMSO control, for 5 or 10μM of bendamustine + 5μM of SGI-1776 treatment, respectively (Figure 48B).

These data indicated that bendamustine was more effective in reducing global protein synthesis in quiescent primary B-cell lymphoma than in replicating JeKo-1 cells. SGI-1776 alone and combination with bendamustine were both effective in reducing global protein synthesis in both model systems.

Aim 3.5. Effect on DNA damage marker γ-H2AX by bendamustine and SGI-1776 combination in JeKo-1 cells.

To determine whether addition of SGI-1776 affects bendamustine-induced DNA damage response, we performed immunostaining of JeKo-1 cells to analyze changes in the levels of phospho-Histone 2A variant X (H2AX) at Ser139, also known as γ-H2AX, following bendamustine and SGI-1776 combination treatments.

Figure 48. Effect of bendamustine and SGI-1776 combination treatment on protein synthesis inhibition in B-cell lymphoma primary samples.

PBMCs isolated from (A)MCL and (B)SMZL patients were treated with DMSO, bendamustine (5, 10μM), SGI-1776 (5μM), or combination of these two drugs are these concentrations (5 or 10μM bendamustine+ 5μM SGI-1776) for 24hr, then cells were incubated with [4,5-^{3}H]-L-leucine at 0.8μCi/mL for 45min. Incorporated radioactivity was measured by scintillation counter and values were calculated into DPM/cell and were further normalized to DMSO control.

B, bendamustine; S, SGI-1776.

Figure 48.

A

MCL#6

B

SMZL#7
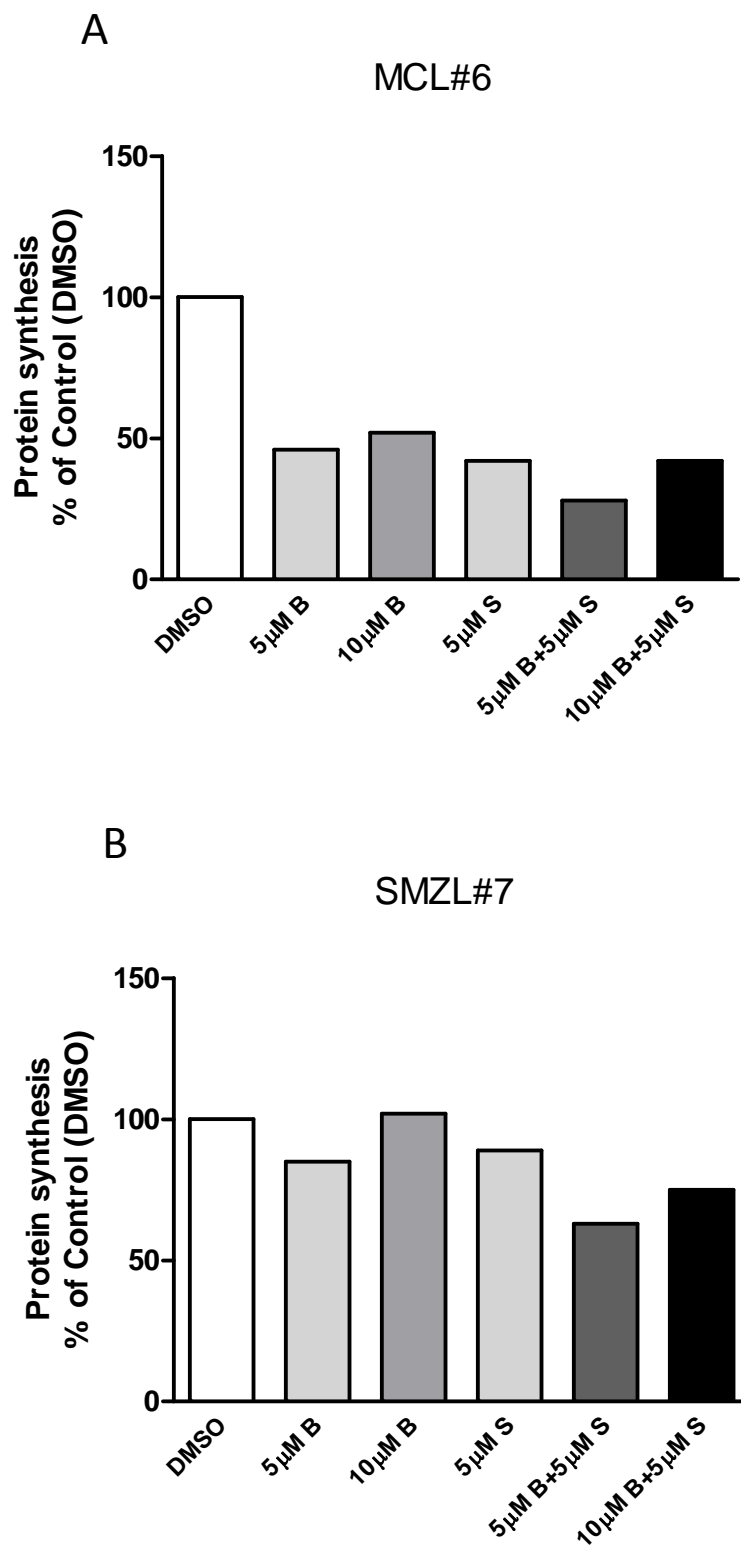
JeKo-1 cells were treated with bendamustine (5, 10μM), with or without 5μM SGI-1776, then cells were fixed and stained with primary antibodies to detect γ-H2AX (Ser139), as a measure for DNA damage (Figure 49).

Consistent with our hypothesis, DNA damage was detected in bendamustine-treated cells, with an increase of 14% and 49% of positive γ-H2AX levels with 5 and 10μM bendamustine, respectively. Addition of SGI-1776 did not resulted in significant increase in γ-H2AX phosphorylation. In combination, 13% and 38% of positive γ-H2AX were detected for 5, 10μM bendamustine +5μM SGI-1776 treatments, indicating that SGI-1776 did not significantly augment bendamustine-induced γ-H2AX formation, and bendamustine-induced DNA damage repair is maintained.

Figure 49. Effect of SGI-1776 treatment on bendamustine-induced γ-H2AX expression in

JeKo-1 cells.

JeKo-1 cells were treated with DMSO, bendamustine (5, 10µM), SGI-1776 (5µM), or combination of these two drugs are these concentrations (5 or 10µM bendamustine+ 5µM SGI-1776) for 24hr, then cells were harvested and fixed by cold 70% ethanol overnight. Cells were then washed and incubated with 0.5% goat serum for 1hr, then probed with primary antibody phospho-histone γ-H2AX (1:500) for 2hr followed by secondary antibody Alexa Fluor mouse IgG (1:200) for 1hr. Cells were then washed and co-incubated with a mixture of 10µg/mL propidium iodine and 2.5µg/mL DNAse-free RNAse for 15min. Cells were analyzed for fluorescence signal shift using flow cytometry to detect the extensiveness of DNA damage. Fluorescence-positive cells were marked as γ-H2AX positive and results were normalized by subtracting endogenous γ-H2AX levels in DMSO-treated cells. Experiments were done in triplicate and results were shown as average ratios ± SEM. Student t-test was perform to calculate statistical significance.
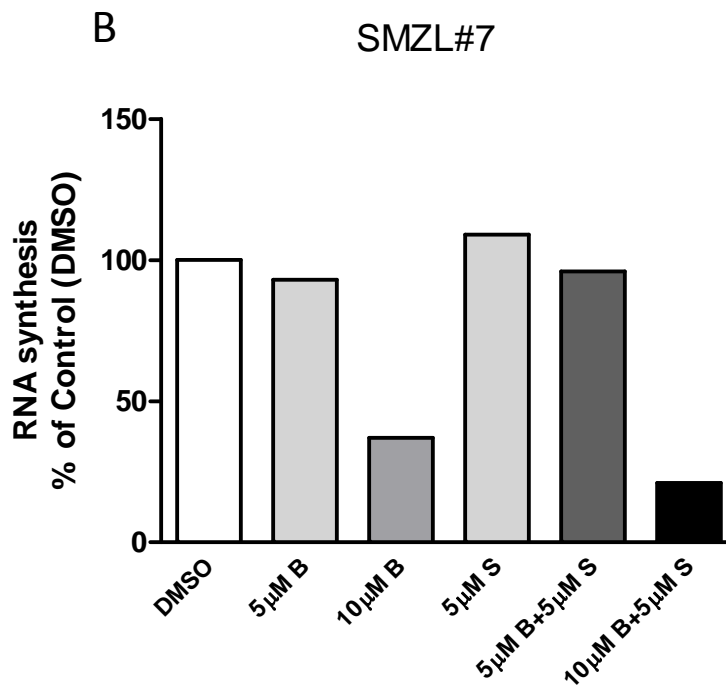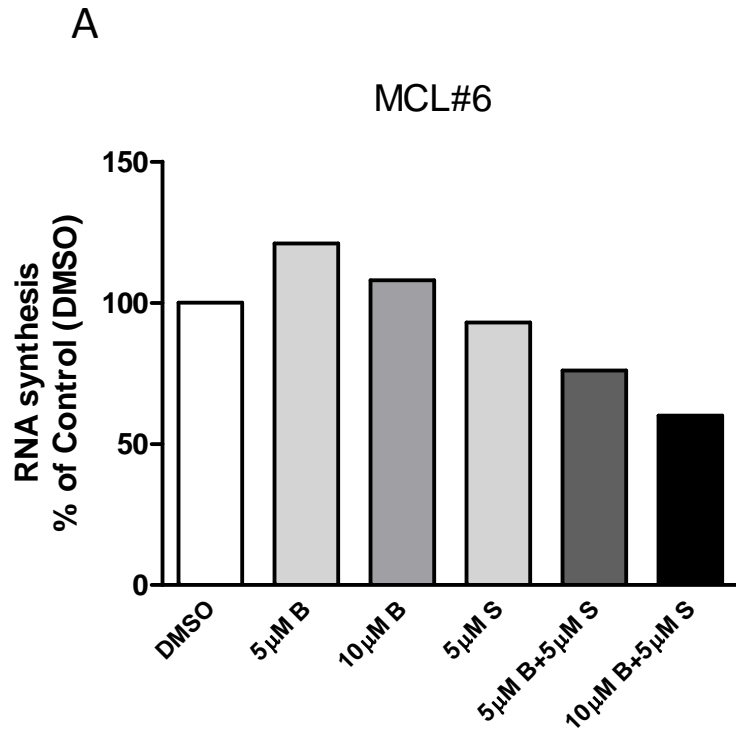
B, bendamustine; S, SGI-1776.

Figure 49.
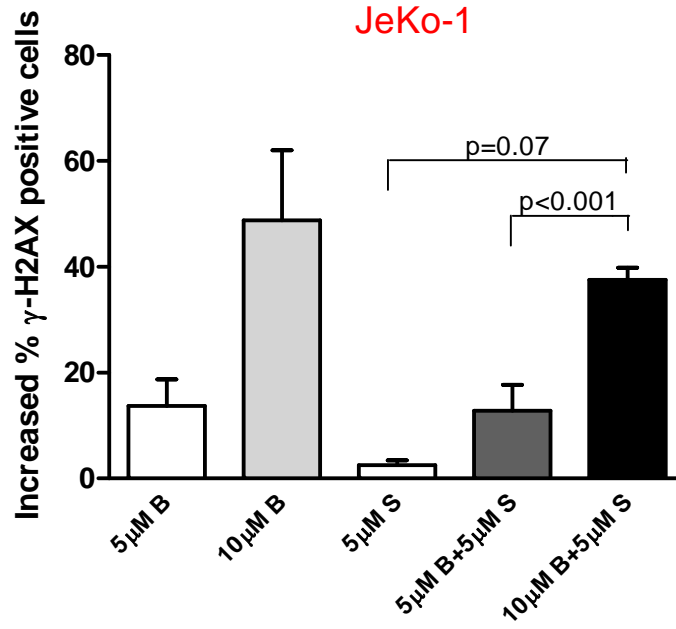
CHAPTER 5: Discussion and Conclusion

I.   Summary

Our results indicated that all three Pim kinases are expressed in MCL cell lines and primary tissue sample (Figures 5-6). Pim kinases are potential therapeutic targets in MCL as Pim kinase inhibitor, SGI-1776 treatment induced moderate to high levels of apoptosis in four MCL cell lines (JeKo-1, Mino, SP-53 and Granta-519) as well as in PBMCs isolated from primary MCL patient samples but not healthy donors (Figures 7-12, 30-33). Primary mechanism of actions of SGI-1776 appears to be targeting c-Myc-driven transcription and cap-dependent translation processes (Figures 13, 15, 30). In addition, levels of short-lived oncoproteins, Mcl-1 and cyclin D1 were decreased in MCL cell line JeKo-1, and primary MCL samples (Figures 18-19, 23, 30). Moreover, SGI-1776 treatments also lead to decline of global RNA synthesis levels in MCL cell lines, correlating with decrease of *MCL1* mRNA level in these cell lines (Figures 17-18). Meanwhile, *MCL1* mRNA levels were also decreased in malignant PBMCs from MCL patients but not in normal PBMCs (Figures 34-35). Collectively, our study suggests Pim kinases as viable drug targets in MCL and that SGI-1776 primarily target Pim kinase functions through disruption transcriptional and translational regulations.

Our studies using bendamustine in combination with SGI-1776 also revealed some interesting results. With bendamustine treatment alone, we observed moderate level of apoptosis in MCL cell lines (JeKo-1 and Mino) as well as in MCL and SMZL primary cells from patients (Figures 42-43). An additive or synergistic effect in cell killing was observed when combined with SGI-1776 (Figure 42-43). SGI-1776 treatment was effective in decreasing global RNA and protein synthesis levels, while bendamustine inhibited DNA synthesis and generated DNA damage response (Figures 44-49). When used in combination, we observed intensified inhibitory effects in DNA, RNA and protein syntheses compared to single agent treatments of either drug (Figures 44-49).

To incorporate main findings of my dissertation, I use a model that summarizes the dissertation project and the cause-and-effect relationships (Figure 50).

Together, these data provided a rationale for using Pim kinase inhibitor in combination with bendamustine, and suggested feasibility of such therapeutic approach in B-cell lymphoma.

II. SGI-1776 primary mechanisms of actions in MCL

<u>MCL cell lines as primary model of study</u>

Primary objective of our investigation was to test Pim kinase inhibition in MCL. This is the first investigation of Pim kinase inhibitor, SGI-1776 in this type of B-cell lymphoma. To fully evaluate consequences of Pim kinase inhibition and to establish our results, we used both MCL cell lines and primary malignant B-cell lymphoma from patients. Furthermore, to explore broad applicability, we used a spectrum of MCL cell lines. These four MCL cell lines possess different cellular morphology, ranging from non-attached single cells to small or large clumps. They acquire different growth media, and doubling time varies from 24-72hr. However, all four cell lines possess hallmark features of MCL such as t(11;14)(q13;q32), cyclin D1 expression (Table 6) and typical MCL surface markers, CD19/20+ (Table 7) (Morice 2008). In addition, these MCL cell lines express cyclin E protein, but very low levels of cyclin D2/D3, while c-Myc, p21 and p27 levels are present in all (Table 8). Meanwhile, anti-apoptotic Bcl-2 family proteins such as Bcl-2, Bcl-X$_L$, and Mcl-1 and pro-apoptotic Bax are present in all cell lines (Table 9).

Interestingly, discrepancies were observed in JeKo-1 and Mino cell lines in SGI-1776-induced responses in the cells, such as apoptosis, disruption of phosphorylation of Pim kinase targets, decrease of global RNA synthesis inhibition and Mcl-1mRNA and protein levels as well as cell cycle arrest (Figures 7-24). JeKo-1 cells were more sensitive and responsive to SGI-1776 treatment compared to Mino cells. Based on the known genetics and molecular characteristics of these two cell lines, we cannot conclude the possible causes of these discrepancies. A gene array or reverse-phase

Figure 50.
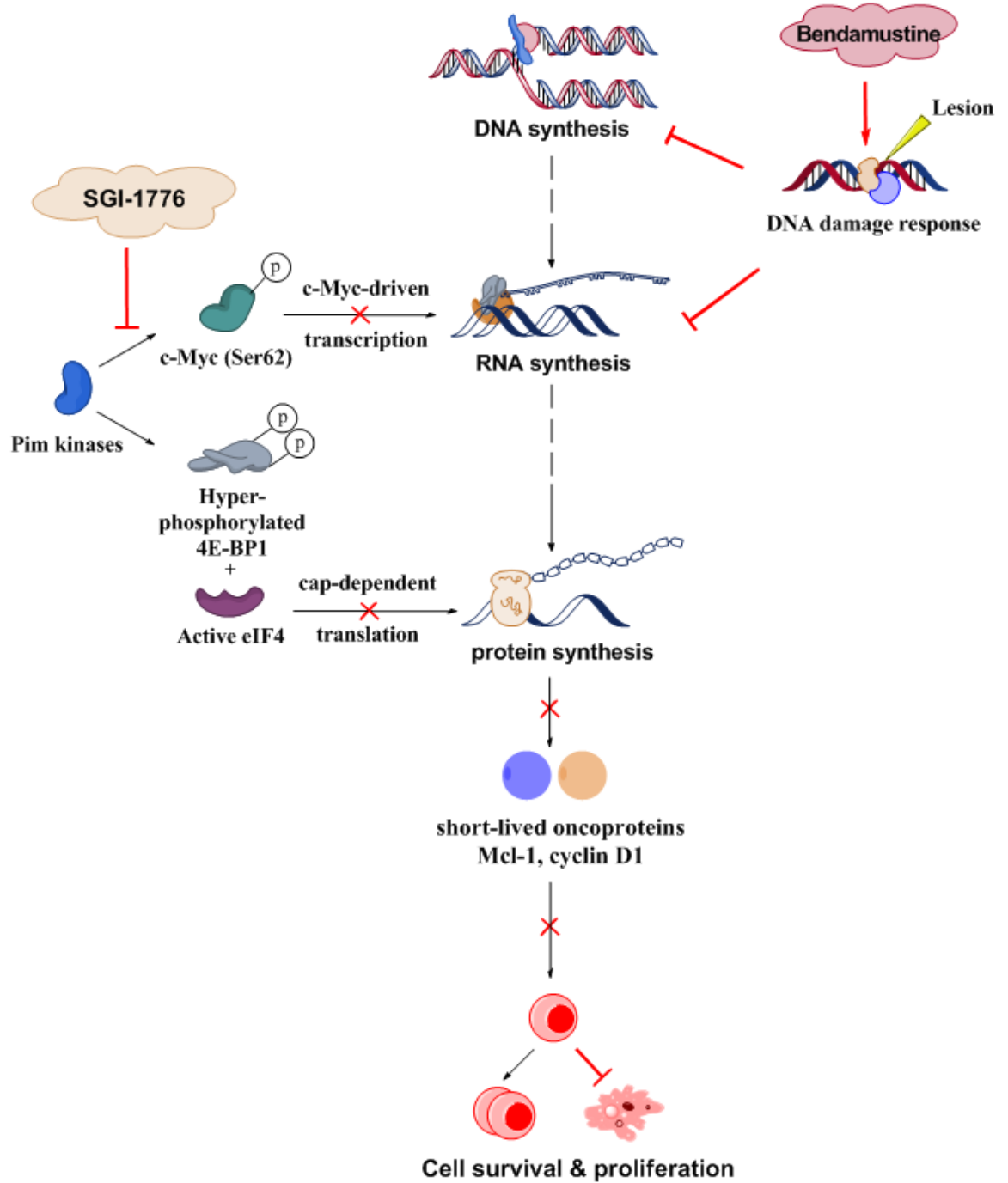
Figure 50. An overall model to summarize main findings.

Table 6.

	JeKo-1	Mino	Granta 519	SP-53
Growth pattern	Single cell	Single cell	Small clumps	Large clumps
Culture media	RPMI 1640+10%FBS	RPMI 1640+20%FBS	DMEM + 20%FBS	RPMI 1640+20%FBS
Doubling time	24hr	24hr	24-72hr	72hr
t(11:14) (q13;q32)	Positive	Positive	Positive	Positive
cyclin D1 expression	High positive	Positive	Positive	Positive

Table 6. MCL cell lines growth condition and MCL charateristics.

Adapted from [Amin HM, McDonnell TJ, Medeiros LJ, Rassidakis GZ, Leventaki V, O'Connor SL, Keating MJ, Lai R, Characterization of 4 mantle cell lymphoma cell lines. *Arch Pathol Lab Med.* 2003;127(4):426] with permission from *Archives of Pathology & Laboratory Medicine.* Copyright 2003 College of American Pathologists.

Table 7.

	JeKo-1	Mino	Granta 519	SP-53
CD5	+	+	-	-
CD10	+	-	-	-
CD19	+	+	+	+
CD20	+	+	+	+
CD22	+	n/a	n/a	n/a
CD23	-	-	+	+

Table 7. Surface CD markers of MCL cell lines.

Adapted from [Amin HM, McDonnell TJ, Medeiros LJ, Rassidakis GZ, Leventaki V, O'Connor SL, Keating MJ, Lai R, Characterization of 4 mantle cell lymphoma cell lines. *Arch Pathol Lab Med*. 2003;127(4):427] with permission from *Archives of Pathology & Laboratory Medicine*. Copyright 2003 College of American Pathologists.

Table 8.

	JeKo-1	Mino	Granta 519	SP-53
Cyclin D2	-	-	-	-
Cyclin D3	+ (w)	-	-	+ (w)
Cyclin E	+	+	+	+
Rb	+	+	+	+
c-Myc	+	+	+	+
p21	+	+	+	+
p27	+*	+	+	+
p53	-	+	+(s)	+

Table 8. Oncogene, tumor suppressor and cell cycle marker expressions in MCL cell lines.

w—weak

s—strong

*p27 band was detected at 53kD in JeKo-1

Adapted from [Amin HM, McDonnell TJ, Medeiros LJ, Rassidakis GZ, Leventaki V, O'Connor SL, Keating MJ, Lai R, Characterization of 4 mantle cell lymphoma cell lines. *Arch Pathol Lab Med.* 2003;127(4):428] with permission from *Archives of Pathology & Laboratory Medicine*. Copyright 2003 College of American Pathologists.

Table 9.

	JeKo-1	Mino	Granta 519	SP-53
Bcl-2	+	+	+	+
Bcl-X$_L$	+	+	+	+
Bcl-X$_S$	-	-	-	-
Bax	+	+	+	+
Mcl-1	+	+	+	+

Table 9. Bcl-2 family protein expressions in MCL cell lines.

Adapted from [Amin HM, McDonnell TJ, Medeiros LJ, Rassidakis GZ, Leventaki V, O'Connor SL, Keating MJ, Lai R, Characterization of 4 mantle cell lymphoma cell lines. *Arch Pathol Lab Med.* 2003;127(4):428] with permission from *Archives of Pathology & Laboratory Medicine*. Copyright 2003 College of American Pathologists.

protein array (RPPA) may be used as exploratory approaches to detect their detailed molecular

characteristics, both before and after drug treatment. These array-type studies could potentially

reveal inherent genomic differences and differentially regulated genes and proteins related to drug

resistance, or other factors that may have contributed to the differences in responding to drug

treatments.

Primary patient samples as important predictor of drugs' clinical outcomes

In our studies, we used primary samples from MCL patients as well as apparently healthy

donors to study the effect of SGI-1776 on cell killing, and to identify potential biomarkers of SGI-

1776 in the clinic. Notably, we only detected SGI-1776-induced apoptosis, decrease of Pim kinase

phosphorylation targets and short-lived oncogenes in lymphocytes isolated from MCL patient blood

but not in PBMCs isolated from healthy donors (Figures 30-35). These results suggested a favorable

therapeutic index of SGI-1776 in the clinic, as it selectively targets malignant cells. Our investigation

did not address the reasons behind this phenomenon, except that more consistent expression of these

oncogenic proteins were detected in MCL primary cells compared to those of healthy donors. More

in-depth study of these cells, such as RPPA studies to identify their molecular characteristics,

expression levels of target proteins, and cellular metabolism patterns are needed to unravel these

differential biological responses.

Targeting c-Myc-driven transcription

Because Pim kinases are expressed in MCL cell line and primary tissue samples (Figures 5-

6), they act as model system to investigate mechanism of action of SGI-1776. Among all proteins, c-

Myc is one of the fastest degrading proteins in human cells (Gregory 2000). Post-translational

modifications, however, alter the short half-life of c-Myc. It has been reported that Pim-1 directly

phosphorylates c-Myc at Ser62, the stabilization site on the protein to prolong its half-life from

minutes to hours, which promotes c-Myc oncogencity (Sears 2000; Zhang 2008). While we did not evaluate half-life of c-Myc, we examined phospho-c-Myc (Ser62) levels in both MCL cell lines and primary cells following SGI-1776 treatment, and observed a consistent decrease in all cells tested (Figures 13, 30). This result confirmed that in MCL, c-Myc is a target of Pim kinases.

Noticeably, along with a decline in phospho-c-Myc (Ser62) levels, there was also a decrease of total c-Myc levels, especially in JeKo-1 cells (Figures 13, 30). In JeKo-1 cells, total c-Myc seemed to decrease more profoundly than phospho-c-Myc (Ser62) (Figure 13A). This is an unavoidable situation since c-Myc (Ser62) phosphorylation is a protein stabilization site for c-Myc, and when Pim kinase function is inhibited by SGI-1776, c-Myc is degraded more rapidly (Zhang 2008). In addition, we consistently observed that the total c-Myc primary antibody used in this immunoblot does not generate as strong signals as the c-Myc (Ser62) antibody; the quality difference in these primary antibodies may also contribute to these results.

It was also reported that Histone H3 phosphorylation at Ser10, a target for Pim kinase, is a critical step to enhance c-Myc-driven transcription (Zippo 2007). However, only in JeKo-1 cells but not Mino, phospho-Histone H3 (Ser10) was reduced upon SGI-1776 treatment (Figure 14). We hypothesize that SGI-1776 prevents Pim kinase from phosphorylate c-Myc (Ser62) and Histone H3 (Ser10) which consequently disrupts c-Myc-driven transcription (Figure 51). Notably, Zippo *et al.* performed their experiments in serum-starved condition, whereas our experiments were done in full-serum condition, an experimental condition that could have contributed to the difference in results. Consistent with c-Myc data, total RNA synthesis declined in all four MCL cell lines (Figure 17A).

Importantly, levels of apoptosis in both MCL cell lines and primary samples were positively correlated with decrease of phospho-c-Myc level in MCL cell lines. In addition, strong correlation was observed between c-Myc phosphorylation and global RNA synthesis as well as *MCL1* mRNA

Figure 51.
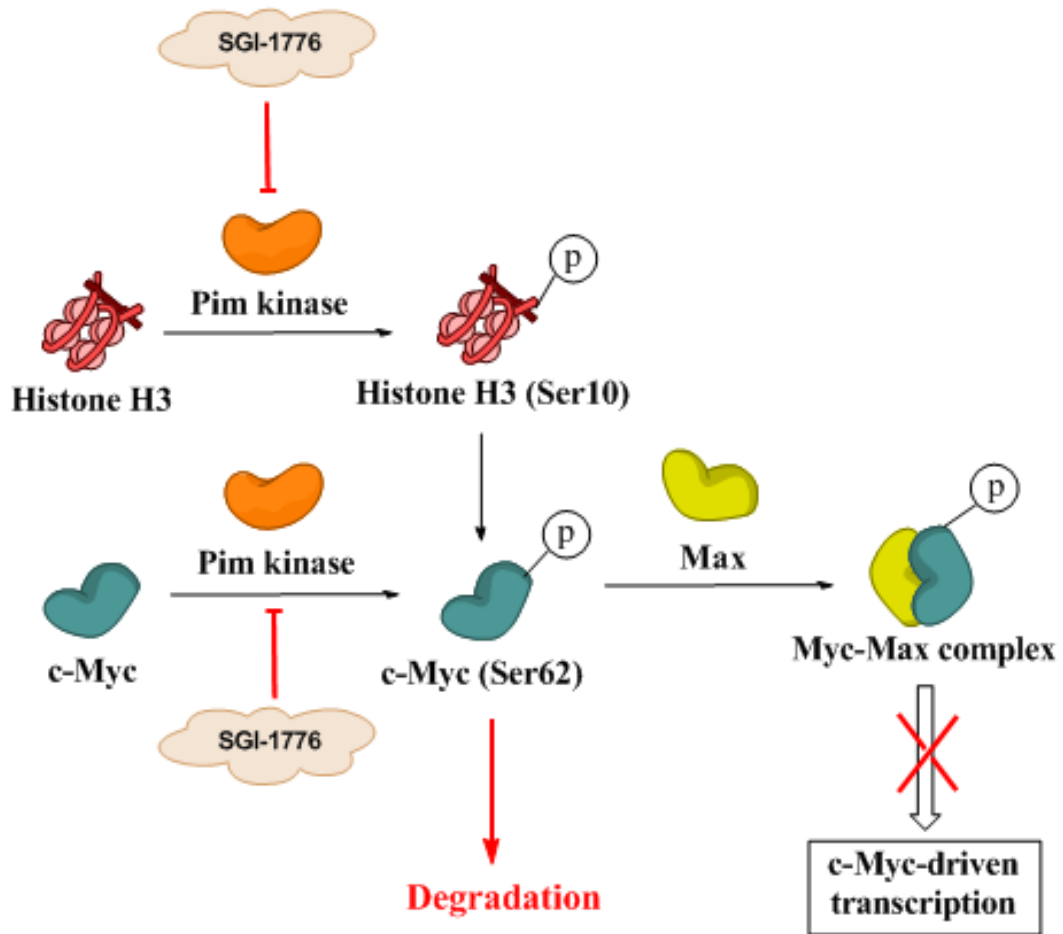
Figure 51. SGI-1776 treatment decreases transcription by disrupting phosphorylation of c-Myc and Histone H3.

SGI-1776 disrupts Pim kinase function, therefore reduced the c-Myc and Histone phosphorylation levels and lead to disruption of Myc-Max complex formation. These processes eventually disrupt c-Myc-driven transcription machineries.

levels, suggesting a c-Myc-driven transcription is involved with SGI-1776 mechanisms of action (Figures 37-38).

<u>Targeting cap-dependent translation</u>

Phosphorylation of 4E-BP1 (Thr37/46) is prerequisite for 4E-BP1 hyper-phosphorylation, which leads to dissociation from eIF4 translation initiation factor (Gingras 2001). Unbound eIF4 will initiate cap-dependent protein translation, a process for translating early response gens including Pim kinases (Hoover 1991; Richter 2005). Pim-1 is known to phosphorylate 4E-BP1 at Thr37/46 site, which triggers hyper-phosphorylation of this protein (Gingras 2001; Tamburini 2009). Pim-2 also phosphorylates 4E-BP1 at Ser65 as part of the hyper-phosphorylation process (Fox 2003). We observed that the 4E-BP1 (Thr37/46) phosphorylation level was consistently decreased in JeKo-1, Mino cell lines and MCL primary samples following SGI-1776 treatment (Figures 15, 30). Our results suggest that SGI-1776 prevents 4E-BP1 priming by Pim kinases which then targets cap-dependent translation processes (Figure 52).

<u>Targeting cell survival machinery</u>

All three Pim kinases phosphorylate Bad protein (Ser112), a pro-apoptotic Bcl-2 family member (Yan 2003; Aho 2004). Un-phosphorylated Bad protein is bound to Bcl-2 family protein (Bcl-X_L or Bcl-2) to sequester their anti-apoptotic function. Once Bad is phosphorylated at Ser112, it dissociates from Bcl-X_L and bind with scaffold protein 14-3-3, where it gets shuttled into the cytoplasm (Aho 2004). Hence, SGI-1776 treatment may lead to a decrease of Bad (Ser112) phosphorylation, which could be a contributing factor to the extensive apoptosis by SGI-1776 treatment observed in MCL cells (Figure 53).

We measured the Bad (Ser112) phosphorylation levels in MCL cell lines JeKo-1 and Mino following SGI-1776 treatment, and interestingly, we were only able to detect a decrease in Bad (Ser112) phosphorylation in JeKo-1 cells but not in Mino cells (Figure 16).

Figure 52.
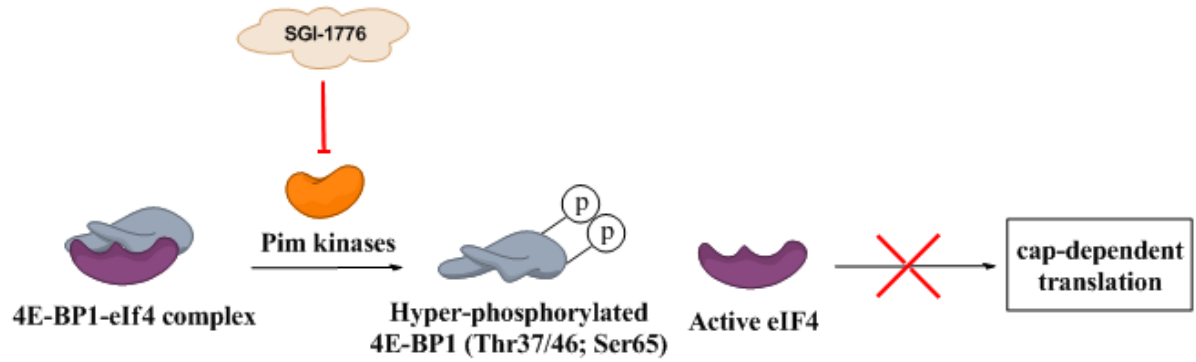
Figure 52. SGI-1776 treatment decreases translation by disrupting phosphorylation of 4E-BP1.

SGI-1776 disrupts Pim kinase function, therefore reduced the 4E-BP1 phosphorylation levels and lead to disruption of initiation of cap-dependent translation.

Figure 53.
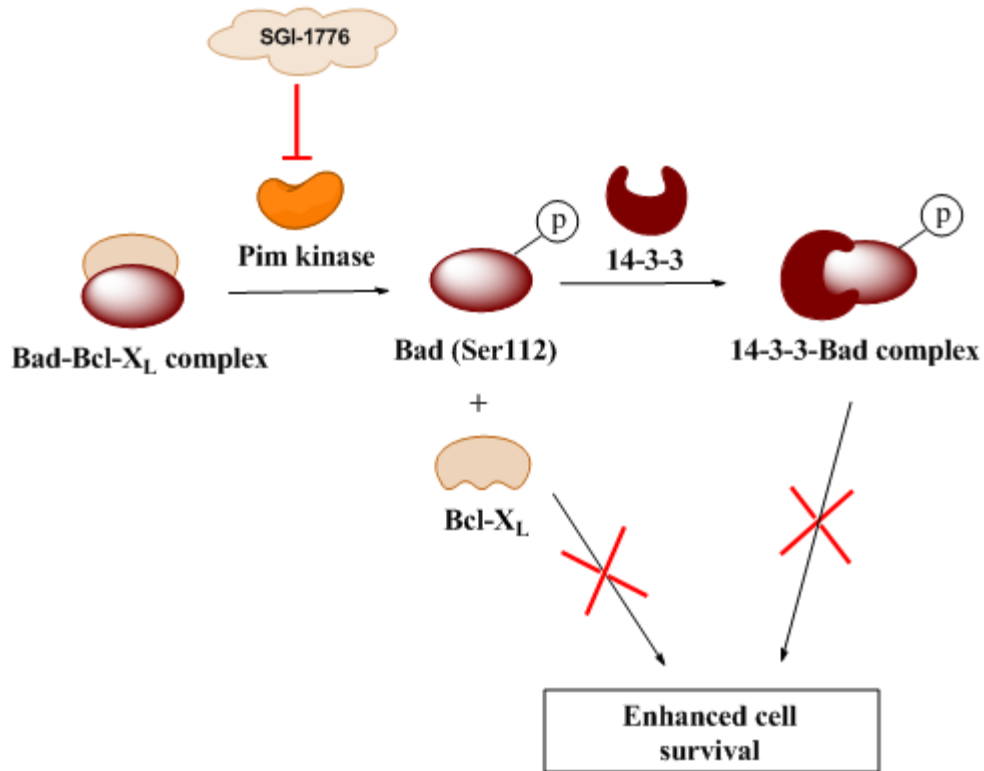
Figure 53. SGI-1776 treatment disrupts phosphorylation of Bad which contribute to cell death.

SGI-1776 disrupts Pim kinase function, therefore reduced the Bad phosphorylation levels and lead to re-gaining function of Bad. Un-phosphorylated Bad also associates with anti-apoptotic Bcl-X$_L$ which then leads to further induction of apoptosis.

In addition, the degree of Bad (Ser112) decrease was less extensive as the level of apoptosis, suggesting that this is not a primary mechanism of action of SGI-1776 in MCL cells (Figures 11, 16).

Furthermore, disruption of c-Myc (Ser62) and 4E-BP1 (Thr37/46) phosphorylation may also lead to cell death following SGI-1776 treatment in MCL cells. However, a time course experiment is needed to correlate decrease of phosphorylation of c-Myc and 4E-BP1 with SGI-1776-induced apoptosis to establish the cause and effect and temporal relationship of these events. Since c-Myc and 4E-BP1 are direct targets of Pim kinases, and decreased phosphorylation of these two proteins lead to disrupted c-Myc-driven transcription and cap-dependent translation, we hypothesize that decrease of phosphorylation levels of these two protein markers would appear prior to extensive cell death, indicating that SGI-1776-induced cell killing is a result of targeting c-Myc and 4E-BP1 phosphorylation by this drug.

Moreover, to establish causal role of c-Myc and 4E-BP1 phosphorylation in cell death, functional inhibitors of c-Myc and 4E-BP1may be tested separately and in combination in MCL cell lines. Alternatively, siRNA treatments to knockdown each protein may establish their roles that disruption of c-Myc and 4E-BP1 phosphorylation lead to cell killing and suggest that SGI-1776-induced apoptosis was through inhibition of c-Myc and 4E-BP1 phosphorylation.

Nonetheless, since c-Myc-driven transcription and cap-dependent translation processes were consistently affected by SGI-1776 treatments, therefore, we hypothesized that early response genes that are regulated by cap-dependent translation may be affected, and those with oncogenic nature, such as Mcl-1 and cyclin D1 may be affected and contributed to the extensiveness of apoptosis induction by SGI-1776 treatment (Fox 2003; Khoury 2003; Schatz 2011).

We tested the levels of Mcl-1 and cyclin D1 in MCL cell lines and primary cells, and detected a consistent decrease of Mcl-1 levels in both cell lines and MCL primary samples (Figures 19-20, 23, 30). Notably, the decrease of anti-apoptotic proteins did not occur in proteins with longer

145

half-lives such as Bcl-2 and Bcl-X$_L$ (Figure 21). Importantly, in both JeKo-1 and Mino cells, decrease of Mcl-1 protein was detected as early as 0.5hr and lasted through the rest of 24hr. Consistently, there was a significant decrease of *MCL1* mRNA levels in both MCL cell lines and primary samples; and in cell lines, *MCL1* levels started to decrease at 0.5hr as well (Figures 18, 34). These observations suggest that Mcl-1 mRNA and protein are rapidly degraded by SGI-1776 treatment, which may contribute to the SGI-1776-induced apoptosis in these MCL cells.

In contrast, we detected heterogeneous outcomes in cyclin D1 levels between the two MCL cell lines. There was a significant and consistent decrease of cyclin D1 levels in JeKo-1 cells, but the opposite was observed in Mino cells (Figure 24). Notably, cyclin D1 levels in untreated Mino cells were much lower than that of JeKo-1 cells. However, in malignant PBMCs isolated from MCL, we detected consistent decrease of cyclin D1 levels (Figure 31). These results indicated that cyclin D1 degradation could be a contributor for high levels of apoptosis in cells express high levels of cyclin D1 but not in cells express low levels of this protein.

Importantly, in PBMCs isolated from MCL patient in remission or healthy donors, we did not detect a decrease of either 4E-BP1 (Thr37/46), or c-Myc (Ser62) phosphorylation levels after treated with SGI-1776, and we detected low levels of apoptosis in these samples (Figure 32). In concordance, neither did Mcl-1, cyclin D1 protein levels, nor *MCL1* mRNA levels decrease in normal PBMCs following SGI-1776 treatment (Figures 33, 35). These observations suggests that SGI-1776 is not toxic in these normal PBMCs, and it does not alter the molecular mechanisms of healthy cells, suggesting that SGI-1776 is therapeutically favorable, and support its feasibility in the clinic.

Targeting cell cycle

Pim kinases are known to target multiple cell cycle proteins, such as p21, p27, cdc25A/C (Figure 2). Phosphorylation of these cell cycle-regulating proteins promote cells to enter G1/S and

G2 phases more efficiently, which makes them more oncogenic in nature (Mochizuki 1999; Wang 2002; Bachmann 2006; Morishita 2008).

Differential effect was observed in cell cycle profile between the two MCL cell lines. In JeKo-1, there wasn't obvious signs for cell cycle arrest, however, in Mino, a dose-dependent G1 phase arrest was detected (Figure 22). Unfortunately, we could not find a well-functioned p21 antibody for western blot analysis, and p27 expression was irregular, running at 54kD in Mino cells and we could not detect p27 expression JeKo-1 cells (data not shown). Therefore, we were not able to analyze these two protein marker responsible to regulate G1 phase. We also analyzed the cdc25C phosphorylation level in the two MCL cell lines. It seemed that in JeKo-1, both phospho- and total cdc25C expression levels were reduced upon SGI-1776 treatment, and total cdc25C level decreased faster and more significant than the phospho-cdc25C (Figure 23). However, we did not detect any changes in phospho-cdc25C level in Mino cells. It seems that G1 arrest may be a cell type-specific phenomenon.

Short-lived oncogene cyclin D1 is also a cell cycle-regulating protein. Cyclin D1 forms complexes with CDK 4/6, both are expressed at high levels in MCL, which regulates G1/2 transition (Perez-Galan 2011). We analyzed the changes of cyclin D1 levels in JeKo-1 and Mino, and we observed opposite response as described above (Figure 24). Besides the differential expression levels of cyclin D1 in untreated JeKo-1 and Mino, the contracting cell cycle profiles of JeKo-1 and Mino caused by SGI-1776 suggests that cyclin D1 may be regulated differently in the two cell lines.

Pim kinase redundant pathways

In our SGI-1776 single agent treatment study in MCL, we consistently detected decrease of c-Myc (Ser62), 4E-BP1 (Thr37/46) and Mcl-1 mRNA and protein levels in all the *in vitro* models tested. However, even taken all of the factors above, these may still not be enough to compensate with the extensiveness of apoptosis observed in these cells. We hypothesize that redundant pathways

to Pim kinase pathways may be contributing to this phenomenon, such as the PI3K/Akt/mTOR and nuclear factor kappa-light-chain-enhancer of activated B cells (NF-kB) canonical pathways, which are also upregulated in MCL (Hammerman 2005; Schatz 2011). These pathways share some common targets such as c-Myc, 4E-BP1, and a common effector Mcl-1, as well as upstream growth factors and cytokines/chemokines (Hammerman 2005; Chen 2010; Fruman 2011; Nawijn 2011). A gene-array and a RPPA assay will be useful to identify these potential redundant pathways, and it is important to perform these assays both before and after SGI-1776 treatments in multiple MCL cell lines, and compare the SGI-1776-induced changes in different oncogene and oncoproteins in their regulating oncogenic pathways, In addition, these screening tests could also reveal additional factors contributing to the extensive cell death observed in the MCL cells.

Our siRNA knockdown studies showed results in accord with the hypothesis of activated redundant pathways in MCL cells, that even when Pim kinase mRNAs are knocked down to almost 50% or less than scrambled control, Pim kinase phospho- targets (c-Myc, 4E-BP1) and Mcl-1 protein showed less extensive level of decrease in their phosphorylation levels, which could be due to activation of the redundant pathways (Figures 13, 15, 25-29). In addition, less extensive cell death levels compared to SGI-1776 treatment were detected in MCL cells treated with Pim kinase siRNAs (Figures 11-12, 25-29). This result indicates that other targets may be impacted by SGI-1776 besides Pim kinases. However, our siRNA treatment results were consistent with Pim kinase knockout mouse embryonic fibroblast (MEF) cells. These Pim kinase knockout MEFs grow and replicate much more slowly compared to wildtype MEF cells (Beharry 2011). Other means of cell death by SGI-1776 remains to be found, such as other short-lived oncogenic proteins and possibly other transcription/translation-regulating pathways, which may be discovered through microarrays and RPPA assays.

SGI-1776 toxicity and second generation Pim kinase inhibitors

SGI-1776 was the first Pim kinase inhibitor to enter clinical trial for refractory prostate cancer or lymphoma, but it was terminated prematurely due to cardiotoxicty, concerns when prolonged cardiac QTc was observed in patients treated with SGI-1776 (ClinicalTrial.gov). This was an unexpected human-only toxicity as it was not observed in other animals during *in vivo* testing during drug development (Astex Pharmaceuticals). A possible reason may be that both Pim-1 and Pim-3 are expressed in human cardiomyocytes, and may be cytoprotective against external toxicities and injuries (Liu 2009; Borillo 2010). In addition, several metabolites of SGI-1776 were observed in human plasma (verbal communication with SuperGen, now Astex Pharmaceuticals) and hence a more stable and targeted inhibitor was in demand.

A plethora of Pim kinase inhibitors is synthesized by several pharmaceutical companies. Several of these next generation Pim kinase inhibitors have been tested in *in vitro* assays (SMI-4a), pre-clinical trial (GNE-652) or clinical trial (AZD-1208); more are underway (Beharry 2011; Keeton 2011; Munugalavadla 2011; Blanco-Aparicio 2012; Keeton 2012). Preliminary data from AZD-1208 in AML cells and AML clinical trials were presented recently (Keeton 2012).

Pim kinases targeting appears to be a valid option for MCL, however, cell death data suggest that combination strategies are needed. Especially for drugs that act synergistically, much lower doses of each drug in the combination method are needed for achieving desired clinical efficacy. These potential partners could be members of the conventional chemotherapeutic drugs that target multiple oncogenic pathways, or targeted therapeutic inhibitors that have specific targets, as long as the combination treatment reaches the goal of repressing multiple redundant oncogenic pathways and lead to sufficient amount of cytotoxicity in cancer cells. To date, no information on SGI-1776's synergy partners has been reported; we investigated a combination approach using bendamustine, a FDA-approved chemotherapeutic agent with SGI-1776, and tested the molecular responses in B-cell lymphoma cells.

**III.	Combination of bendamustine with SGI-1776 in B-cell lymphoma**

Bendamustine is a DNA damaging agent that causes both inter- and intra-strand DNA crosslinks, which lead to disruption in DNA replication, repair and transcription processes (Leoni 2011). Single-drug bendamustine treatment during clinical trials showed promising efficacy with overall response rate at >70% and duration of response as >9 months, although toxicity was observed in both non-hematological and hematological nature (National Cancer Institute). Overall, this drug is well-tolerated by patients (Goy 2011). Based on our results with SGI-1776, c-Myc-driven transcription and cap-dependent-translation appear to be primary mechanisms of action, and the molecular mechanism as well as favorable clinical efficacy of bendamustine, we speculate that bendamustine is an appropriate agent to be combined with SGI-1776 and we expect an additive effect in cell killing in B-cell lymphoma cells (Figure 42-43). We examined the effect of each drug as well as the combination approach on aspects of DNA, RNA and protein synthesis inhibition along with cell death in B-cell lymphoma cell lines and primary patient samples, as described in details below.

Targeting DNA synthesis

Bendamustine demonstrates a unique cytotoxicity profile compared to other alkylating agents, which involves induction of caspase-dependent and -independent apoptosis (Roue 2008), increased DNA repair gene expression through base excision repair and S-phase arrest (Torres-Garcia 1989), as well as degrading mitotic checkpoint-regulating proteins that disrupts G2-M transition which ultimately results in mitotic catastrophe (Leoni 2011).

Gamma-H2A is a known marker for DNA double-stranded breaks, which is associated with DNA inter-strand crosslinks (Leoni 2008). Gamma-H2A phosphorylation is an important step for recruiting DNA repair proteins and cell cycle-checkpoint proteins to the site of DNA damage, and can be detectable by flow cytometry (Paull 2000; Fillingham 2006). Our studies showed that single-

agent bendamustine treatment in MCL cell line JeKo-1 was effective in inducing γ-H2A, especially

at higher concentrations (15%-50% induction at 5-10μM, Figure 49). In addition, single agent

bendamustine was also effective in disrupting global DNA synthesis in JeKo-1, measured by

radioactive-thymidine incorporation assay, which is also consistent with previous findings (30%-50%

reduction, Figures 44).

Since SGI-1776 single agent treatment on DNA damage in MCL cells is unknown, we used

thymidine incorporation assay to detect the changes on level of DNA synthesis and found that SGI-

1776 was less effective in reducing DNA synthesis levels compared to bendamustine (24% reduction,

Figure 44). In addition, we did not see increased levels of γ-H2A from SGI-1776 treatment alone

(Figure 49). These results are expected, as the primary mechanism of action of SGI-1776 in MCL

cells appears to be through transcription and translation inhibition, which are both are downstream of

DNA synthesis. Interestingly, combination of bendamustine with SGI-1776 showed additive effect in

blocking global DNA synthesis in JeKo-1 cells without showing an increase in γ-H2A induction

(Figures 44, 49). For future studies, molecular markers related to DNA damage and repair, such as

p53, ATM, and cell cycle checkpoint proteins and aurora kinases may play a role in this process and

are potentially relevant clinical markers for studying DNA damage response using bendamustine

with a Pim kinase inhibitor.

Targeting RNA synthesis

Our study has demonstrated that SGI-1776 targets c-Myc-driven transcription process and

also reduced global RNA synthesis levels in MCL (Yang 2012). Bendamustine, a DNA-damaging

alkylating agent, is known to break DNA crosslinks which halts DNA synthesis, and subsequently

results in transcription inhibition (Leoni 2008).

Using radioactive-uridine incorporation in JeKo-1 cells and B-cell lymphoma primary cells

to measure RNA synthesis, single agent SGI-1776 resulted in significant decrease in RNA synthesis,

whereas in bendamustine-treated cells, there was little or no effect (Figures 45-46). More significant decrease in global RNA synthesis was observed in the MCL and SMZL primary samples compared to JeKo-1 cell line using combination treatments (Figures 45-46). This may be due to the difference in cellular physiology between replicating cell line and non-proliferating primary cells, where the relevant transcription regulator proteins are expressed differently. This result needs to be further explored in a larger number of cell lines and primary samples and the regulating molecules needs to be validated.

Targeting protein synthesis

Our previous study indicated inhibition of 4E-BP1-mediated cap-dependent translation as a mechanism of action of SGI-1776 in MCL cells (Yang 2012). Our experiments using radioactive-leucine incorporation assay confirmed this finding that SGI-1776 was effect in reducing global translation levels in both JeKo-1 cell line and MCL, SMZL primary samples (10%-60% decrease, Figures 47-48).

Bendamustine has not been demonstrated to affect translation processes; however, our results indicated a 13%-50% decrease of global protein synthesis level using single agent bendamustine in both MCL cell line and primary cells, with variability among the two primary B-cell lymphoma samples (Figure 47, 48). We suspect that this was not a direct effect but rather a secondary or tertiary result, following bendamustine-induced DNA damage response and disruption of transcription process. However, the decrease of global protein synthesis by bendamustine was extensive, suggesting that there may be an unknown mechanism of action that contributed to this result. To confirm this hypothesis, further explorations and molecular studies are needed.

Combination of bendamustine and SGI-1776 resulted in variable responses in global protein synthesis inhibition in JeKo-1 cell lines and B-cell lymphoma primary samples. Heterogeneity among patient samples may be a reason, however, consistent in both JeKo-1 and primary patient

152

samples, combination treatment lead to more significant decrease in global protein levels compared to either single agent treatment (Figures 48, 48). Interestingly, similar to uridine-incorporation studies, more prominent results were shown in primary MCL patient cells compared to cell lines. Greater number of cells lines and primary patient cells are needed to verify these results and understand the molecular mechanism.

Additive to synergistic effect in cell killing

Both bendamustine and SGI-1776 are cytotoxic agents (Leoni 2008; Yang 2012), and based on the known mechanisms of actions, we hypothesized that when used in combination, there would be an additive to synergistic effect in cell killing in B-cell lymphoma cells (Figure 41). We used annexin V/PI assays to analyze the apoptosis induction by each agent alone, and in combination then used fractional analysis to determine whether the results were less than, equal to or more than additive (Figures 42-43, Table 3).

In MCL cell lines, JeKo-1 and Mino, we observed additive to synergistic effects in apoptosis (Figure 42). In the two B-cell lymphoma samples, we observed additive effects (Figure 43). Although the molecular mechanisms were not investigated, our results measuring apoptosis induction, as well as the results on macromolecule synthesis inhibition, suggested that combination of bendamustine with a Pim kinase inhibitor such as SGI-1776 could be a viable therapeutic approach in the clinic. A larger number of cell lines and primary cells are needed to conduct molecular marker studies in order to identify the underlying mechanisms of actions.

Other combination methods involving Pim kinase inhibitors

Combination strategies using small molecule inhibitors or established chemotherapeutic agents with Pim kinase inhibitors have been investigated to augment cytotoxicity in both hematological malignancies and solid tumors. In prostate cancer, where Pim kinases contribute to tumorigenesis and chemoresistance, Pim kinase inhibitor, SMI-4a was used in combination with

Bcl-2 inhibitor, ABT-737, which is also a clinical trial agent, to overcome chemoresistance and successfully boosted cell killing efficiency in *in vitro* prostate cancer cells that overexpress Bcl-2 (Song 2012). Another Pim-1 inhibitor, ETP-45299, was shown to act synergistically with a PI3K inhibitor, GDC-0914, in apoptosis induction and translation inhibition in AML cells. The study also demonstrated that Bad and 4E-BP1 phosphorylation were double-targeted by this combination strategy and lead to extensive cell killing (Blanco-Aparicio 2011). In addition, in multiple myeloma (MM), a Pim-2-specific inhibitor, (Z)-5-(4-propoxybenzylidene) thiazolidine-2,4-dione, and PI3K inhibitor, LY294002 cooperatively enhanced MM cell death levels (Asano 2011).

Combinations of Pim kinase inhibitors with FDA-approved chemotherapeutic agents or other investigational agents have been reported to have greater effects compared to single agent therapies. A study in renal cell carcinoma (RCC), where c-Myc is overexpressed and known to drive tumorigenesis, addition of Pim kinase inhibitor, SGI-1776 enhanced the effect of sunitinib (an FDA-approved receptor tyrosine kinase inhibitor for treating RCC) in reducing phospho- and total c-Myc levels as well as expression levels of c-Myc-regulated genes, in addition to promoting anticancer activities (Mahalingam 2011). Furthermore, another study in MM demonstrated that reduction of cell viability by mTOR inhibitor rapamycin was enhanced when Pim-2 expression was repressed by *PIM2* siRNA due to a cooperative effort in repressing 4E-BP1-regulated translation processes (Asano 2011). Moreover, combination of Vorinostat, (suberoylanilide hydroxamic acid, SAHA–an FDA-approved inhibitor of class I&II histone deacetylases for treating cutaneous T-cell lymphoma) with a Pim kinase inhibitor, ETP-39010 resulted in an additive to synergistic effect in multiple cell lines tested (Wozniak 2010). In addition, SGI-1776 single agent treatment was able to increase cell death levels in a multidrug resistance 1 protein (ABCB1)–based prostate cancer cell line that are refractory to taxane, a widely used chemotherapeutic agent for many cancers. SGI-1776 was also able to re-sensitize chemoresistant cells to taxane-base therapies by inhibiting ABCB1 expression (Mumenthaler 2009).

The examples described above provided strong rationale for the feasibility of Pim kinase inhibitors used in combination treatment, which could improve efficacy and decrease Pim kinase inhibitor-derived toxicity in clinic.

<u>Advantage of using Pim kinase inhibitor to prevent drug resistance</u>

In addition to oncogenic pathways described above, all three Pim kinases are mediators for drug resistance development (Brault 2010). A common mechanism for drug resistance is through insufficient drug transportation into cancer cells, due to changes or overexpression of trans-membrane transporter molecules, known as drug efflux pumps. Pim-1 is able to phosphorylate and activate the ATP-biding cassette (ABC) transporters p-glycoprotein (ABCB1) and breast cancer resistance protein (ABCG2), which are transporter molecules strongly associated with acquired drug resistance in cancers such as AML (Ji 2009; Natarajan 2013).

By knocking down Pim-1 expression, ABCB1/ABCG2-mediated drug resistance was inhibited in AML cells overexpression ABCB1/ABCG2 (Natarajan 2013). In leukemia cells with high levels of Mcl-1 (another factor known to cause chemoresistance), increased the sensitivity to cytotoxic agents was made possible, by specifically targeting both Mcl-1 and ABCB1 (Ji 2009). These studies indicated that targeting Pim kinases along with one or more oncogenic pathways to which the tumor cells are addicted may be a desirable approach for treatment refractory cancer patients.

IV.   Conclusion and future directions

The investigations described in this dissertation focuses on investigating Pim kinases as therapeutic targets and evaluating the effect of Pim kinase inhibitor, SGI-1776 in MCL, as well as combination approach of SGI-1776 with chemotherapeutic agent, bendamustine in B-cell lymphoma. We were able to identify that SGI-1776 is a cytotoxic agent in MCL, that targets c-Myc-driven transcription and cap-dependent translation processes to disrupt MCL survival. In addition, global

RNA and protein synthesis were disrupted, and short-lived oncogene *MCL1* mRNA and its protein expression were decreased. Meanwhile, SGI-1776-induced cytotoxicity was not observed in normal PBMCs. In B-cell lymphoma cells, bendamustine was effective in disrupting DNA synthesis as well as inducing DNA-damage response, whereas SGI-1776 decreased RNA and protein syntheses. When used in combination, additive to synergistic effect in cell killing was observed, and more extensive decrease of macromolecule synthesis was detected in B-cell lymphoma cell line and primary cells.

Our study in SGI-1776 provides a mechanism of action that may be used to guide future clinical trial studies of Pim kinase inhibitors, and the combination study with bendamustine supports the feasibility of using Pim kinase inhibitor with other chemotherapeutic agents. However, two questions remain unclear –whether other mechanism of apoptosis induction are involved in SGI-1776-induced cell death, and if redundant pathways are activated when Pim kinases are repressed either by a small molecular inhibitor or siRNAs. To identify other mechanisms of SGI-1776-induced cytotoxicity, we may look outside of direct phosphorylation targets Pim kinase, and to look more closely into the intrinsic/extrinsic apoptosis-regulating pathways, and other members of Bcl-2 family, and examine the regulating molecule more closely. We will also conduct screening studies to look for upregulated oncogenes in PI3K, NF-κB, and Wnt pathways (all are known to be deregulated in MCL) in order to identify redundant pathways of Pim kinases (Perez-Galan 2011).

Due to limited number of lymphoma primary patient cells, we were unable to examine the molecular mechanism of the combination treatment, and greater number of MCL cell lines and primary samples are needed to confirm our findings of macromolecule synthesis inhibition and identify the important players and oncogenic pathways affected by combination treatment.

In addition, other Pim kinase inhibitors could be tested in B-cell lymphomas, to compare and validate the mechanisms of actions of SGI-1776. We hypothesize that pan Pim kinase inhibitors may have a greater effect in apoptosis induction in MCL cells, and the output of downstream

phosphorylation targets may be different for selective Pim-2 or Pim-3 inhibitors compared to SGI-1776.

Moreover, effect of SGI-1776 under microenvironment conditions is another important aspect of study to better understand the mechanism of actions of the drug in patient body. Microenvironments contain many growth factors and cytokines/chemokines are known to upregulate oncogenic pathways such as JAK/STAT or PI3K/Akt/mTOR to enhance oncogenecity and drug resistance of lymphoma cells (Chen 2010; Burger 2011). Importantly, Pim kinases are known to be regulated and interact with growth factors and cytokine/chemokines from microenvironment. Specifically, it was reported that Pim-2 is downstream of B lymphocyte stimulator (BLyS), and it acts independently from Akt/mTOR pathway to enhance B cell growth and survival (Woodland R.T. 2008). In addition, expression of Mcl-1, a reporter protein downstream of BLyS was also increased in the presence of BLyS and activated BCR pathways (Woodland R.T. 2008). Moreover, Pim-1 was reported to regulate C-X-C chemokine receptor 4-12 (CXCR4-CXCR12)-mediated homing and migration processes in AML (Grundler 2009). Based on these evidences, it is reasonable to speculate that the effect of Pim kinase inhibitors such as SGI-1776 may be different under the influence of microenvironment compared to microenvironment-free conditions.

Finally, effect of SGI-1776 and other Pim kinase inhibitors need to be investigated in mouse models to better understand the dose-efficacy relationship, and to predict potential toxicities in patients before they enter the clinic. Xenograph models are good systems to study the efficacies of Pim kinase inhibitors, as they readily reflect the drugs' effect by easily-measured reduction of tumor volumes and prolonged survival in mice. However, xenograph models differ from human physiology by lacking immune systems, which may become important in study hematological malignancies. Additional *in vivo* models such as gene knockout mice may also be used to complement *in vitro* studies. Importantly, metabolites of each Pim kinase inhibitor needs to be analyzed and investigated to more accurately predict toxicity in the clinic.

157

References

Aho TL, Sandholm J, Peltola KJ, Mankonen HP, Lilly M, Koskinen PJ, Pim-1 kinase promotes inactivation of the pro-apoptotic Bad protein by phosphorylating it on the Ser112 gatekeeper site. *FEBS Lett,* 2004. **571**(1-3): p. 43-49.

Akyurek N, Ren Y, Rassidakis GZ, Schlette EJ, Medeiros LJ, Expression of inhibitor of apoptosis proteins in B-cell non-Hodgkin and Hodgkin lymphomas. *Cancer,* 2006. **107**(8): p. 1844-1851.

Allen JD, Verhoeven E, Domen J, van der Valk M, Berns A, Pim-2 transgene induces lymphoid tumors, exhibiting potent synergy with c-myc. *Oncogene,* 1997. **15**(10): p. 1133-1141.

Amaravadi R. TCB, The survival kinases Akt and Pim as potential pharmacological targets. *The Journal of Clinical Investigation,* 2005. **115**(10): p. 2618-2624.

Amin HM, McDonnell TJ, Medeiros LJ, Rassidakis GZ, Leventaki V, O'Connor SL, Keating MJ, Lai R, Characterization of 4 mantle cell lymphoma cell lines. *Arch Pathol Lab Med,* 2003. **127**(4): p. 424-431.

Amson R, Sigaux F, Przedborski S, Flandrin G, Givol D, Telerman A, The human protooncogene product p33pim is expressed during fetal hematopoiesis and in diverse leukemias. *Proc Natl Acad Sci U S A,* 1989. **86**(22): p. 8857-8861.

An N, Kraft AS, Kang Y, Abnormal hematopoietic phenotypes in Pim kinase triple knockout mice: Pim kinase regulates hematopoiesis. *J Hematol Oncol,* 2013. **6**(1): p. 12.

Asano J, Nakano A, Oda A, Amou H, Hiasa M, Takeuchi K, Miki H, Nakamura S, Harada T, Fujii S, Kagawa K, Endo I, Yata K, Sakai A, Ozaki S, Matsumoto T, Abe M, The serine/threonine kinase Pim-2 is a novel anti-apoptotic mediator in myeloma cells. *Leukemia,* 2011. **25**(7): p. 1182-1188.

Bachmann M, Kosan C, Xing PX, Montenarh M, Hoffmann I, Moroy T, The oncogenic
serine/threonine kinase Pim-1 directly phosphorylates and activates the G2/M specific
phosphatase Cdc25C. *Int J Biochem Cell Biol,* 2006. **38**(3): p. 430-443.

Balakrishnan K, Wierda WG, Keating MJ, Gandhi V, Mechanisms of cell death of chronic
lymphocytic leukemia lymphocytes by RNA-directed agent, 8-NH2-adenosine. *Clin Cancer
Res,* 2005. **11**(18): p. 6745-6752.

Beharry Z, Mahajan S, Zemskova M, Lin YW, Tholanikunnel BG, Xia Z, Smith CD, Kraft AS, The
Pim protein kinases regulate energy metabolism and cell growth. *Proc Natl Acad Sci U S A,*
2011. **108**(2): p. 528-533.

Blanco-Aparicio C, Carnero A, Pim kinases in cancer: Diagnostic, prognostic and treatment
opportunities. *Biochem Pharmacol,* 2012.

Blanco-Aparicio C, Collazo AM, Oyarzabal J, Leal JF, Albaran MI, Lima FR, Pequeno B, Ajenjo N,
Becerra M, Alfonso P, Reymundo MI, Palacios I, Mateos G, Quinones H, Corrionero A,
Carnero A, Pevarello P, Lopez AR, Fominaya J, Pastor J, Bischoff JR, Pim 1 kinase inhibitor
ETP-45299 suppresses cellular proliferation and synergizes with PI3K inhibition. *Cancer
Lett,* 2011. **300**(2): p. 145-153.

Bodrug SE, Warner BJ, Bath ML, Lindeman GJ, Harris AW, Adams JM, Cyclin D1 transgene
impedes lymphocyte maturation and collaborates in lymphomagenesis with the myc gene.
EMBO J, 1994. **13**(9): p. 2124-2130.

Borillo GA, Mason M, Quijada P, Volkers M, Cottage C, McGregor M, Din S, Fischer K, Gude N,
Avitabile D, Barlow S, Alvarez R, Truffa S, Whittaker R, Glassy MS, Gustafsson AB,
Miyamoto S, Glembotski CC, Gottlieb RA, Brown JH, Sussman MA, Pim-1 kinase protects
mitochondrial integrity in cardiomyocytes. *Circ Res,* 2010. **106**(7): p. 1265-1274.

Brault L, Gasser C, Bracher F, Huber K, Knapp S, Schwaller J, PIM serine/threonine kinases in the
pathogenesis and therapy of hematologic malignancies and solid cancers. *haematologica,*
2010. **95**(6): p. 1004-1015.

Brault L. GC, Bracher F., Huber K., Knapp S., Schwaller J., PIM serine/threonine kinases in the pathogenesis and therapy of hematologic malignancies and solid cancers. *haematologica,* 2010. **95**(6): p. 1004-1017.

Bullock AN, Debreczeni J, Amos AL, Knapp S, Turk BE, Structure and substrate specificity of the Pim-1 kinase. *J Biol Chem,* 2005. **280**(50): p. 41675-41682.

Burger JA, Ford RJ, The microenvironment in mantle cell lymphoma: cellular and molecular pathways and emerging targeted therapies. *Semin Cancer Biol,* 2011. **21**(5): p. 308-312.

Chen LS, Balakrishnan K, Gandhi V, Inflammation and survival pathways: chronic lymphocytic leukemia as a model system. *Biochem Pharmacol,* 2010. **80**(12): p. 1936-1945.

Chen LS, Redkar S, Bearss D, Wierda WG, Gandhi V, Pim kinase inhibitor, SGI-1776, induces apoptosis in chronic lymphocytic leukemia cells. *Blood,* 2009. **114**(19): p. 4150-4157.

Chen WW, Chan DC, Donald C, Lilly MB, Kraft AS, Pim family kinases enhance tumor growth of prostate cancer cells. *Mol Cancer Res,* 2005. **3**(8): p. 443-451.

Chen X.P. LJA, Cowan S., Donahue E., Fay S., Vuong B.Q., Nawijn M.C., Capece D., Cohan V.L., Rothman P., Pim serine/threonine kinases regulate the stability of Socs-1 protein. *PNAS,* 2002. **99**(4): p. 2175-2180.

Cheney IW, Yan S, Appleby T, Walker H, Vo T, Yao N, Hamatake R, Hong Z, Wu JZ, Identification and structure-activity relationships of substituted pyridones as inhibitors of Pim-1 kinase. *Bioorg Med Chem Lett,* 2007. **17**(6): p. 1679-1683.

Chiang CW, Kanies C, Kim KW, Fang WB, Parkhurst C, Xie M, Henry T, Yang E, Protein phosphatase 2A dephosphorylation of phosphoserine 112 plays the gatekeeper role for BAD-mediated apoptosis. *Mol Cell Biol,* 2003. **23**(18): p. 6350-6362.

Culjkovic B, Topisirovic I, Skrabanek L, Ruiz-Gutierrez M, Borden KL, eIF4E is a central node of an RNA regulon that governs cellular proliferation. *J Cell Biol,* 2006. **175**(3): p. 415-426.

Cuypers HT, Selten G, Quint W, Zijlstra M, Maandag ER, Boelens W, van Wezenbeek P, Melief C, Berns A, Murine leukemia virus-induced T-cell lymphomagenesis: integration of proviruses in a distinct chromosomal region. *Cell,* 1984. **37**(1): p. 141-150.

Danial NN, Gramm CF, Scorrano L, Zhang CY, Krauss S, Ranger AM, Datta SR, Greenberg ME, Licklider LJ, Lowell BB, Gygi SP, Korsmeyer SJ, BAD and glucokinase reside in a mitochondrial complex that integrates glycolysis and apoptosis. *Nature,* 2003. **424**(6951): p. 952-956.

Dautry F, Weil D, Yu J, Dautry-Varsat A, Regulation of pim and myb mRNA accumulation by interleukin 2 and interleukin 3 in murine hematopoietic cell lines. *J Biol Chem,* 1988. **263**(33): p. 17615-17620.

Domen J, Von Lindern M, Hermans A, Breuer M, Grosveld G, Berns A, Comparison of the human and mouse PIM-1 cDNAs: nucleotide sequence and immunological identification of the in vitro synthesized PIM-1 protein. *Oncogene Res,* 1987. **1**(1): p. 103-112.

Ek S, Dictor M, Jerkeman M, Jirstrom K, Borrebaeck CA, Nuclear expression of the non B-cell lineage Sox11 transcription factor identifies mantle cell lymphoma. *Blood,* 2008. **111**(2): p. 800-805.

Fernandez PC, Frank SR, Wang L, Schroeder M, Liu S, Greene J, Cocito A, Amati B, Genomic targets of the human c-Myc protein. *Genes Dev,* 2003. **17**(9): p. 1115-1129.

Fillingham J, Keogh MC, Krogan NJ, GammaH2AX and its role in DNA double-strand break repair. *Biochem Cell Biol,* 2006. **84**(4): p. 568-577.

Fox CJ, Hammerman PS, Cinalli RM, Master SR, Chodosh LA, Thompson CB, The serine/threonine kinase Pim-2 is a transcriptionally regulated apoptotic inhibitor. *Genes Dev,* 2003. **17**(15): p. 1841-1854.

Fruman DA, Rommel C, PI3Kdelta inhibitors in cancer: rationale and serendipity merge in the clinic. *Cancer Discov,* 2011. **1**(7): p. 562-572.

Gandhi V, Burger JA, Bendamustine in B-Cell Malignancies: The New 46-Year-Old Kid on the Block. *Clin Cancer Res,* 2009. **15**(24): p. 7456-7461.

Gingras AC, Raught B, Gygi SP, Niedzwiecka A, Miron M, Burley SK, Polakiewicz RD, Wyslouch-Cieszynska A, Aebersold R, Sonenberg N, Hierarchical phosphorylation of the translation inhibitor 4E-BP1. *Genes Dev,* 2001. **15**(21): p. 2852-2864.

Gomez-Abad C, Pisonero H, Blanco-Aparicio C, Roncador G, Gonzalez-Menchen A, Martinez-Climent JA, Mata E, Rodriguez ME, Munoz-Gonzalez G, Sanchez-Beato M, Leal JF, Bischoff JR, Piris MA, PIM2 inhibition as a rational therapeutic approach in B-cell lymphoma. *Blood,* 2011. **118**(20): p. 5517-5527.

Goy A, Kahl B, Mantle cell lymphoma: the promise of new treatment options. *Crit Rev Oncol Hematol,* 2011. **80**(1): p. 69-86.

Greaves MF, Differentiation-linked leukemogenesis in lymphocytes. *Science,* 1986. **234**(4777): p. 697-704.

Gregory MA, Hann SR, c-Myc proteolysis by the ubiquitin-proteasome pathway: stabilization of c-Myc in Burkitt's lymphoma cells. *Mol Cell Biol,* 2000. **20**(7): p. 2423-2435.

Grundler R, Brault L, Gasser C, Bullock AN, Dechow T, Woetzel S, Pogacic V, Villa A, Ehret S, Berridge G, Spoo A, Dierks C, Biondi A, Knapp S, Duyster J, Schwaller J, Dissection of PIM serine/threonine kinases in FLT3-ITD-induced leukemogenesis reveals PIM1 as regulator of CXCL12-CXCR4-mediated homing and migration. *J Exp Med,* 2009. **206**(9): p. 1957-1970.

Halldorsdottir AM, Fruhwirth M, Deutsch A, Aigelsreiter A, Beham-Schmid C, Agnarsson BA, Neumeister P, Richard Burack W, Quantifying the role of aberrant somatic hypermutation in transformation of follicular lymphoma. *Leuk Res,* 2008. **32**(7): p. 1015-1021.

Hammerman PS, Fox CJ, Birnbaum MJ, Thompson CB, Pim and Akt oncogenes are independent regulators of hematopoietic cell growth and survival. *Blood,* 2005. **105**(11): p. 4477-4483.

Hammerman PS, Fox CJ, Cinalli RM, Xu A, Wagner JD, Lindsten T, Thompson CB, Lymphocyte transformation by Pim-2 is dependent on nuclear factor-kappaB activation. *Cancer Res,* 2004. **64**(22): p. 8341-8348.

Herrmann A, Hoster E, Zwingers T, Brittinger G, Engelhard M, Meusers P, Reiser M, Forstpointner R, Metzner B, Peter N, Wormann B, Trumper L, Pfreundschuh M, Einsele H, Hiddemann W, Unterhalt M, Dreyling M, Improvement of overall survival in advanced stage mantle cell lymphoma. *J Clin Oncol,* 2009. **27**(4): p. 511-518.

Hinds PW, Dowdy SF, Eaton EN, Arnold A, Weinberg RA, Function of a human cyclin gene as an oncogene. *Proc Natl Acad Sci U S A,* 1994. **91**(2): p. 709-713.

Hogan C, Hutchison C, Marcar L, Milne D, Saville M, Goodlad J, Kernohan N, Meek D, Elevated levels of oncogenic protein kinase Pim-1 induce the p53 pathway in cultured cells and correlate with increased Mdm2 in mantle cell lymphoma. *J Biol Chem,* 2008. **283**(26): p. 18012-18023.

Hoover D, Friedmann M, Reeves R, Magnuson NS, Recombinant human pim-1 protein exhibits serine/threonine kinase activity. *J Biol Chem,* 1991. **266**(21): p. 14018-14023.

Hoover DS, Wingett DG, Zhang J, Reeves R, Magnuson NS, Pim-1 protein expression is regulated by its 5'-untranslated region and translation initiation factor elF-4E. *Cell Growth Differ,* 1997. **8**(12): p. 1371-1380.

Hsi ED, Jung SH, Lai R, Johnson JL, Cook JR, Jones D, Devos S, Cheson BD, Damon LE, Said J, Ki67 and PIM1 expression predict outcome in mantle cell lymphoma treated with high dose therapy, stem cell transplantation and rituximab: a Cancer and Leukemia Group B 59909 correlative science study. *Leuk Lymphoma,* 2008. **49**(11): p. 2081-2090.

Ji M, Li J, Yu H, Ma D, Ye J, Sun X, Ji C, Simultaneous targeting of MCL1 and ABCB1 as a novel strategy to overcome drug resistance in human leukaemia. *Br J Haematol,* 2009. **145**(5): p. 648-656.

Keeton E, McEachern K, Alimzhanov M, Wang S, Cao Y, Bao L, Palakurth iS, Grondine M, Chen Y, Dillman K, Chinnappan D, Shen M, Dakin L, Zheng X, Lamb M, Wu A, Chen H, Lyne P, Huszar D, Abstract 2796: Efficacy and biomarker modulation by AZD1208, a novel, potent and selective pan-Pim kinase inhibitor, in models of acute myeloid leukemia. *Cancer Research,* 2012. **72**(8 Supplement): p. 2796.

Keeton E, Palakurthi, S, Alimzhanov, M, et al., AZD1208, a Novel, Potent and Selective Pan PIM Kinase Inhibitor, Demonstrates Efficacy in Models of Acute Myeloid Leukemia. *53rd ASH Annual Meeting: 2011,* 2011: p. Abstract 1540.

Khoury JD, Medeiros LJ, Rassidakis GZ, McDonnell TJ, Abruzzo LV, Lai R, Expression of Mcl-1 in mantle cell lymphoma is associated with high-grade morphology, a high proliferative state, and p53 overexpression. *J Pathol,* 2003. **199**(1): p. 90-97.

Kim O, Jiang T, Xie Y, Guo Z, Chen H, Qiu Y, Synergism of cytoplasmic kinases in IL6-induced ligand-independent activation of androgen receptor in prostate cancer cells. *Oncogene,* 2004. **23**(10): p. 1838-1844.

Klapper W, Histopathology of mantle cell lymphoma. *Semin Hematol,* 2011. **48**(3): p. 148-154.

Konietzko U, Kauselmann G, Scafidi J, Staubli U, Mikkers H, Berns A, Schweizer M, Waltereit R, Kuhl D, Pim kinase expression is induced by LTP stimulation and required for the consolidation of enduring LTP. *EMBO J,* 1999. **18**(12): p. 3359-3369.

Kuppers R, Mechanisms of B-cell lymphoma pathogenesis. *Nat Rev Cancer,* 2005. **5**(4): p. 251-262.

Kuppers R, Dalla-Favera R, Mechanisms of chromosomal translocations in B cell lymphomas. *Oncogene,* 2001. **20**(40): p. 5580-5594.

Kuppers R, Klein U, Hansmann ML, Rajewsky K, Cellular origin of human B-cell lymphomas. *N Engl J Med,* 1999. **341**(20): p. 1520-1529.

Leoni LM, Bailey B, Reifert J, Bendall HH, Zeller RW, Corbeil J, Elliott G, Niemeyer CC, Bendamustine (Treanda) displays a distinct pattern of cytotoxicity and unique mechanistic features compared with other alkylating agents. *Clin Cancer Res,* 2008. **14**(1): p. 309-317.

Leoni LM, Hartley JA, Mechanism of action: the unique pattern of bendamustine-induced cytotoxicity. *Semin Hematol,* 2011. **48 Suppl 1**: p. S12-23.

Levy D, Davidovich A, Zirkin S, Frug Y, Cohen AM, Shalom S, Don J, Activation of cell cycle arrest and apoptosis by the proto-oncogene Pim-2. *PLoS One,* 2012. **7**(4): p. e34736.

Linn DE, Yang X, Xie Y, Alfano A, Deshmukh D, Wang X, Shimelis H, Chen H, Li W, Xu K, Chen M, Qiu Y, Differential regulation of androgen receptor by PIM-1 kinases via phosphorylation-dependent recruitment of distinct ubiquitin E3 ligases. *J Biol Chem,* 2012. **287**(27): p. 22959-22968.

Liu D, He M, Yi B, Guo WH, Que AL, Zhang JX, Pim-3 protects against cardiomyocyte apoptosis in anoxia/reoxygenation injury via p38-mediated signal pathway. *Int J Biochem Cell Biol,* 2009. **41**(11): p. 2315-2322.

Losman JA, Chen XP, Vuong BQ, Fay S, Rothman PB, Protein phosphatase 2A regulates the stability of Pim protein kinases. *J Biol Chem,* 2003. **278**(7): p. 4800-4805.

Lovec H, Grzeschiczek A, Kowalski MB, Moroy T, Cyclin D1/bcl-1 cooperates with myc genes in the generation of B-cell lymphoma in transgenic mice. *EMBO J,* 1994. **13**(15): p. 3487-3495.

Macdonald A, Campbell DG, Toth R, McLauchlan H, Hastie CJ, Arthur JS, Pim kinases phosphorylate multiple sites on Bad and promote 14-3-3 binding and dissociation from Bcl-XL. *BMC Cell Biol,* 2006. **7**: p. 1.

Mahalingam D, Espitia CM, Medina EC, Esquivel JA, 2nd, Kelly KR, Bearss D, Choy G, Taverna P, Carew JS, Giles FJ, Nawrocki ST, Targeting PIM kinase enhances the activity of sunitinib in renal cell carcinoma. *Br J Cancer,* 2011. **105**(10): p. 1563-1573.

Merkel AL, Meggers E, Ocker M, PIM1 kinase as a target for cancer therapy. *Expert Opin Investig Drugs,* 2012. **21**(4): p. 425-436.

Mikkers H, Nawijn M, Allen J, Brouwers C, Verhoeven E, Jonkers J, Berns A, Mice deficient for all PIM kinases display reduced body size and impaired responses to hematopoietic growth factors. *Mol Cell Biol,* 2004. **24**(13): p. 6104-6115.

Mochizuki T, Kitanaka C, Noguchi K, Muramatsu T, Asai A, Kuchino Y, Physical and functional

    interactions between Pim-1 kinase and Cdc25A phosphatase. Implications for the Pim-1-

    mediated activation of the c-Myc signaling pathway. *J Biol Chem,* 1999. **274**(26): p. 18659-

    18666.

Morice WG, Kurtin PJ, Hodnefield JM, Shanafelt TD, Hoyer JD, Remstein ED, Hanson CA,

    Predictive value of blood and bone marrow flow cytometry in B-cell lymphoma

    classification: comparative analysis of flow cytometry and tissue biopsy in 252 patients.

    Mayo Clin Proc, 2008. **83**(7): p. 776-785.

Morishita D, Katayama R, Sekimizu K, Tsuruo T, Fujita N, Pim kinases promote cell cycle

    progression by phosphorylating and down-regulating p27Kip1 at the transcriptional and

    posttranscriptional levels. *Cancer Res,* 2008. **68**(13): p. 5076-5085.

Mozos A, Royo C, Hartmann E, De Jong D, Baro C, Valera A, Fu K, Weisenburger DD, Delabie J,

    Chuang SS, Jaffe ES, Ruiz-Marcellan C, Dave S, Rimsza L, Braziel R, Gascoyne RD, Sole F,

    Lopez-Guillermo A, Colomer D, Staudt LM, Rosenwald A, Ott G, Jares P, Campo E,

    SOX11 expression is highly specific for mantle cell lymphoma and identifies the cyclin D1-

    negative subtype. *haematologica,* 2009. **94**(11): p. 1555-1562.

Mumenthaler SM, Ng PY, Hodge A, Bearss D, Berk G, Kanekal S, Redkar S, Taverna P, Agus DB,

    Jain A, Pharmacologic inhibition of Pim kinases alters prostate cancer cell growth and

    resensitizes chemoresistant cells to taxanes. *Mol Cancer Ther,* 2009. **8**(10): p. 2882-2893.

Munugalavadla V, Berry, L, Chen, Y-H, et al., A selective PIM kinase inhibitor is highly active in

    multiple myeloma: mechanism of action and signal transduction studies. *53rd ASH annual*

    meeting: 2011, 2011: p. Abstract 4084.

Natarajan K, Bhullar J, Shukla S, Burcu M, Chen ZS, Ambudkar SV, Baer MR, The Pim kinase

    inhibitor SGI-1776 decreases cell surface expression of P-glycoprotein (ABCB1) and breast

    cancer resistance protein (ABCG2) and drug transport by Pim-1-dependent and -independent

    mechanisms. *Biochem Pharmacol,* 2013. **85**(4): p. 514-524.

Nawijn MC, Alendar A, Berns A, For better or for worse: the role of Pim oncogenes in tumorigenesis. *Nat Rev Cancer,* 2011. **11**(1): p. 23-34.

Pasqualucci L, Neumeister P, Goossens T, Nanjangud G, Chaganti RS, Kuppers R, Dalla-Favera R, Hypermutation of multiple proto-oncogenes in B-cell diffuse large-cell lymphomas. *Nature,* 2001. **412**(6844): p. 341-346.

Paull TT, Rogakou EP, Yamazaki V, Kirchgessner CU, Gellert M, Bonner WM, A critical role for histone H2AX in recruitment of repair factors to nuclear foci after DNA damage. *Curr Biol,* 2000. **10**(15): p. 886-895.

Peltola KJ, Paukku K, Aho TL, Ruuska M, Silvennoinen O, Koskinen PJ, Pim-1 kinase inhibits STAT5-dependent transcription via its interactions with SOCS1 and SOCS3. *Blood,* 2004. **103**(10): p. 3744-3750.

Perez-Galan P, Dreyling M, Wiestner A, Mantle cell lymphoma: biology, pathogenesis, and the molecular basis of treatment in the genomic era. *Blood,* 2011. **117**(1): p. 26-38.

Polotskaya A, Zhao Y, Lilly ML, Kraft AS, A critical role for the cytoplasmic domain of the granulocyte-macrophage colony-stimulating factor alpha receptor in mediating cell growth. *Cell Growth Differ,* 1993. **4**(6): p. 523-531.

Popivanova BK, Li YY, Zheng H, Omura K, Fujii C, Tsuneyama K, Mukaida N, Proto-oncogene, Pim-3 with serine/threonine kinase activity, is aberrantly expressed in human colon cancer cells and can prevent Bad-mediated apoptosis. *Cancer Sci,* 2007. **98**(3): p. 321-328.

Qian KC, Wang L, Hickey ER, Studts J, Barringer K, Peng C, Kronkaitis A, Li J, White A, Mische S, Farmer B, Structural basis of constitutive activity and a unique nucleotide binding mode of human Pim-1 kinase. *J Biol Chem,* 2005. **280**(7): p. 6130-6137.

Richter JD, Sonenberg N, Regulation of cap-dependent translation by eIF4E inhibitory proteins. *Nature,* 2005. **433**(7025): p. 477-480.

Rosenwald A, Wright G, Wiestner A, Chan WC, Connors JM, Campo E, Gascoyne RD, Grogan TM, Muller-Hermelink HK, Smeland EB, Chiorazzi M, Giltnane JM, Hurt EM, Zhao H, Averett

L, Henrickson S, Yang L, Powell J, Wilson WH, Jaffe ES, Simon R, Klausner RD, Montserrat E, Bosch F, Greiner TC, Weisenburger DD, Sanger WG, Dave BJ, Lynch JC, Vose J, Armitage JO, Fisher RI, Miller TP, LeBlanc M, Ott G, Kvaloy S, Holte H, Delabie J, Staudt LM, The proliferation gene expression signature is a quantitative integrator of oncogenic events that predicts survival in mantle cell lymphoma. *Cancer Cell,* 2003. **3**(2): p. 185-197.

Rossi D, Berra E, Cerri M, Deambrogi C, Barbieri C, Franceschetti S, Lunghi M, Conconi A, Paulli M, Matolcsy A, Pasqualucci L, Capello D, Gaidano G, Aberrant somatic hypermutation in transformation of follicular lymphoma and chronic lymphocytic leukemia to diffuse large B-cell lymphoma. *haematologica,* 2006. **91**(10): p. 1405-1409.

Roue G, Lopez-Guerra M, Milpied P, Perez-Galan P, Villamor N, Montserrat E, Campo E, Colomer D, Bendamustine is effective in p53-deficient B-cell neoplasms and requires oxidative stress and caspase-independent signaling. *Clin Cancer Res,* 2008. **14**(21): p. 6907-6915.

Rummel MJ, Gregory SA, Bendamustine's emerging role in the management of lymphoid malignancies. *Semin Hematol,* 2011. **48 Suppl 1**: p. S24-36.

Schatz JH, Oricchio E, Wolfe AL, Jiang M, Linkov I, Maragulia J, Shi W, Zhang Z, Rajasekhar VK, Pagano NC, Porco JA, Jr., Teruya-Feldstein J, Rosen N, Zelenetz AD, Pelletier J, Wendel HG, Targeting cap-dependent translation blocks converging survival signals by AKT and PIM kinases in lymphoma. *J Exp Med,* 2011. **208**(9): p. 1799-1807.

Sears R, Nuckolls F, Haura E, Taya Y, Tamai K, Nevins JR, Multiple Ras-dependent phosphorylation pathways regulate Myc protein stability. *Genes Dev,* 2000. **14**(19): p. 2501-2514.

Selten G, Cuypers HT, Boelens W, Robanus-Maandag E, Verbeek J, Domen J, van Beveren C, Berns A, The primary structure of the putative oncogene pim-1 shows extensive homology with protein kinases. *Cell,* 1986. **46**(4): p. 603-611.

168

Shay K.P. WZ, Xing P., McKenzie I.F.C., Magnuson N.S., Pim-1 Kinase Stability Is Regulated by Heat Shock Proteins and the Ubiquitin-Proteasome Pathway. *Mol Cancer Res,* 2005. **3**(3): p. 170-181.

Shirogane T, Fukada T, Muller JM, Shima DT, Hibi M, Hirano T, Synergistic roles for Pim-1 and c-Myc in STAT3-mediated cell cycle progression and antiapoptosis. *Immunity,* 1999. **11**(6): p. 709-719.

Sivertsen EA, Galteland E, Mu D, Holte H, Meza-Zepeda L, Myklebost O, Patzke S, Smeland EB, Stokke T, Gain of chromosome 6p is an infrequent cause of increased PIM1 expression in B-cell non-Hodgkin's lymphomas. *Leukemia,* 2006. **20**(3): p. 539-542.

Song JH, Kraft AS, Pim kinase inhibitors sensitize prostate cancer cells to apoptosis triggered by Bcl-2 family inhibitor ABT-737. *Cancer Res,* 2012. **72**(1): p. 294-303.

Stevenson FK, Sahota SS, Ottensmeier CH, Zhu D, Forconi F, Hamblin TJ, The occurrence and significance of V gene mutations in B cell-derived human malignancy. *Adv Cancer Res,* 2001. **83**: p. 81-116.

Swords R, Kelly K, Carew J, Nawrocki S, Mahalingam D, Sarantopoulos J, Bearss D, Giles F, The Pim kinases: new targets for drug development. *Curr Drug Targets,* 2011. **12**(14): p. 2059-2066.

Tamburini J, Green AS, Bardet V, Chapuis N, Park S, Willems L, Uzunov M, Ifrah N, Dreyfus F, Lacombe C, Mayeux P, Bouscary D, Protein synthesis is resistant to rapamycin and constitutes a promising therapeutic target in acute myeloid leukemia. *Blood,* 2009. **114**(8): p. 1618-1627.

Telerman A, Amson R, Zakut-Houri R, Givol D, Identification of the human pim-1 gene product as a 33-kilodalton cytoplasmic protein with tyrosine kinase activity. *Mol Cell Biol,* 1988. **8**(4): p. 1498-1503.

Thomas M, Lange-Grunweller K, Weirauch U, Gutsch D, Aigner A, Grunweller A, Hartmann RK, The proto-oncogene Pim-1 is a target of miR-33a. *Oncogene,* 2012. **31**(7): p. 918-928.

Torres-Garcia SJ, Cousineau L, Caplan S, Panasci L, Correlation of resistance to nitrogen mustards in chronic lymphocytic leukemia with enhanced removal of melphalan-induced DNA cross-links. *Biochem Pharmacol,* 1989. **38**(18): p. 3122-3123.

Trivigno D, Bornes L, Huber SM, Rudner J, Regulation of protein translation initiation in response to ionizing radiation. *Radiat Oncol,* 2013. **8**: p. 35.

Vasef MA, Medeiros LJ, Koo C, McCourty A, Brynes RK, Cyclin D1 immunohistochemical staining is useful in distinguishing mantle cell lymphoma from other low-grade B-cell neoplasms in bone marrow. *Am J Clin Pathol,* 1997. **108**(3): p. 302-307.

Verbeek S, van Lohuizen M, van der Valk M, Domen J, Kraal G, Berns A, Mice bearing the E mu-myc and E mu-pim-1 transgenes develop pre-B-cell leukemia prenatally. *Mol Cell Biol,* 1991. **11**(2): p. 1176-1179.

Walpen T, Kalus I, Schwaller J, Peier MA, Battegay EJ, Humar R, Nuclear PIM1 confers resistance to rapamycin-impaired endothelial proliferation. *Biochem Biophys Res Commun,* 2012. **429**(1-2): p. 24-30.

Wang M, Okamoto M, Domenico J, Han J, Ashino S, Shin YS, Gelfand EW, Inhibition of Pim1 kinase prevents peanut allergy by enhancing Runx3 expression and suppressing T(H)2 and T(H)17 T-cell differentiation. *J Allergy Clin Immunol,* 2012. **130**(4): p. 932-944 e912.

Wang Z, Bhattacharya N, Mixter PF, Wei W, Sedivy J, Magnuson NS, Phosphorylation of the cell cycle inhibitor p21Cip1/WAF1 by Pim-1 kinase. *Biochim Biophys Acta,* 2002. **1593**(1): p. 45-55.

Winn LM, Lei W, Ness SA, Pim-1 phosphorylates the DNA binding domain of c-Myb. *Cell Cycle,* 2003. **2**(3): p. 258-262.

Woodland R.T. FCJ, Schmidt M.R., Hammerman P.S., Opferman J.T., Korsmeyer S.J., Hilbert D.M., Thompson C.B., Multiple singnaling pathways promote B lymphocyte stimulator-dependent B-cell growth and survival. *Blood,* 2008. **111**: p. 750-760.

Wozniak MB, Villuendas R, Bischoff JR, Aparicio CB, Martinez Leal JF, de La Cueva P, Rodriguez ME, Herreros B, Martin-Perez D, Longo MI, Herrera M, Piris MA, Ortiz-Romero PL, Vorinostat interferes with the signaling transduction pathway of T-cell receptor and synergizes with phosphoinositide-3 kinase inhibitors in cutaneous T-cell lymphoma. *haematologica,* 2010. **95**(4): p. 613-621.

Yan B, Zemskova M, Holder S, Chin V, Kraft A, Koskinen PJ, Lilly M, The PIM-2 kinase phosphorylates BAD on serine 112 and reverses BAD-induced cell death. *J Biol Chem,* 2003. **278**(46): p. 45358-45367.

Yang Q, Chen LS, Neelapu SS, Miranda RN, Medeiros LJ, Gandhi V, Transcription and translation are primary targets of Pim kinase inhibitor SGI-1776 in mantle cell lymphoma. *Blood,* 2012. **120**(17): p. 3491-3500.

Zhang Y, Wang Z, Li X, Magnuson NS, Pim kinase-dependent inhibition of c-Myc degradation. *Oncogene,* 2008. **27**(35): p. 4809-4819.

Zippo A, De Robertis A, Serafini R, Oliviero S, PIM1-dependent phosphorylation of histone H3 at serine 10 is required for MYC-dependent transcriptional activation and oncogenic transformation. *Nat Cell Biol,* 2007. **9**(8): p. 932-944.

Vita

Qingshan (Carly) Yang was born in Tianjin, China on April 14th, 1986 to parents of Lin Chen and Benping Yang as a single child. She grew up in Tianjin where she attended Tianjin Xinhua High School from 2001-2005. During 2002-2003, Carly came to Scituate, Massachusetts, United States with American Field Service (AFS) intercultural exchange program as a high school exchange student, where she attended Scituate High School as a junior student, and stayed with her host family Robin and Phillip Elliott and their children Phillip and Kimberly Qiaoya Elliott. After the completion of the AFS program, Carly went back to China to complete her high school education, and in fall of 2005, she is admitted the Ohio Wesleyan University, Delaware, Ohio, where she studied Biochemistry and Microbiology. In august 2009, Carly enrolled at the University of Texas, Graduate School of Biomedical Sciences at Houston, and later joined the laboratory of Dr. Varsha Gandhi in the Department of Experimental Therapeutics in MD Anderson Cancer Center, and she also became a member of the Experimental Therapeutics Academic Program (ETAP). Carly conducted her Ph.D. work under Dr. Gandhi's advisory, and she will complete all requirements of Doctor of Philosophy degree in April, 2013.

During Carly's Ph.D. training, she received multiple travel awards from both UT-GSBS and ETAP program to attend the annual conferences of American Association of Cancer Research (AACR) where she presented her works. In addition, she received a research award from ETAP in 2010. In addition, Carly is the sole recipient of a prestigious Cancer Answers/Sylvan Rodriguez Scholarship of 2012-2013 through UT-GSBS where the Sylvan Rodriguez Foundation sponsors a GSBS student per year based on their outstanding achievements in both research and leadership and community services.

Publications:

-**Yang Q**, Chen LS, Neelapu SS, Gandhi V. Combination of Pim kinase inhibitor, SGI-1776 with Bendamustine in B-cell lymphoma. *Clinical Lymphoma, Myeloma & Leukemia*, in press.

-**Yang Q**, Chen LS, Neelapu SS, Miranda RN, Medeiros LJ, Gandhi V. Transcription and Translation are Primary Targets of Pim Kinase Inhibitor, SGI-1776, in Mantle Cell Lymphoma. *Blood*, 2012 Oct 25; 120 (17):3491-500.

Permanent address:

69-1-301 Xinan Cun, Nankai University

Tianjin, China, 300071